THE BINDING OF GLYCOSAMINOGLYCANS TO PEPTIDES

A thesis presented in partial fulfilment
of the requirements for the degree of
Master of Science in Biochemistry
at Massey University

GRANT JOHN TAYLOR
1994

ABSTRACT

The overall aim this study was to examine the possibility of using immobilised polypeptide chains to fractionate/separate Glycosaminoglycans (GAG's) from mixtures.

Initially individual samples of three GAG classes (chondroitin sulphate, dermatan sulphate and heparin) were characterised to establish purity and provide basic information. Once these samples had been characterised the samples were treated as standards.

Three short poly-l-lysine (PLL) chains with defined length and orientation were synthesized. As a control a PLL chain with 633 residues was immobilised. The interaction of the GAG standards with these resins did not replicate published solution binding behaviour of longer PLL chains. This suggested a different mode of binding. The interaction of two lengths of PLL (126 and 633 residues) and the K_8G peptide with the GAG standards in solution was investigated. These studies demonstrated that the mode of binding of GAG's to short PLL chains was radically different to the earlier reported solution binding studies. ß-Strand dominates with the short PLL chains instead of α-helix established in the published solution binding studies.

The interaction of two peptides PCI (264-283) and thrombospondin peptide with the GAG standards was studied using circular dichroism spectroscopy. In the case of the PCI peptide, each GAG induced different secondary structures. Chondroitin sulphate and heparin induced an α-helix, whereas dermatan sulphate gave ß-strands. Heparin and dermatan sulphate induced double the amount of secondary structure compared to chondroitin sulphate. The strength of the interaction of GAG's with the peptide was also measured by the concentration of salt required to dissociate 50% of the complex. The figures for dermatan sulphate and heparin were found to be 0.1 and 0.3 M salt respectively. The binding of the GAG standards to the thrombospondin

peptide did not elicit any detectable change in conformation of the peptide.

Critical examination of published material on the interaction of GAG's (principally heparin) with short peptides, prompted the writer to propose two **new** complementary models. The first model examines binding in terms of the conformation of the peptide induced by binding to the GAG. It is composed of three components, the periodicity of polar and nonpolar residues within the peptide sequence, the spacing of pairs of basic residues and the spacing of pairs of acidic and basic residues. This model is successfully able to rationalise the binding behaviour of a number of GAG/peptide interactions in terms of the dominant secondary structure and the biological activity. The model is able to make a number of specific predictions. The second model examines the strength of the interaction between heparin and peptides containing the proposed consensus sequences for GAG binding sites. A significant correlation between the binding strength and an attribute derived from the sequence of the peptide was found using only one assumption. The assumption was that the peptides in the correlation bound to heparin with significant levels of ß-strand.

For the **first time** it is possible to rationalise the behaviour of GAG/peptide interactions in a coherent manner. The design of peptides that are capable of binding to specific GAG's now seems possible.

This thesis is dedicated to the most unappreciated group of chemicals in the science of biochemistry: glycosaminoglycans. Thanks to my long suffering laboratory companions: Simon Burton, Lou Wen and Estela Campanella (a.k.a dancing in the streets). I can honestly say that it has certainly been an experience. Thanks to my supervisor David Harding for his support and intellectual contribution, at several critical points in the research project and the drafting of the thesis. Thanks to Darren Englebretsen (a.k.a. Dr Cellulose) and Jenny Cross of the former SSU for helpful advice on peptide synthesis and the synthesis of three peptides. Thanks to Marcia Baker of the Separation Science Programme (formerly the Separation Science Unit) for looking after the finances of the project. It is with regret that I must acknowledge the demise of the SSU, that supplied the intellectual climate in which enabled this project to be fostered. I hope that the unique climate will be allowed to continue to exist by the powers that be.

Thanks to Rod Mackenzie and Carol Flyger of the Chemistry and Biochemistry Department of Massey University for calcium, A.A.S analysis and amino acid analysis respectively. Thanks to John Hastie and Ken Jolley of the Physics and Biophysics Department of Massey University for C^{13} NMR analysis of GAG standards. Thanks to Duncan MaKay and Selwyn Yorke of New Zealand Pharmaceuticals (NZP) for advice on GAG electrophoresis and supplying GAG samples respectively. Thanks to Gavin Manderson and Laurie Creamer of the protein separation section of the Dairy Research Institute for advice on the use of the CD instrument.

To my friends Paul and Linda Hoek, Philip Howard and Marie Wong for their friendship, support and encouragement over the years, I owe you all a debt of gratitude which I can never repay. Heartfelt appreciation to Alicia Pogoni and Dianna Elliott for dispensing fermented malt beverages and stimulating conversations during many evenings while I was writing this thesis. Finally I would like to thank NZ FORST for the financial support of this project, through NZP. It was greatly appreciated.

List of Figures

List of Tables

Abbreviations

α	Alpha helix
ß	Beta sheet
C^{13}	Carbon thirteen
CS	Chondroitin sulphate
C4S	Chondroitin-4-sulphate
C6S	Chondroitin-6-sulphate
CD	Circular dichroism
DS	Dermatan sulphate
GAG	Glycosaminoglycan
Gal	Galactose
GalN	Galactosamine
GalNAc	N-acetyl-galactosamine
GlcN	Glucosamine
GlcNAc	Nacetylglucosamine
GlcNS	Glucosamine-Nsulphate
GlcNS(5S)	Glucosamine-Nsulphate-5Osulphate
GlcN($6SO_3$)	Glucosamine-Nsulphate-6Osulphate
GluA	Glucuronic acid
Hep	Heparin
HexA	Hexuronic acid
HS	Heparan sulphate
Ido2S	Iduronic acid-2Osulphate
IdoA	Iduronic acid
N_{eff}	Number of theoretical plates
PLA	Poly-L-arginine
PLL	Poly-L-lysine
R	Random coil

Chapter 1: Introduction

1.1 REVIEW OF GLYCOSAMINOGLYCANS STRUCTURE AND FUNCTION

1.1.1 Classification of Glycosaminoglycans (GAG'S)

1.1.1.1 Common GAG types.

Glycosaminoglycans (GAG's) are linear heteropolysaccharides with characteristic disaccharide repeat sequences (AB). Usually GAG's are found to be covalently associated (with the exception of hyaluronic acid) with proteins. GAG's associated with proteins are termed as proteoglycans. Proteoglycans are widely distributed in animal tissues such as connective tissue and fluids, cell membranes and in the cerebral cortex of the brain. Common naturally occurring GAG's are grouped into seven classes, of which six are structurally related (Table 1.1). The seven different GAG types can be distinguished by differences in the following factors:

1. The monomer composition
2. The position and configuration of the glycosidic linkages.
3. The amount and location of the sulphate residues.

All GAG's consist of an alternating sequence of a hexose sugar (Figure 1.1) and hexosamine residues. Both units can be variably O-sulphated, and the hexosamine sugar residue is N-acetylated or N-sulphated. The seven GAG types can be easily divided into three classes of disaccharide units by examining the basic structure of the glycan backbone. The three classes are as follows:

1. $(HexA\text{-}GalN)_n$
2. $(HexA\text{-}GlcN)_n$
3. $(Gal\text{-}GlcN)_n$

Table 1.1: Classification of glycosaminoglycans

GAG type	Unit A	Unit B	Anomeric Linkage	Additional sulphation positions	N
Hyaluronic acid	Gluc acid	GluNAc	(1-3)/(1-4)	-	250-25000
Keratan sulphate	Gal6S	GluNAc6S	(1-3)/(1-4)	-	
Chondroitin 4 sulphate	Gluc acid	GalNAc4S	(1-3)/(1-4)	C2 of Gluc acid (but this is not common)	50-125
Chondroitin 6 sulphate	Gluc acid	GalNAc6S	(1-3)/(1-4)	oversulphated 4,6 disulphation has been recorded	50-125
Dermatan sulphate	Gluc/Idu acid proportion may vary	GalNAc	(1-3)/(1-4)	C4 of GALN C2 of Idu acid	25-90
Heparan sulphate	Mostly Gluc	GlcN (N-acetylated, N sulphated or O sulphated)	(1-4)	C2 and/or C6 of GALN	30-200
Heparin	Mostly IduA	GlcN (N sulphated or O sulphated, some N-acetylation)	(1-4)	C2,C3 or C6 of GLCN C2 of Idu acid	30-200

Source: adapted from Kjellen and Lindahl 1991, N: Number of disaccharide units

Figure 1.1: Structures of monosaccharide units in GAG's

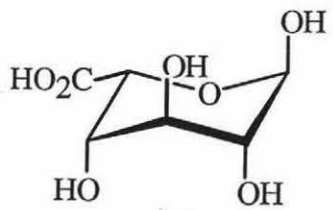

L-iduronic acid

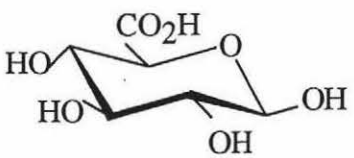

D-glucuronic acid

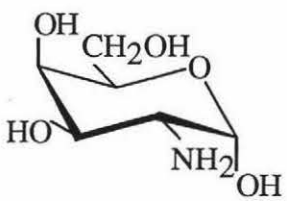

N-acetyl Galactosamine

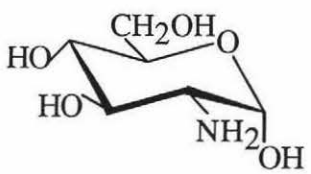

N-acetyl glucosamine

The type 3 disaccharide unit has only been found in keratan sulphate. Types 1 and 2 may be further subdivided. Type 1 contributes to chondroitin sulphate and dermatan sulphate. Type 2 can be found in heparin and heparan sulphate respectively. Type 2 also includes hyaluronic acid which has a slightly different pattern of glycosidic linkages and is not sulphated. The hexose unit in the first two classes of GAG's is modified at the C6 position, containing a carboxylic acid group instead of the usual primary alcohol group at the C6 position. These modified units are referred to as uronic acid residues, of which there are two types glucuronic and iduronic acid, which are C5 epimers of each other (Figure 1.1).

The individual GAG species are represented by a heterogenous disaccharide repeat sequence with corresponding heterogeneous properties. Sequence heterogeneity is particulary important in the three different GAG types; dermatan sulphate, heparin and heparan sulphate. This is due to two variable structural properties:

(i) The proportion of glucuronic to iduronic acid residues in the chain may vary over a wide range e.g. for dermatan sulphate iduronic acid can vary from 10 to 90% of the total uronic acid content.

(ii) The position and extent of sulphation of the polymer can also vary widely.

1.1.1.2 Heterogeneity of disaccharide repeat sequences

The basic disaccharide repeat sequences of GAG chains would seem to provide for the occurrence of regular polymer sequences. However the analysis of GAG preparations often reveals heterogeneity within as well as between the individual polysaccharide chains. This is readily explained in terms of the mechanism of GAG biosynthesis. The initial polymerisation reaction generate products of strictly repeating disaccharide units. Subsequent modification processes, involves sulphate substitution at various positions and may include C5 epimerisation of glucuronic to iduronic acid. These modification processes are incomplete and yield polymer sequences at various stages of modification.

In the case of the glucosaminoglycans, heparin and heparan sulphate, the N-acetyl groups may be partially removed and the resulting amino group is sulphated. The removal goes almost to completion for heparin, with 70 to 90 percent removal, however in the case of heparan sulphate only 50% of these groups are removed. The heterogeneity is greatest in the case of heparin which allows for the existence of 17 different HexAGlcN and 10 (possibly 12) GlcNHexA disaccharide sequences (Kjellen and Lindahl 1991). In the case of the galactosaminoglycans (chondroitin and dermatan sulphate) which are generated by similar biosynthetic pathways, the structural diversity in less pronounced (since the GalNAc units remains acetylated) than heparin related species. As many as nine different disaccharide units have been identified (Kjellen and Lindahl 1991).

The GalNAc residue in chondroitin and dermatan sulphates can be nonsulphated, 4O-sulphated, 6O-sulphated or 4O/6O-disulphated. When the uronic acid is glucuronic all four variants have been found, however iduronic is usually associated

with GalNAc4OS. This restriction is thought to arise during the biosynthesis of the GAG chain (Cheng et al 1992). Whether the majority of the different possible disaccharide repeats in chondroitin sulphate and dermatan sulphate are distributed randomly or in some orderly fashion is still under investigation.

The situation for GAG sequencing at present is similar to the early days of protein sequencing with the same barriers to sequencing i.e. a lack of good purification procedures, and sequencing protocols are hampered by the lack a wide range of specific GAG cleaving reagents. A variety of sequencing strategies for the examination of the distribution of the disaccharides near the linkage region of the GAG chains to the core protein for chondroitin and dermatan sulphate chain have been advanced (Uchiyamal et al 1987, Cheng et al 1992, Fransson et al 1990). All of these strategies involve the chemical labelling of the reducing end of the GAG chain and degradation of the labelled chain with chemicals or GAG degrading enzymes (GAG lyases). In shark C6S chains 4O-sulphation and nonsulphation of disaccharides appears to be concentrated close to the linkage region (Uchiyamal et al 1987). Whereas 6O-sulphation in shark cartilage and nasal chondroitin sulphate appears to be distally concentrated from the linkage region (Uchiyamal et al 1987 and Cheng et al 1992). Glc-GalNAc repeats in pig skin dermatan sulphate are prevalent in position 1-3 and 7-12 from the linkage region of the GAG chain (Fransson et al 1990). These preliminary studies suggest that the overall distribution of disaccharides within the polysaccharide chain is not random, but there is not a defined primary sequence to each polysaccharide molecule. Part of the remaining heterogeneity observed could be due to the fact that the GAG chains are derived from many sites in different core proteins synthesized by a variety of cell types. Since the biosynthetic machinery may be tissue specific and receive information from the core protein.

Heparan sulphate contains an equal proportion of N-acetylated and N-sulphated disaccharides. The distribution of these disaccharides within the chain is not random. They tend to occur in separate domains within the chain. In addition O-sulphate

groups are located in or near N-sulphate domains (Gallagher et al 1992).

1.1.2. Biological roles of GAG's

Over the last few years the biological roles of GAG's and proteoglycans has come under increasing scrutiny. Previously it was assumed that they played a mainly structural rather than a chemical role (B. Chakrabarti and J.W. Park 1980). There is now an increased appreciation of the roles that they play in the body. These roles range from regulation of the intrinsic blood coagulation cascade, to a possible involvement in a variety of diseases.

The initial function that was ascribed to proteoglycans was the result of the interaction between proteoglycans and fibrillar collagen and elastin in connective tissues. The large sizes of the GAG chains result in large excluded volumes. The interactions between the components are electrostatic since they are disrupted by increasing salt concentration (Scott 1988a for a recent review). The proteoglycans seem to be important for maintaining the structural integrity of connective tissue. The large excluded volumes of the GAG chain on the proteoglycans serve two functions:

- In cartilage they serve as a mechanical shock absorber since the long chains and their associated water of hydration resist compression.
- They also regulate the distribution of macromolecules by steric exclusion.

Three types of GAG's have been shown to be involved in the regulation of blood coagulation (Bourin and Lindahl 1993). Two of these GAG's (heparin and dermatan sulphate) activate SErine Protease INhibitors (SERPINs) and act on the serine proteases of the intrinsic blood coagulation pathway. Heparin binds to antithrombin III and accelerates the inhibition of thrombin and other serine proteases of the blood coagulation pathway. A second serpin, heparin cofactor II is activated by both heparin and dermatan sulphate. This selectively inactivates thrombin. Heparin has been used for over sixty years in the treatment of blood clots, as it inhibits the

formation of clots by inactivating thrombin. There is considerable interest in the possible use of dermatan sulphate as an alternative to heparin as it appears to have less side effects. Finally another regulatory species of blood coagulation, the protein C pathway involves the proteoglycan thrombomodulin, which contains a functionally important chondroitin sulphate chain. The protein C pathway inactivates the auxiliary coagulation proteins and prevents the generation of active thrombin. Thrombomodulin plays a key role in the activation of the protein C pathways by thrombin.

Injection of heparin results in an increased clearance of triglycerides in the body. The effect is due to the release of lipoprotein lipase and hepatic lipase from the surface of capillary endothelial cells and from the liver respectively. Lipoprotein lipase hydrolyses lipids in the plasma (located in low density lipoproteins and chylomicrons), resulting in the transfer of fatty acids to tissues. The release of lipoprotein lipase on addition of heparin is the result of heparin competition with cell surface heparan sulphate proteoglycans which bind lipoprotein lipase. It is also involved in the receptor mediated uptake of lipoproteins, the process being linked to the presence of HSPG on the surface of the cell membranes. Heparin has also been shown to inhibit the growth (antipoliferative effect) of several cell types (Wright et al 1989).

Proteoglycans containing either heparan or chondroitin sulphate play an important role in the organisation and function of the basement membrane (a specialised extracelluar matrix). The proteoglycans interact with the other components of the basement membrane (laminin, collagen etc) to form the supramolocular architecture typical of the basement membrane. The final structure forms an almost impenetrable net with a nett negative charge. This final structure of the basement membrane serves such functions as controlling the filtration of large molecules, and the binding of growth factor and protease inhibitors (Timp 1993). In addition the components of the extracelluar matrix, including proteoglycans, regulate the differentiation and development of cells (Adams and Watt 1993, Wight 1992). It has also been suggested that they may also be involved in signal transduction of some growth

factors to the nucleus.

Heparan sulphate has been shown to be a modulator of fibroblast growth factor (FGF) activity. The surface of cells has two receptor classes for the FGF, the high and low affinity receptor systems. The low affinity receptors have been identified as heparan sulphate proteoglycans. The high affinity receptors are responsible for the transmission of the cellular signal to the inside of the cell. Experiments with mutant cells that lack cell surface heparan sulphate chains after treatment with heparitinase or treatment of cells with chlorate (which inhibits the sulphation of heparan sulphate) have demonstrated that activation of the high affinity receptors is greatly reduced (Klagsbrun and Baird 1991). These FGF unresponsive cells can be activated by FGF in vitro by the presence of heparin. The structure of the heparan sulphate oligosaccharide that binds to basic FGF (Habuchi et al 1992) and acidic FGF (Mach et al 1993) has been determined. The involvement of HSPG's in the regulation of FGF activity is now almost complete. Since the FGF receptor (FGF-R1) has also been shown to have a heparin binding site (Kan et al 1993). Examination of the binding interaction of heparin with FGF (Thompson et al 1994) and FGF-R1 (Pantaliano et al 1994) has demonstrated that HSPG and FGF binding to FGF-R1 occurs in such a manner that the receptor dimerises. The dimerisation is thought to be an essential step for signal transduction.

It is well known that heparan sulphate (and heparin) bind to a large range of cytokines that affect cell growth and differentiation, of which FGF is an example. It is interesting to speculate as to whether the dual requirement of growth factor receptor and GAG-type receptors is a general phenomenon among heparin binding growth factors. The interaction of heparin binding epidermal like growth factor (HB-EGF) with the EGF receptor has recently been shown to also be modulated by heparin and heparinase treatment in a similar manner to FGF (Besner et al 1993). Preliminary evidence suggest that the activity of hepatocyte growth factors mitogenic activity on hepatoctyes is also regulated by heparin-like molecules on the hepatocyte cell surface (Naka et al 1993).

Cell surface heparan sulphate proteoglycans have been shown to facilitate the initial binding of some viruses and bacteria to the cell membrane and allow their internalisation. In some cases the binding appears to be specific to these chains since other GAG's are unable to compete for the binding and internalisation process. The interaction has been shown to range from low affinity (Liang et al 1993) to high affinity (Lycke et al 1991). The binding of the Herpes simplex virus to heparan sulphate (Lycke et al 1991) has been demonstrated to be the first step in the internalisation of the virus into the cell. The in vitro anti HIV-1 activity of heparin has been explained by a specific low affinity interaction between heparin and the major envelope protein of HIV-1 (Mbemba et al 1992). Staphylococcus aureus and other staphylococcal bacteria that are capable of causing diseases in humans, interact with various connective tissue proteins. To date the binding of heparan sulphate proteoglycans to three staphylococcus species have been demonstrated S. aureus (Herrmann et al 1988 and Liang et al 1992), S.pyrogens (Berggey and Stinson 1988) and S.mutans (Choi and Stinson 1989). In these cases the binding has been shown to be saturatable, but not specific since the binding can be inhibited by other GAG's to various extents, the general order of inhibition being

Heparin > HS > DS > CS > Hyaluronic acid

Amyloidosis is the deposition of insoluble protein fibrils resulting in organ dysfunction and death. GAG's in the form of proteoglycan, in particular heparan sulphate proteoglycan has been implicated in the development of at least five different forms of amyloidoses (Kiselevsky 1990 and 1992), including Alzheimers disease, Creutzfeldt-Jakob disease and Scrapie. There is a coincident deposition of heparan sulphate proteoglycans occurs while the amyloid deposits of these diseases form. High affinity interaction between HS-PG and the amyloid protein of Alzheimers disease have been demonstrated and suggest that they may play more than a passive role in the development of amyloid deposits. Although the major component of the amyloid deposits in Alzheimers disease beta-A4 peptide has been shown to form fibrils in vitro in the absence of GAG's and proteoglycans. However it has been demonstrated that the fibrils of the correct size and morphology will only

form in the presence of sulphate or heparan sulphate (Fraser et al 1992). This demonstrates that at least in vitro, the formation of significant amounts of Alzheimers amyloid deposits of appropriate morphology requires the presence of GAG's to pack the amyloid fibrils in the appropriate manner. The preferential localisation of diffuse plaques in the hippocampus but not the cerebellum of the brains of Alzheimers disease patients has been related to the presence of perlecan (a particular HSPG) in the hippocampus of the brain (Snow et al 1994). Additional information on the connection between HSPG and other amyloidoses is given in Section A1.2 of Appendix 1.

The biological roles of proteoglycans are highly diverse. This is perhaps a reflection of the diversity in the disaccharide repeat sequences in each GAG class. The anti-proliferative and anticoagulant effects of heparin and heparan sulphate are effected by the free GAG chains. However most of the biological effects of proteoglycans depends at least to some extent on the presence of the protein core. It is not clear however whether the protein core acts primarily as a scaffold for the appropriate immobilisation and spacing of the GAG chains, or whether the core protein plays a more important role in some cases. However to a large extent most of the biological function of proteoglycans appear to depend on the binding interaction of GAG chains to heparin.

1.1.3. GAG properties

1.1.3.1 pK_a of ionizable groups

GAG's are polyanionic species, and to a large extent most of their properties can be related to this. The pK_a of the carboxyl group in sulphated GAG's varies over the pH range 3.95 to 5.30, the precise value depending on the **GAG concentration** (Gatti et al 1979), and on the **ionic strength of the solution being used** (Nieduszynski 1989).

1.1.3.2 Flexibility of uronic acid sugar residues

Iduronic acid residues that are present in some GAG types (heparin, heparan sulphate, and dermatan sulphate) impart a variety of properties to the GAG chain. As discussed in the previous section, iduronic acid containing GAG's have important roles in a variety of biological processes. Theoretical, and experimental studies (using NMR) indicate that iduronic acid residues are in an equilibrium between two different conformations (Casu et al 1988 for a review). The relative proportions of these different conformations depend upon the sulphation pattern and sequence of the GAG chain in question.

When inside a polysaccharide sequence, the iduronic acid residues are in equilibrium between the two forms, $^1C_4$ and $^2S_0$ (footnote [1]) in approximately the same proportion for both nonsulphated (dermatan sulphate series) and sulphated (heparin series) residues. A 3-O-sulphate residue in the preceding aminosugar residue (as in the case for the binding sequence of the binding site for antithrombin III) drives the equilibrium towards the $^2S_0$ form which can represent more than sixty percent of the iduronic acid in such sequences. This flexibility of the iduronic acid residues compared to glucuronic acid residues explains the decreasing order of affinity of GAG chains for polyvalent cations and proteins (such as lipoprotein lipase):

Heparin > Dermatan sulphate > Chondroitin-6-sulphate > Chondroitin-4-sulphate

The flexibility of these units allows the GAG chain to adopt a greater variety of conformations when binding to proteins or polyvalent cations. In addition these residues may be forced into unusual conformations by the presence of adjacent sulphated residues.

---

[1] C and S stand for the chair and skew-boat forms of these sugar, the superscript gives the number of equatorial groups, while the subscript gives the number of axial groups.

1.1.3.3 Hydrophobic patches

The presence of large clusters of contiguous (8 or 9) CH groups forming patches of highly hydrophobic character, repeated at regular intervals on alternative side of the GAG chain have been detected in molecular models of GAG disaccharides of chondroitin sulphate, keratan sulphate and hyaluronic acid (Scott and Tigwell 1978, Hounsell 1989, and Scott 1988b). The hydrophobic patches are smaller in the case of dermatan sulphate since the carboxyl replaces one CH group in each patch. In addition when the uronic residue is iduronic acid, the patch is eliminated since all the CH groups are equatorial (if the conformation is $^1C_4$). Molecular models of heparan sulphate disaccharide (Scott and Healy 1982) suggest that such hydrophobic patches are not as extensive as in the case of chondroitin and keratan sulphate disaccharides.

1.1.3.4 Secondary Structure

Secondary structures of GAG chains in solution have been detected by the kinetics of periodate oxidation and proton NMR spectroscopy of oligosaccharides. Hydrogen bonding between the carboxyl of the acetyl group on C2 of glucuronic acid and the C6 carboxyl and the NH group of GluNAc induce two fold helices in HA. Solid state structures of GAG fibres have indicated that depending on the conditions of pH and ambient cations 2, 3, 4 and 8 fold helices can form. The extensive hydrogen bonding between sugar units in HA reduces the flexibility of the GAG chain ie increases stiffness and to some extent diminishes its capacity for interaction with other molecules (Scott 1988b). A similar 2 fold helix is present in the solution conformation of chondroitin and keratan sulphate, however the axial C4 hydroxyl of GalNAc is unable to hydrogen bond to the GluUA ring oxygens. While 2,3,and 8 fold helices have been inferred from solid state structures of dermatan sulphate, solution NMR evidence suggests that the NH-carboxyl hydrogen bond is not so extensive.

1.1.3.5 Stereochemistry of charged groups

Studies of the structure and conformational analysis of keratan sulphate oligosaccharides reveal that the backbone has repetitive disaccharides which repeat relatively hydrophobic and hydrophillic areas on each face of the molecule (Hounsell 1989). The sulphates are arranged in pairs spatially removed for the backbone. The sulphate and N-acetamindo groups have a distinct topology characterising the top and bottom of the polymer. A similar trans arrangement of the carboxyl groups is also apparent. It appears there is a tendency in GAG chains to try and space out the sulphate and carboxyl groups. The broad similarity of chondroitin and keratan sulphate disaccharides in terms of secondary structure, spacing of hydrophobic and hydrophillic patches has been noted (Scott 1991).

1.1.3.6 Binding to polycations

The interaction of heparin with polycations provides a useful model for heparin protein interactions. A large body of work by Gelman and coworkers exists on the interaction of polybasic amino acids, ie lysine, arginine and ornithine (Gelman and Blackwell 1973a, 1973b, 1973c; Schodt et al 1976 and Blackwell et al 1977). These studies showed that some GAG's were able to effect a change in the conformation of the polypeptide chains as determined by changes in the circular dichroism (CD) spectra. An extended charged coil ordered structure is exhibited by poly-L-lysine (PLL) at neutral pH's. This is a left handed helix with 2.5 residues per turn, due primarily to the electrostatic repulsion between side chains. Using the shape of the CD spectra after binding GAG's they were able to assess the extent of the induced conformation. The strength of the interaction was monitored in two ways: the temperature that was required to disrupt 50% of the interaction (melting temperature or T_m) and the salt concentration that was required to inhibit the interaction. The success of Gelman's group in characterising the interaction of GAG's with polybasic amino acid chains was due to the fact that they used GAG standards of **known** properties, ie molecular weight and charge density (SO_3^-/ COO^- ratio), Table A1.1 in Appendix 1.

The maximum interaction between the respective polypeptide and GAG's was judged by the highest proportion of induced alpha helix or random conformation. This occurred at a aminoacid to disaccharide ratio characteristic for each pair of GAG and polybasic aminoacids. Arginine appeared to have the tendency to interact with both the sulphate and the carboxyl groups, whereas lysine only interacts with the sulphate. This effect is probably due to the length of the side chains. Arginine is able to approach both groups without disrupting the alpha helix. A summary of their **solution** binding experiments is shown in Table 1.2.

The interaction of PLA with GAG's are stronger than PLL and does not appear to be disrupted with increasing ionic strength. Increasing the temperature or increasing the ionic strength are both likely to effect the polysaccharide conformation, but not necessarily in the same way. The GAG's induced changes from charged coil to alpha-helix conformation with an order of efficiency of

Heparin > DS > KS > C6S > HS > C4S > Hyaluronate

(i.e. an order dependant upon the number of sulphate groups in the GAG type). The strength of the interaction with different polypeptides was found to follow the order

Polyarginine > Polylysine > Polyornithine

Results for nonsulphated polysaccharides indicate that the sulphate group, rather than or in addition to the carboxyl group, is necessary for the interaction (Gelman and Blackwell 1973).

The interesting facts about the poly-l-lysine GAG interaction is that the interaction does not seem to be dependant on the sulphation degree of the polysaccharide (dermatan sulphate binds more strongly than heparin). The interaction of chondroitin sulphate with polylysine is also greatly dependant on the position of the sulphation (C4S binds much tighter than C6S).

Table 1.2: Summary of Gelmans solution binding experiments

Polypeptide	HA	KS2	C4S	HS	C6S	KS1	DS	Heparin
PLA ratio	1:1	1.4:1	2:1	1:1	2:1	1.2:1	1.4:1	3.3:1
Induced conformation	R	α	α	α	α	α	α	α
T_m (°C)	35	46	54.5	65	76	>90	>90	>90
PLL ratio	1:1	1.4:1	1:1	2:1	1:1	1.2:1	1.4:1	2.3:1
Induced conformation	R	R	α	R	α	R	α	α
T_m (°C)	-	-	23	-	47	-	72	>90
Sigmoid Transition (M NaCl)	0.5	-	0.80		0.27		>2.0	1.5

KEY TO ABBREVIATIONS: HA: hyaluronic acid, KS2: keratan sulphate 2, C4S: chondroitin 4-sulphate, HS: heparan sulphate, C6S: chondroitin 6-sulphate, KS1: keratan sulphate 1, DS: dermatan sulphate, R: random coil, α: alpha helix, PLA: poly-L-arginine, PLL: poly-L-lysine, PLO: poly-L-ornithine.

1.1.3.4 Summary of important GAG properties

In summary, a number of the properties of GAG's must be considered when attempting to separate these molecules. These properties hamper the isolation of pure GAG fractions and the separation protocol must be designed so as to minimize their effects with the following points in mind:

1. The overall similarity of the GAG types.
2. The existence of the heterogeneity of the disaccharide repeat sequences.
3. The fact that the pK_a of the carboxyl groups are not constant. The pK_a depends on the ionic strength of the GAG and on the concentration of the GAG solution.
4. As a consequence of the biosynthetic process for GAG's final product is not a single molecular species but a mixture of closely related species.
5. The fact that GAG samples are often polydisperse with respect to molecular weight even if the repeating units and sulphation patterns are constant for a single source or species.

1.2 SEPARATION OF GAG's

A review of the classical separation and characterisation technologies for GAG's was last reported in 1972 (Roden 1972). *"There have been few, if any, fundamental advances in separation and fractionation methods for glycosaminoglycans since 1972"* (Fransson 1985). This statement is probably as true now as it was in 1985. A variety of techniques can and have, been used in the separation of GAG's, but to a large extent (with the possible exception of chondroitin sulphate and heparin) all techniques used at present result in only partial fractionation of the individual GAG species. At present there is no single **preparative** technique that is capable of complete separation of **all** the known GAG types. The complete separation of all the GAG types requires the use of several chromatographic column techniques using one or more separation technologies (Bohn and Kalben 1971a and 1971b). However analytical techniques that are used at present have no large scale application such as electrophoresis, can be used to completely resolve all seven GAG species from each other. This is not as drastic a situation as it may seem as all the GAG types rarely occurs in large amount in the same tissue, eg beef lung is a rich source of heparin and heparan sulphate with small amounts of other GAG's. Intestinal mucosa is a rich source of heparin, but it is complicated by large amounts of other GAG being present.

General methods for large scale separation of GAG's include: ion exchange, fractional solvent precipitation and salt concentration-controlled interaction with long chain aliphatic ammonium compounds. *"Most of the procedures used for the separation of glycosaminoglycans depend on properties that are only partially, if at all, structure specific. Often, different kinds of properties (eg charge and chain length) influence the result simultaneously." (Fransson 1985).* In each of the above separation methods, the overall similarities of the various GAG species and in the case of iduronic acid containing species, the heterogeneity of the disaccharide repeat sequence means that quantitative separation of GAG mixtures is problematical.

1.2.1. Ion exchange resins

Discrete separation of all GAG species by ion exchange chromatography on a single matrix, from a GAG mixture has yet to be achieved. Separation of iduronic acid containing GAG's, on ion exchange resins results in overlapping fraction of the individual GAG types. Heparin the most highly charged of the GAG's (Table A1.3 in Appendix 1) is eluted from the above resins at higher salt concentrations than the other GAG's. As a result it is often easier to obtain relatively "pure" heparin fractions.

When optimizing the separation of any biological material from a mixture by ion exchange chromatography, several factors must be taken in account. Firstly the separation must be carried out under conditions of buffer pH and ionic strength so the different ionizable groups carry a charge. Under these conditions the different GAG types will have different charge densities (Table A1.3 in Appendix 1). The selection of the ideal ion exchanger for the separation would be based on the following criteria.

1. The ion exchange resin must be inexpensive, and easily obtainable.
2. The resin must have a similar charge density to the GAG's being separated.
3. The resin should have a good porosity for the molecules concerned (dextran determined porosity). This will influence the strength of the interaction and the capacity of the exchanger. Both are improved by a suitable porosity.
4. Finally for optimal separation of the GAG types in a mixture, the resin should have a similar accessible distribution of charges along the surface of the resin particles. This will result in tight binding of the molecule concerned.

At present **no** ion exchange resin which fulfils all of the above criteria has been reported. Careful consideration of ion exchange chromatography leads the writer to strongly conjecture that separation of **all** the GAG types, solely on the basis of charge, will not be successful. This is because of the similar charge densities of the different GAG types. In addition the estimates of the pK_a of the carboxyl groups,

indicate that they are not sufficiently different (chondroitin sulphate and heparin being exceptions) to allow complete separation of the species. The existence of heterogeneity in the disaccharide repeat sequence of iduronic acid containing polymers causes additional problems. The separation of a GAG mixture into three fractions containing hyaluronic acid, galactosaminoglycans (chondroitin and dermatan sulphate) and heparin should be easily achieved by most ion exchange resins on the basis of their different charge densities (Table A1.3 in Appendix 1). The existence of certain heparan sulphates and to a smaller extent keratan sulphates which have similar charge densities to the galactosaminoglycans cause problems in separation of homogeneous GAG fractions from GAG mixtures containing these materials.

1.2.2. Fractional solvent precipitation

GAG's may be separated by careful fractional precipitation of their calcium salts in ethanol water mixtures (Kennedy 1978). The solubility of GAG in organic solvent-water mixtures is greatly influenced by the presence of divalent cations (usually Ca^{2+} and Ba^{2+}). The difference of GAG salts of individual GAG classes has been exploited and used for the preparation of enriched GAG fractions using ethanol precipitation of calcium salts of GAG mixtures (Meyer et al 1956). There are two specific GAG precipitation methods for particular GAG types. The first is an alkaline copper precipitation of dermatan sulphate (Jeanloz 1965). A selective precipitation method for heparin has been patented by Scott and coworkers (Scott et al 1968). This technique separates GAG's on the basis of the charge density, the lower the charge density the higher the concentration of potassium acetate required to precipitate it.

1.2.3. Polylysine resins

The interaction of GAG's with polylysine has been known for some time and has already been briefly discussed earlier is this Chapter (Section 1.1.3.6). Immobilized polylysine columns have been used on numerous occasions to separate proteins (Nevaldine and Kassell 1971). The poly-L-lysine chains usually being immobilised

through the cyanogen bromide procedure. A method for the fractionation of GAG's, principally heparan sulphate using polylysine columns has been published (Suzuki and Koide 1984a). This method is primarily based on Gelman's work (Blackwell et al 1977) and was the subject of a successful patent application (Suzuki and Koide 1984b). However there are some large discrepancies between this paper and Gelman's work. These will be outlined below. The elution behaviour of the GAG samples tested for immobilised polylysine compared to the binding strength found by Gelman and coworkers is summarised in Table A1.2 in Appendix 1. The first fact that is apparent is that the immobilised polylysine resin no longer has differential binding capacity for chondroitin sulphates that it had in the solution binding. The binding of dermatan sulphate is much weaker when compared to the solution studies. This could be due to the fact that the dermatan sulphate used in their study had a lower charge density than that used by Gelman.

1.2.4 Hydrophobic interactive chromatography

Hydrophobic interactive chromatography on Phenyl-Sepharose or Sepharose CL-4B has been used to fractionate GAG's. While the technique does not appear to be able at separate the different GAG classes, the fractionation procedure is unusual in that it is able to fractionate porcine heparin into two groups of high and low affinity (Ogamo et al 1980). Increased retention on the Phenyl Sepharose is reflected by increased potency in Antithrombin III activation and an increased proportion of high affinity binding to antithrombin III affinity columns. Elution of bound GAG's is effected by stepwise decreasing gradients of ammonium sulphate or linear decreasing gradients. Increased retention on hydrophobic resins has been correlated with increased molecular weight and/or increased N-acetyl group content. The fractionation of shark cartilage chondroitin 6 sulphate (Ogamo et al 1987) and whale cartilage chondroitin 6 sulphate (Ogamo et al 1990) has demonstrated that the unit disaccharide composition also has some effect on the retention in that increased C6S disaccharide is related with increased retention. The retention behaviour of the unit disaccharide of the GAG classes seems to be related to the size and extent of the hydrophobic patches on the unit disaccharide (Section 1.1.3.3.). Since model studies

of C4S,C6S and DS oligosaccharides of similar degrees of polymerisation on Phenyl Sepharose gels (Uchiyama et al 1985) have shown that decreased retention follows the order

C6S > C4S > DS

The solubility of the GAG classes in ammonium sulphate agrees well with the chromatographic binding behaviour. The binding depends largely on the ability of the GAG's to precipitate onto the gel rather than on the hydrophobic interaction between the gel and the polysaccharide.

1.2.5. Bioaffinity chromatography

The interaction of GAG's with proteins has been known for some time (Lindahl and Hook 1978) but in general most of the binding is not highly specific. The problems encountered in the separation of proteoglycans species are similar to those in the separation of free GAG chains. There are several reports in the literature of the use of protein-GAG interaction in the purification of heparan sulphate proteoglycans. Two immobilised bioaffinity columns have been used in this regard. These are platelet factor four (Culp et al 1986) and lipoprotein lipase (Klinger et al 1985). However only in the case of lipoprotein lipase has the interaction between all of the GAG types been documented. The relative strength of binding of lipoprotein lipase to immobilised GAG columns (Bengtsson et al 1980) has been shown to occur in the following order:

Heparin > Heparan sulphate > Dermatan sulphate > Chondroitin sulphate

Unfortunately lipoprotein lipase interacts with the various GAG types in a way that precludes the complete differentiation of the different GAG types. However immobilised lipoprotein lipase columns have been used to isolate a heparan sulphate proteoglycan from rat brain tissue. It had not previously been possible to isolate the highly purified heparan sulphate proteoglycan, because of the similarities in size, charge, and density with the other proteoglycans. It was **only** by the use of

immobilised lipoprotein lipase bioaffinity columns that the separation became achievable (Klinger et al 1985). The column was operated in a ligand displacement mode during the separation. Although the two proteoglycan species were both able to bind to the bioaffinity column to different extents, the heparan sulphate proteoglycan is able to displace or compete for the binding sites on lipoprotein lipase.

The use of immobilised proteins in the separation of free GAG chains in mixtures seems possible in principle. At present immobilised protein bioaffinity chromatography has only been applied to the fractionation of free heparin chains in solution, using two different proteins, antithrombin III and tissue plasminogen activator (Hook et al 1976, Adrade and Stickland 1990).

In summary the application of immobilised protein bioaffinity columns for GAG fractionation has been of limited value for the following reasons:

1. Often the binding of the different GAG types has not been of sufficient specificity resulting in the overlapping fractionation of GAG's (e.g. lipoprotein lipase affinity columns).
2. Other applications such as the use of immobilised antithrombin III columns have resulted in the separation of a limited number of GAG types.
3. The large scale use of bioaffinity column technology is expensive.

1.2.5 Summary of GAG purification procedures

A wide range of purification protocols have been used for GAG's these range from ion exchange to fractional solvent precipitation. However the heterogeneity of the disaccharide repeat sequence results is diverse properties for the GAG chains in a mixture. This results in difficulties in purifying GAG's (chondroitin sulphate and heparin being exceptions) often resulting in the incomplete fractionation of most GAG species.

1.3 BINDING OF GAG'S TO PROTEINS

Recently the binding of GAG's to proteins has been examined with particular reference to the specificity of the interaction and the amino-acid residues and amino acid sequences responsible for binding (Jackson et al 1991). In many cases the residue sequences that are involved in binding of GAG have been identified as being clusters of positively charged amino acids (Arg, Lys, and to a lesser extent His). In general there are two types of binding between GAG's and proteins (Lindahl and Hook 1978).

1. *Cooperative electrostatic binding*: *"In positive, cooperative binding, heparin binds to a protein at different sites, and the affinity shown at each individual interacting site contributes to the overall affinity of the heparin for its protein ligand"* (Farooqui et al 1994). This tends to be of low affinity and increases with increasing charge density of the polysaccharide, and with the presence of iduronic acid e.g. the binding of GAG's to lipoprotein lipase.

2. *Sequence specific binding*: Represents high affinity binding to particular sequences on the GAG chain. At present there are four examples of this type of binding to the binding.

1.3.1 Sequence specific binding

Four sequence specific binding sites on GAG chains have presently been elucidated, representing types one and two disaccharide repeat sequence (Section 1.1.1.1). These sequences are outlined in Table 1.3. The first sequence identified was the pentasaccharide required for the interaction between heparin and antithrombin III. The occurrence of an 3-O-sulphate group on an internal glucosamine unit appear essential for high affinity interaction. Structural variants in the antithrombin III are allowed in two positions without decreasing the high affinity interaction.

A hexasaccharide (Table 1.3), derived from dermatan sulphate that binds to heparin

cofactor II with high affinity has been identified (Maimone and Tollefsen 1990). The sequence on the heparan sulphate chain that is essential for high affinity binding of the FGF is a pentasaccharide of defined sequence (Table 1.3). Recent evidence suggest that the minimum size of heparin/ heparan sulphate oligosaccharides required to potential the activity of FGF is a dodecasaccharide (Guimond et al 1993). The three sequences elucidated so far contain iduronic acid sequences, which as has already been mentioned are flexible. The presence of unusual sulphation patterns in adjacent residues can also force the iduronic residues into unusual conformations. The comparative rarity of these sequences in the case of heparin cofactor II and FGF binding sites, along with their short length means that they may selectively influence their biological activities. The sequence of the high affinity site on heparin for LPL has recently been characterised (Parathasarathy et al 1994), as being distinct from the ATIII and FGF binding sites. There is a broad similarity to the HCII binding site on dermatan sulphate (Table 1.3) with the same repetition of the two sugars iduronic acid 2sulphate and N-sulphated hexosamine which is sulphated at the 6 position. The two major differences being that in heparan sulphate heparin the anomeric linkages alternate between the 1-3 /1-4 positions, whereas in dermatan sulphate the linkages are all the 1-4 type and the site in LPL is elongated slightly, with 5 instead of 3 disaccharide units.

Table 1.3: Sequences specific binding sites on GAG's

Function	GAG	Sequence	% Chains carrying this sequence
AT III- heparin binding	Heparin/HS	GlcN6S-GlcA-GlcNS-Ido2S-GlcNS(5S)	30
FGF binding	Heparin/HS	HexA-GlcNS-HexA-GlcNS-Ido2S	nd
HC II-DS interaction	Dermatan sulphate	$[\text{-IdoA2S-GalNS(6S)-}]_3$	<5
LPL-HS interaction	Heparin/HS	$[\text{-IdoA2S-GlcNS(6S)-}]_5$	<5

1.3.2 Protein consensus sequences for GAG binding

To date five different protein consensus sequences for GAG binding have been proposed. The first was the result examining twelve known heparin-binding sequences in four proteins to formulate two *search strings* for identifying potential heparin binding regions in other proteins (Cardin and Weintraub 1989). The identified consensus sequences (Table 1.4) correctly predicted the GAG binding domains of several proteins such as antithrombin III, heparin cofactor II and neural cell adhesion molecule (Cardin et al 1991).

A different consensus sequence for heparin binding was proposed after examining the amino acid sequences of a six heparin binding peptides (Sobel et al 1992). The motif is palindromic containing a central cluster of three cationic residues, flanked on either side by additional doublets of cationic residues separated by two neutral amino acids. This consensus peptide was then used to locate the punitive heparin binding domains in a human plasma protein von Willebrand factor. Human von Willebrand factor is a plasma glycoprotein which plays a critical role in regulating haemostasis.

A common hyaluronic acid binding motif in three hyaluronic acid binding proteins has been identified (Yang et al 1994), BY_7B. The seven residues (Y) contain contains no acidic residues and at least one basic residue. Earlier work on the binding of hyaluronic acid to cartilage binding protein (Goetinick et al 1987), which contains this motif demonstrated that the other GAG's were unable to compete with hyaluronic acid for the binding of this protein. Taken together these results suggest that the BY_7B motif is a consensus for the binding of only hyaluronic acid.

Unfortunately some of the proteins known to bind heparin do not conform to the above consensus sequences eg platelet factor four residues 46-70 and bFGF residues 25-46. In addition the identification of short sequences such as BBXBX seems incompatible with requirement of a pentasaccharide as the minimum functional unit of heparin for antithrombin III binding (Margalitt et al 1993). The existence of heparin binding peptides that contain no basic residues is also puzzling (Guo et al

1992a) if one is influenced by the above reasoning.

Table 1.4: Proposed consensus sequences for Heparin binding

Sequence	GAG Class	Reference
XBBXBX XBBBXXBX	Heparin/all GAG's ?	Cardin and Weintraub 1989
XBBXXBBBXXBBX	Heparin/all GAG's ?	Sobel et al 1992
$B(Y)_7B$	Hyaluronic acid	Yang et al 1994

KEY: B is the high probability of a basic residue, X is hydrophobic residue, Y is any non-acidic residue

However a recent comparative analysis of structurally defined heparin binding sequences revealed a distinct distribution of basic residues within these sequences (Margalit et al 1993). The sequences of eighteen peptides known to bind heparin were compared. For nine of these sequences, the three dimensional structure was known. Alignment of the sequences with a alpha helical fold demonstrated that they all contained two basic residues twenty angstroms apart on opposite sides of an amphipathic helix. Although the binding site of antithrombin III is thought to be in a beta strand type conformation, the position of two basic residues twenty angstroms apart on opposite sides of the fold is retained. The distance of twenty angstroms between basic residues fits the pentasaccharide sequence.

So far the binding of GAG's to protein has primarily been focused on the heparin domains of these proteins. The affinity for the various GAG types for two heparin binding proteins have been reported (Dawes et al 1988) antithrombin III and thrombin. These results show that even for proteins that have been shown to bind heparin, have an intrinsic ability to bind other GAG types, although only weakly in some cases.

1.3.3 Conformational change of protein

The binding of heparin to proteins is often accompanied by a conformation of the protein concerned. The induction of a conformational change on the binding of GAG's may be of functional importance. The conformational change in the case of some serpins is related to their function (Gettins et al 1993). The binding of heparin to antithrombin III brings about a conformational change and increases the rate of inhibition of thrombin by antithrombin III.

Conformational changes have been studied by a number of model systems. The changes in conformation of polylysine upon binding GAG's has already been discussed in Section 1.1.3.6. The interaction of mixed polypeptides poly(lysine:tyrosine, 1:1) and poly (lysine: phenylalanine, 1.4:1) has been characterised using CD technique (Stone and Epstein 1977). The induced conformation of the two polypeptides is different. The polylysine-phenylalanine copolymer forms an alpha helix after binding heparin. Whereas the lysine-tyrosine copolymer formed a beta sheet. This was the first demonstration that the character of the induced conformation depended of the sequence of the polypeptide chain.

A peptide model of the heparin binding site of antithrombin III has been synthesized (Lellouch and Lansbury 1992) and the interaction with three sulphated polysaccharides with this peptide was monitored by CD spectroscopy. As a negative control a random peptide with the same AA composition, but with the basic residues evenly distributed around the helical cylinder was synthesized. The peptide was predicted to be α-helical using the secondary structure predictive protocol of Chou and Fasman (Chou and Fasman 1978). Both peptides had no detectable secondary structure when alone, but ATIII (123-139) when complexed with polysaccharide had induced secondary structure (Table 1.5). The strength of the complex was measured by monitoring the elipticity at 217nm with increasing salt concentration. The concentration required for 50% dissociation was measured. The complex was found to be saturatable. The increasing charge density of the sulphated polysaccharide, was

paralleled by an increased salt concentration required for 50% dissociation of the complex. The conformational behaviour of these peptides from apolipoprotein B and E upon binding heparin has also been studied (Cardin et al 1989, 1991). The results are outlined in Table 1.5

The formation of beta sheets in murine serum amyloid A protein (SAA) after binding heparan sulphate has been related to the development of amyloid deposits. Murine SAA levels increase up to one thousand times during the first twenty four hours of inflammation. The conformation of two closely related SAA isoforms (SAA_1 and SAA_2) has been studied by the use of CD spectroscopy (Mc Cubbin et al 1988). SAA_2 is the precursor to the amyloid deposits of this disorder, whereas SAA_1 is not. The changes in the CD spectra of both proteins after binding chondroitin sulphate, heparan sulphate and heparin were studied. The main elements of the structure of both proteins in the absence of GAG are beta sheets and beta turns. Binding of heparan sulphate to SAA_2 increases the proportion of beta sheets at the expense of the random structure, whereas the structural element of SAA_1 was essentially unchanged. A strain of mice resistant to amyloidogeneis has been characterised (de Beer et al 1993). The resistance of this strain is not due to a lack of SAA synthesis, rather it is the existence of a new SAA isoform. The new isoform had elements of both SAA_1 and SAA_2. SAA_1 differs from SAA_2 in only nine of its 103 amino acids. The new isoform differs in only six positions. This new isoform fails to undergo the characteristic increase in beta sheet after binding heparan sulphate proteoglycans. Since the binding of heparan sulphate to SAA_2 has been shown to be a prerequisite for the formation of a beta sheet. The resistance of this strain of mice to the development of amyloidosis and the lack of beta sheet formation in SAA after binding heparan sulphate is perhaps related.

The binding of GAG's to peptides can also lead to changes in the conformation of the peptide chain, but does not necessarily increase the established secondary structures. The conformational changes of a peptide derived from the von Willebrand factor associated with the binding of heparin have been studied (Sobel et al 1992). The free peptide displays a spectrum typical of a peptide containing mostly

beta sheet and beta turn element, 5% beta turn, 60% ß-sheet, 10% α-helix, and 25% random coil. After binding of heparin the spectral envelope is displaced towards higher wavelengths. Analysis of the spectra did not indicate any significant change in the proportion of the secondary structure. However displacement of the spectra is consistent with a conformational change in the peptide after binding heparin.

1.3.4 Examples of GAG binding peptides

Synthetic peptides derived from thrombospondin (Guo et al 1992) are potent inhibitors of heparin binding to thrombospondin. These peptides are unusual in two respects. They lack the postulated consensus sequences for heparin binding. Secondly and more importunately they typically contain only one basic amino acid. The three type I repeats in the N terminal domain of thrombospondin all inhibited heparin binding. The optimum consensus sequence for binding was defined as SXWSPWXS. These peptides were also shown to inhibit heparin binding to apolipoprotein E and laminin. The interaction between these peptides and heparin was demonstrated directly by application of the peptide to a heparin affinity column, requiring 0.13 to 0.18 molar salt for elution. This consensus sequence for binding is preserved in several other superfamilies, notably the cytokine receptor

superfamily and the transforming growth factor beta superfamily. The structural requirement for heparin binding in the consensus peptide has been studied (Guo et al 1992). Synthetic peptides corresponding to variant of the consensus sequence were made. Substitution of the first tryptophan in the most highly active sequence (SHWSPWSS) resulted in a complete loss of activity. The serine residue following the first tryptophan was established to be essential, along with the fifth residue, proline.

1.4 Scope of this study

The experimental work forming the conceptual basis of this thesis is divided into two parts. The interaction of GAG's with polylysine in solution has long been known. Indications are that it may provide the basis of a novel separation technique. The

Table 1.5: Influence of Polysaccharide binding on peptide conformation

Peptide	Polysaccharide	% α-helix	% ß-sheet	$[NaCl]_{0.5}$	Stoichiometry	Reference
Antithrombin III (123-139)	Heparin	8	80	0.6	20	Lellouch and Landsbury 1992
	Dextran sulphate	6	51	0.6	8	
	C6S	23	35	0.2	20	
Apo E 129-139	peptide alone peptide + heparin	20 49	5 <1	0.35	nd	Cardin et al 1989
Apo B 3345-3381	peptide alone peptide + heparin	10 34	28 15	-	nd	
Apo E 202-243	peptide alone peptide + heparin	11 9	16 67	0.2	nd	Cardin et al 1991

ND: not determined

binding of GAG's to defined sequences in proteins is related to the diverse biological function of GAG's. Bioaffinity chromatography has been used to separate proteoglycans but little work has been performed of the fractionation of free GAG chains. To further understand the binding of GAG to protein, the binding behaviour of two peptides to GAG's was examined.

The behaviour of immobilised polylysine in the separation of GAG's has so far been less than satisfactory (Suzuki and Koide 1984a and 1985b). It is theorized that the changes in the conformation the polylysine chains are the operationally important part of the separation of GAG's using immobilised polylysine. Firstly immobilised poly-l-lysine columns with the varying lengths of the poly-L-lysine chain were synthesized. This was achieved using published (Englebretsen and Harding 1991, 1992, 1993, 1994a, 1994b and 1994c) and in house solid phase peptide synthesis (SPPS) technology, whereby lysines were coupled one at a time in a stepwise fashion to a solid support. The resulting lysine chains were then deprotected but not cleaved from the matrix. Thus the maximum confidence is achieved concerning the nature of the immobilised species. Lengths of 4, 8 and 12 amino acids were chosen as initial target resins to be used to make comparisons on the binding of different GAG classes. These columns were then examined for their GAG binding ability, with particular reference to their binding affinities for chondroitin sulphate, dermatan sulphate, and heparin. The binding behaviour of these resins was directly compared to the solution binding behaviour in terms of the binding strength of DS and heparin (relative to chondroitin sulphate) and the stoichiometry of the interaction. As a control of the binding behaviour of these resins, a full length PLL chain (with 633 residues) was immobilised in a directed manner. The solution binding behaviour of the K_8G peptide along with two lengths of PLL (with 126 and 633 residues) to the GAG standards in terms of the conformation and the stoichiometry of the interaction was also studied.

Two peptide sequences from GAG binding proteins have been identified as potential candidates for further peptide GAG interaction work. These were the most active heparin binding peptide from thrombospondin (Guo et al 1992) and the peptide

fragment of protease inhibitor C (Pratt and Church 1992). The sequences of these peptides are shown in Table 1.6. In general these peptides have been shown to bind to a variety of GAG types with varying affinities and are of defined sequences. Although the binding affinities of these peptides for the various GAG types are not known, the affinities were postulated as being widely different. These three peptides were separately synthesized using published Separation Science Program (SSP) technology. The interaction of these two peptides PCI (264-283) and thrombospondin with the three GAG standards was examined to determine the dominant secondary structure induced upon binding the GAG. The strength of the interaction between the peptide and DS and heparin was also determined.

Table 1.6: Free peptides synthesized as part of this thesis

Peptide origin	Sequence	Reference
Polylysine based	K_8G	This thesis
Protease inhibitor C residues 264-283	SEKTLRKWLKMFKKRELEEY	Pratt and Church 1992b
Heparin binding peptide from Thrombospondin	SHWSPWSS	Guo et al 1992

To understand the binding behaviour of both the PLL chains resins and the three peptides synthesized. Three GAG standard (CS, DS and Heparin) were prepared by classical techniques were characterised. The use of pure GAG's with defined properties simplified the analysis of the binding behaviour of the K_xG resins, the PLL resin, and the three peptides synthesized (Table 1.6).

The binding behaviour of a number of GAG binding peptides described in the literature was critically examined and as a result two complementary models were proposed by the writer. The two models rationalise different aspects of the binding behaviour. The first model a stereochemical model is able to rationalise the dominant secondary structure that is induced upon binding GAG's. The second model based on Cardin and Weintraub's consensus sequences (Section 1.3.2) indicated the existence of two correlation (one for each of the consensus sequences)

between an attribute derived from the amino acid sequence and the binding strength of the interaction.

CHAPTER TWO: GAG STANDARDS

2.1 INTRODUCTION

The binding behaviour of a subset of all the GAG classes was attempted in this thesis. The majority of the biological functions of GAG's is carried out by five of the seven GAG types. These are chondroitin-4-sulphate, chondroitin-6-sulphate, dermatan sulphate, heparan sulphate and heparin (Section 1.1.2). Since sizable samples of heparan sulphate were not available to the writer, the binding behaviour of this material was not pursued. Samples of all of the remaining GAG classes were available for this study.

To be able to fully characterise the binding behaviour of GAG's to either chromatographic resins or peptides, pure samples of GAG's of known properties **must** be used. However as discussed in Chapter 1 (Section 1.1.1.2) the existence of heterogenous disaccharide repeat sequences and the polydisperse nature of these molecules, complicates the determination of GAG purity. A number of criteria were evaluated to establish the minimum purity of a particular GAG fraction. If a GAG sample fulfilled the majority of the above criteria it was regarded as being of sufficient purity to warrant its use in binding experiments. These criteria were:

1. The presence of a single band on cellulose acetate electrophoresis, using the barium acetate ethanol precipitation method (Cappelletti et al 1979a and 1979b).

2. The determination of the optical rotation of a sample of each of the GAG should be of comparative value to literature values of each of the GAG types.

3. Appropriate enzymatic breakdown behaviour i.e. for dermatan sulphate is broken down by chondroitinase ABC (which degrades C4S, C6S and DS) but not chondroitinase AC (which degrades C4S and C6S).

4. The samples must be homogenous on the basis of C^{13} NMR spectroscopy i.e. no

evidence for the existence of contaminating GAG's within the sample.

5. Determination of the average charge density (i.e. the sulphate to carboxyl ratio) of the GAG chains.

6. Determination of the mean molecular weight and the molecular weight distribution of each sample must be determined to be able to compare the results of different GAG binding studies.

The two absolute methods of measurements of molecular weight of GAG's are sedimentation by ultracentrifuge and light scattering. Both of these methods were unavailable for this study. However published correlation between viscosity and molecular weight was used for standardization of molecular weight. The absence of suitable molecular weight standards for the calibration of gel filtration of GAG's has prompted several authors to make their own (Melrose and Ghosh 1993, Gigli et al 1992). The process involves the separation of GAG into size classes by gel-filtration, followed by measurement of their molecular weights. An empirical relationship exists between the intrinsic viscosity of GAG solution and the polymers molecular weight. It is termed the Mark-Houwink relationship (see equation 2.1).

Equation 2.1: $n = KM^{\alpha}$

where: n is the intrinsic viscosity, M is the molecular weight, and K and α are empirical constants. The exact values of K and α depend on the GAG class and the buffer used. These have been measured for each GAG class (Table 2.1).

Several fractional precipitation techniques have been introduced over the years for the preparation of pure GAG fractions. These are as follows: alkaline copper precipitation of dermatan sulphate (Jeanloz 1965), potassium acetate precipitation of heparin (Scott 1968) and ethanol precipitation of calcium salts of GAG's (Meyer et al 1956). Preliminary experiments using each of these methods were performed to determine which of the above methods would fractionate GAG mixtures into

fractions pure enough for use in this study.

Table 2.1: Constants for Mark-Houwink Equation

GAG	Buffer	K X 10^4	Exponent
C4S/C6S	0.2 M NaCl in 0.15 M Phosphate buffer pH 7.0	3.1	0.74
DS	0.2 M NaCl in 0.15 M Phosphate buffer pH 7.0	3.1	0.74
Heparin	0.5 M NaCl	0.355	0.90

Approximate molecular weight range 10^4 to 5 X 10^4
Source: Roden et al 1972

2.2 MATERIAL AND METHODS

2.2.1 Equipment

The following equipment was supplied by Biorad (Hercules, California USA): a computer controlled electrophoresis power supply (model 3000Xi), horizontal electrophoresis cell fitted to a refrigerated recirculator (model 4860). Sample applicators (code number 18-1618-01) were supplied by Pharmacia (Uppsala, Sweden). A Amicon ultrafiltration membrane (YM2 i.e. has a 2 kdaltons MW cutoff) and a 50 ml stirred ultrafiltration cell were both supplied by New Zealand Medical and Scientific Limited (Auckland, NZ). Titan III cellulose acetate plates of dimensions 70 x 60 mm were supplied by Helena laboratories (Beumont, Texas USA). An AA-100 polarimeter (optical rotation meter) was supplied by Optical activity Ltd (Ramsey, England). A Cannon-Fenske routine viscometer was supplied by John Morris Scientific Ltd (Auckland, NZ). A Stopwatch capable of reading 0.1 seconds was used in this study. A thermostated water bath (temperature control to within 0.1 ^{0}C) was used in this study.

2.2.2 Chemicals

The following chemicals were obtained form Sigma: chondroitin sulphate A (C4S) from bovine Trachea (70% chondroitin 4 sulphate, remainder chondroitin 6 sulphate), Dowex 50x2-100 ion exchange resin, sodium citrate and D-glucuronic acid. The GAG degrading enzymes chondroitinase AC lyase from Arthrobacter aureus and chondroitinase ABC lyase from Proteus vulgaris were also obtained from Sigma (St Louis USA).

The following GAG samples were obtained from New Zealand Pharmaceuticals (Linton, NZ): sodium heparin from pig intestinal mucosa (batch 2288T03), mucopolysaccharide from pig intestinal mucosa (batch 13088, type 1271): a GAG mixture containing both chondroitin sulphates and dermatan sulphate, and an extract of mucosa from pig intestinal mucosa (batch 2516): a GAG mixture containing both chondroitin-4-sulphate (and 6-sulphate) and dermatan sulphate.

The following chemicals were supplied by BDH (Palmerston North, NZ): Toluidine Blue, Alcian Blue, Phenol Red, concentrated sulphuric acid (high grade purity), anhydrous copper sulphate, sodium carbonate and sodium 3-trimethylsilyl propane sulphonate (spectroscopic grade). Deuterium oxide and meta-hydoxyldiphenyl were supplied by Aldrich (St Louis, MO, USA). Sodium tetraborate manufactured by Reindel-de Haen was supplied by Scientific Supplies Limited (Auckland, NZ).

2.2.3 Preparative GAG fractionation procedures

2.2.3.1. Calcium salt ethanol fractionation

The procedure is essentially that of Meyer's (Meyer et al 1956) with some modifications. The GAG mixture to be fractionated was dissolved in a five percent (w/v) calcium acetate solution containing acetic acid (0.5 M) typically to a level of 5 mg/ml. Fractional precipitation was performed in three steps of 20, 30, and 40 percent ethanol. After sufficient ethanol was added to bring the ethanol

concentration to the required level, the resulting mixture was allowed to stand for twenty four hours at 4°C. The precipitate was recovered by centrifugation at 17k g for ten minutes. The supernatant was retained for the next stage in the procedure. The precipitate was washed twice with 95% ethanol and dried by washing with diethyl ether. After standing in a vacuum desiccator overnight, under vacuum over phosphorus pentoxide, the precipitates from each stage were retained for further analysis.

2.2.3.2. Calcium salt to sodium salt conversion

A solution of the calcium salt was passed down a strong acid cation exchange resin (Dowex 50W) in its hydrogen form, to effect the conversion of the GAG fraction to the acid form. Less than one and half milligrams of the salt was added per ml of resin. Fractions containing dermatan sulphate were pooled and the pH adjusted to 7 with 1M NaOH. The resulting solution was freeze dried. To check that the conversion had taken place, GAG samples before and after treatment were dissolved in distilled water (typically 0.5 mg/ml). Calcium levels were determined by atomic absorbtion spectroscopy in the analytical facility of the Department of Chemistry and Biochemistry of Massey University.

2.2.3.3. Selective precipitation of heparin

The selective precipitation method patented by Scott and coworkers (Scott et al 1968) was used with some modifications. A solution of a GAG mixture containing heparin (10 mg/ml) was added to an equal volume of 4M potassium acetate (pH 5.7) and allowed to stand for one hour at 0°C. The precipitate was recovered by centrifugation at 12k g for ten minutes. To recover the remaining GAG, two volumes of 95% ethanol were added to the supernatant and the solution was stood over night at 4°C. The resulting precipitate was recovered by centrifugation at 12k g for ten minutes. Both of the recovered precipitates were separately washed with ethanol twice, and then washed with diethyl ether. The samples were retained for analysis and chemical characterisation.

2.2.3.4. Alkaline copper precipitation

The procedure involves the use of Benedicts solution the preparation of which is described below:
Solution A: 1.73 grams of copper (II) sulphate was dissolved in 100 ml of milli Q water. Solution B: 17.3 grams of sodium citrate and 10 grams of sodium carbonate were dissolved in 80 ml of milli Q water. Both solutions were mixed and made up to volume in a 1 litre volumetric flask. The solution was stable for up to a week at room temperature.

This method is essentially that described by Jeanloz (Jeanloz 1965) and is briefly outlined here. A 10 mg/ml solution of GAG was mixed with saturated sodium hydroxide and Benedicts solution in the ratio of 10:1:8. This solution was allowed to stand at room temperature for fifteen minutes with intermittent shaking. The precipitate was recovered by centrifugation and washed with a minimum volume of 2M sodium hydroxide containing 0.5 volume of Benedicts solution. The precipitate was dissolved in a minimum volume of acetic acid and precipitated with five volumes of glacial acetic acid, washed with 95% ethanol and diethyl ether. The samples was retained for characterisation.

2.2.4 Characterisation of GAG samples

2.2.4.1. Cellulose acetate electrophoresis

This analytical procedure for the identification of components in a GAG mixture is essentially the method described by Cappelletti and coworkers with some modifications (Cappelletti et al 1979a, 1979b). The modifications were the alteration of the ethanol concentrations (D McKay, NZP personal communication) in the soak buffers and the use of a cooling plate during electrophoresis instead of decane and crushed ice.

The electrophoresis tank buffer used was 1.0 M barium acetate pH 5.0. The

following soak buffers were used: 0.1 M barium acetate pH 5.0, 0.1 M barium acetate pH 5.0, 3% ethanol and 0.1 M barium acetate pH 5.0, 20% ethanol. The stain solutions used were: 0.1% toluidine blue in 1% acetic acid and 0.1% Alcian blue in 1% acetic acid. A tracking dye solution of 5% phenol red was also used in the analysis

Pretreatment of the plates: cellulose acetate plates were immersed at one end for two to three seconds in distilled water to a height of 1.5 cm. The plate was then immediately blotted between two sheets of filter paper. The opposite end was then immersed in the 0.1 M barium acetate solution, not reaching the wet zone of the previous immersion, leaving a narrow band (2-4mm wide) visibly dry between water and buffer.

GAG samples were dissolved in milli Q water (typically 10 mg/ml) and diluted with an equal volume of tracing dye solution. This solution was applied in the dry zone on plate using a sample applicator. This procedure allowed the application of known volumes (usually 1 µl was sufficient) onto the plate.

The plate was then placed in the electrophoresis chamber of the flat bed electrophoresis system and electrophoresed for 5 minutes at a constant voltage of 100 volts. During the electrophoresis the chamber was cooled with a refrigerated recirculator set at 5^0C. At the end of this time the plate was removed from the chamber and soaked in 0.1 M barium acetate with 3% ethanol for several minutes. This effected the precipitation of any heparin that may be present. After blotting with filter paper, the plate was electrophoresed for 40 min at a constant voltage of 100 volts. The plates were then removed and soaked in a 20% ethanol solution, blotted and electrophoresed for a final 30 min.

Staining procedure: The plates were first soaked in the toluidine blue solution for 5 min, washed with water, then soaked in Alcian blue solution for 1 min. Destaining of the plates was effected by soaking in several changes of 1% acetic acid solution. The plates were then air dried for photography and storage.

2.2.4.2 Optical rotation measurements

The optical rotation of GAG samples were determined by measuring the rotation of GAG solution (typically 3 to 5 mg/ml) at 589 nm, using a ten centimetre pathlength cell. All determinations were performed at 22°C. Typical values for each GAG class are shown in Table 2.2

Table 2.2: Typical Optical rotations of GAG classes

GAG Class	$[\alpha]^{20}_{D}$
Hyaluronic Acid	-70 to -80
C4S	-28 to -33
C6S	Slightly lower
DS	-60 to -70
Heparin	+48
Heparan sulphate	+38 to -78

Source: Kennedy 1978

2.2.4.3. Chondroitinase ABC and AC lyase digestion

Reagents: 30 mM HCl, chondroitinase ABC lyase 5 units/ml, chondroitinase AC lyase 5 units/ml. Concentrated digestion buffer: the buffer (at five times the strength used in the digestion mixture) was made up as follows: Tris 0.25 M, sodium acetate 0.180 M, NaCl 0.25 M, 0.5% bovine serum albumin pH 8.00.

A sample of GAG solution 60 µl (typically 10 mg/ml) was mixed with 30 µl of water, 30 µl of the chondroitinase ABC solution and 30 µl of concentrated buffer solution. All digestions were performed in duplicate. Positive and negative controls were used during each digestion. Negative control consisted of the digestion mixture minus the enzyme. The positive control was a chondroitin sulphate sample (CSA from Sigma) which both enzymes were able to digest. The mixture was incubated at 37^{0}C. The reaction was monitored by taking 10 µl samples at various time intervals diluting them with 0.99 ml of 30 mM HCl and reading the absorbance of the diluted

aliquots at 232 nm. The depolymerization of the sample was judged to be complete when the absorbance levelled off at a constant value. The final mixture was stored frozen for electrophoretic analysis.

Chondroitinase AC lyase digestions were performed in a similar manner except that samples containing dermatan sulphate were treated with 60 µl of enzyme solution and water was omitted from the digestion mixture. This was done as dermatan sulphate is known to inhibit the activity of chondroitinase AC lyase. As an additional internal control for the chondroitinase AC lyase digestion, dermatan sulphate with a small amount of chondroitin sulphate contamination (DS from an earlier stage of the purification) was used in the digestion procedure.

2.2.4.4. C^{13} NMR spectroscopy

A 10% (w/v) solution of the GAG in deuterium oxide was prepared for C13 spectroscopy at the NMR facility of the Physics and Biophysics Department of Massy University. The proton decoupled C^{13} NMR spectra at 270 MHz were recorded on a JEOL 270 spectrometer fitted with a 5mm probe. Because of the high viscosity of the solution, the spectra were recorded at 60^{0}C to reduce the line widths. The pulse width used was 3.5 µsec, sensitivity enhancement was 16 or 17, and the acquisition time was 0.511 or 0.603 seconds. Depending on the GAG sample, between 12 to 25 thousand scans of the solution were performed to average the spectra. Chemical shifts were measured with reference to an external standard, sodium 3-(trimethylsilyl)-1-propanesulphonate.

2.2.4.5. Elemental analysis

To facilitate the calculation of the charge density (i.e. ratio of sulphate to carboxyl group) of the purified GAG samples, the percentage of nitrogen and sulphur were measured by elemental analysis. Dried samples of each GAG was submitted to the micro analytical service in the Chemistry Department of the University of Otago.

2.2.4.6 Uronic acid assay

The concentrations of the GAG solutions used in the viscosity studies (Section 2.2.4.8) were determined by uronic acid levels (Blumenkrantz and Ashoe-Kansen 1973) and converted to GAG concentration with the relevant conversion factor. The assay involves the reaction of m-hydroxyldiphenyl with the unstable acid-hydrolysed dehydrated derivative of hexuronic acid.

Reagents: 0.15% m-hydroxyldiphenyl in 0.5% NaOH, 0.0125 M sodium tetraborate in concentrated H_2SO_4, and 10 mg/ml D-glucuronic acid solution

1.2 ml of sodium tetraborate reagent was added to 0.2 ml of chilled GAG containing samples (containing 0.5 to 20 µg GAG). The tubes were then heated at 100°C for 5 min, and cooled on ice for several minutes. To each tube 20 µl of m-hydroxyldiphenyl solution was added, and the absorbance at 520 nm was read within 5 min. A 0.2 ml sample of 0.5% NaOH was used as a blank.

2.2.4.7 Dimethylmethene blue assay for GAG's

The concentration of GAG's was measured by the dimethylmethene blue assay (Farndale et al 1986). The method is based on a metachromatic increase in absorbance of the dye after binding sulphated GAG's. Other polyanions such as hyaluronic acid and DNA do not interfere under the assay conditions.

The dye solution was prepared by dissolving 8 mg of dimethylmethene blue in 10 ml of 95% ethanol and added to a solution of 3.04 g of glycine, 2.37 g of sodium chloride and 95 ml of 0.1M HCl in 900 ml of milli Q water, then made up to volume (1 L).

100 µl of sample is added to 2.5 ml of the dimethylmethene blue solution and mixed. The absorbance of the solution is measured at 525 nm within 1 min of mixing. The assay could be turned into a quantitative assay by the use of pure GAG standards.

2.2.4.8 Intrinsic viscosity determination

The viscometer was cleaned with 1M KOH in 50% ethanol (filtered), washed out with several changes of distilled water and oven dried. GAG samples were dissolved in the relevant buffer (Table 2.1). The viscometer was clamped inside a water bath equilibrated to 25 ^{0}C. After ensuring that the viscometer was vertical, 2.5 ml of buffer was added to the viscometer. After allowing time for the temperature to equilibrate, a rubber tube was attached to the right hand arm of the viscometer and the solution sucked to above the top mark. The time taken to vertically drop between the two marks was measured using a stopwatch. Readings were repeated until the average deviation from the mean was less than 0.1 percent. An aliquot of the GAG solution (0.5 ml) was added to the viscometer and the procedure repeated. Further aliquots of the GAG solution were added and the efflux times for the different concentrations of GAG were measured. To accurately measure the concentration of the GAG solution, the uronic acid levels of the GAG solution were measured using the m-hydroxyldiphenyl assay (Section 2.2.4.6).

Viscosity data analysis

The ratio of the times for each sample with respect to the buffer (relative viscosity) is converted into the specific viscosity by subtracting one. The specific viscosity divided by the solutions concentration is plotted versus the concentration (in g/100 ml). A regression line is fitted to the results. The y intercept is the intrinsic viscosity. The Mark-Houwink relationship for the GAG (Table 2.1) was then used to estimate the samples molecular weight.

2.2.4.9 Iduronic-2Osulphate assay

The percentage of Ido2OS in fast and slow heparin was estimated by the alkali-induced optical rotation assay (Piani et al 1993). Under the conditions outlined by the authors, αL-iduronic acid 2-O-Sulphate undergoes a selective epoxidation reaction between C2 and C3 of this residue. The formation of this epoxide residue in

heparin and heparan sulphate chain is accompanied by a large increase in the optical rotation of the sample.

A 4% solution of fast or slow heparin in 1 M NaOH was heated at 60°C for 210 min. At the end of this time the solutions were neutralized and salt was removed by repeated ultrafiltration followed by dilution, using a YM2 membrane. The process was repeated three times. The solution was then freeze dried. Optical rotations of the fast and slow heparin before and after epoxidation were then measured. The proportion of Idu2OS was then measured using the correlation (equation 2.2) established by the authors.

Equation 2.2: % Idu2OS = Optical rotation increment X 1.72

2.3 RESULTS AND DISCUSSION

2.3.1 Alkaline copper precipitation

The alkaline copper precipitation method was performed on GAG mixtures (mucoid). Results for this procedure were somewhat disappointing. The procedure was attempted three times but in each case chondroitin sulphate coprecipitated with the dermatan sulphate (data not shown). To examine the purity of the precipitated samples, the cellulose acetate electrophoretic analysis was performed using heavily overloaded samples (with 20 µg loadings).

The method is not as specific for dermatan sulphate as is commonly believed. Dermatan sulphate from a variety of sources: livers from hog, rat, rabbit and beef spleens from hog, rat, and dog and hog skin have been isolated (Poblacion and Michelacci 1986). The isolation was performed with 0.5 M and 2 M KOAc pH 5.7, along with the alkaline copper procedure. It was found that **only** hog-liver dermatan sulphate could be specifically precipitated using this technique. As a result of these results the alkaline copper precipitation methods was not used in this study to fractionate GAG mixtures.

2.3.2 Ethanol precipitation of calcium salts

Preliminary ethanol fractionation experiments were performed on two GAG mixtures containing dermatan sulphate. Each step of the purification was monitored by cellulose acetate electrophoresis and optical rotation. The detection limit for GAG's for the staining procedure is quoted as being 1-2 ng/ band (Cappelletti et al 1979b). The first two steps of the fractionation did not result in completely pure GAG fractions and consequently these fractions were refractionated. On the basis of these experiments one of the GAG mixtures (viz mucopolysaccharide NZP batch 13088 type 1271) was established to be the richer source of dermatan sulphate. Following small scale experiments to validate the procedure, larger scale fractionation were performed on mucopolysaccharide sample (four gram). Cellulose acetate electrophoresis (Figure 2.1) with large sample loading (20 µg) showed that the 20% ethanol fraction (lane 2) was essentially pure dermatan sulphate. However to ensure complete purity, the samples were refractionated again. The refractionated samples gave a single band on electrophoresis (lane 3). The 30% fraction (lane 5) was a mixture of chondroitin and dermatan sulphate. The 40% fraction (lane 8) also appeared to be a mixture of dermatan sulphate, chondroitin-4-sulphate and, chondroitin-6-sulphate. Refractionation of the 30% sample did not result in a homogenous GAG preparation (lanes 6 and 7). A summary of the large scale experiment showing the yields obtained and the optical rotations, is outlined in Table 2.3. The fractional precipitation behaviour of the mucopolysaccharide sample was similar to the fractionation of GAG from whale cartilage (Habuchi et al 1973). The final step of the procedure, the conversion of the calcium salt to the sodium salt of dermatan sulphate using the method outlined in section 2.2.3.2 reduced calcium levels from 9.8 % to 0.13%.

The optical rotation of the final dermatan sulphate sample was slightly lower than the literature value (column 6 Table 2.3). The lower value could be an indication that the glucuronic acid levels may be higher than typically expected. As a comparison the optical rotation of the chondroitin sulphate sample (CSA, Sigma) was measured as -20.6°. Dermatan sulphate from mucosal sources (like the source used in this

study) typically contains lower amounts of glucuronic acid when compared to dermatan sulphate isolated from pig skin, 1-3% compared to 15-20% respectively (Mascellani et al 1993). The results of the electrophoretic analysis for the mucoid sample are shown in Figure 2.2 (lanes 4 to 7). As can be seen the procedure gave similar results to the mucopolysaccharide sample. The fractional precipitation of the calcium salts of the mucopolysaccharide sample, using ethanol, as a result was chosen as the method used to prepare the dermatan sulphate sample used in this study.

Figure 2.1: Electrophoretic analysis of Calcium ppt Technique

Legend: Lanes 1-8; lane 1: Mucopolysaccharide, lane 2: 20% EtOH ppt, lane 3: 20% EtOH ppt refractionated in 20% EtOH, lane 4: 20% EtOH ppt refractionated in 30% EtOH, lane 5: 30% EtOH ppt, lane 6: 30% EtOH ppt refractionated in 20% EtOH, lane 7: 30% EtOH ppt refractionated in 30% EtOH, Lane 8: 40% EtOH ppt. All samples had 20 µg.

Table 2.3: Preparative precipitation of calcium salts

Percent Ethanol	INITIAL Weight	$[\alpha]_D$	REFRACTIONATED Weight	$[\alpha]_D$	$[\alpha]_D$
Twenty	1.8444	-50.3	1.3643	-51.8	-60
Thirty	0.8425	-37.3	0.0313	-42.7	-51
Forty	0.1249	-18.0	-	-	-19

Legend: Source of results in column 6, Habuchi et al 1973

2.3.3 2M KOAc, pH 5.7 precipitation

Heparin samples can be separated into two forms using electrophoresis: slow moving and fast moving heparin. These two forms are different in terms of sulphation level and molecular weight. Fast heparin is less sulphated and has a lower molecular weight compared to slow heparin (Volpi 1993a and 1993b). The slow moving heparin was precipitated by the Scott procedure (Scott et al 1968) whereas the residual fast moving heparin required the addition of ethanol to the supernatant to effect its precipitation. To assess the purity of the recovered GAG fractions, cellulose acetate electrophoresis and optical rotation readings were performed. A results of these experiments are outlined in Table 2.4.

As can be seen from the results the total yield of the fractional precipitation procedure was less than the initial weight. This is a common problem with fractional GAG precipitation procedures in that the final yield is always less than 100%, since some GAG is always left in solution. Electrophoretic analysis (lanes 1-3, Figure 2.2) of the initial heparin sample, and the fractions from the precipitation procedure demonstrated that it was able to cleanly separate fast (supernatant) and slow (ppt) heparin. Assuming that the solubility of slow and fast heparin under the conditions used to precipitate them was similar, the proportion of slow and fast heparin in the starting material can be estimated as being 53% and 47% respectively. Using these proportions and the optical rotations for slow and fast heparin, the optical rotation of the original unfractionated heparin could be calculated, as being 39°. It compares favourably to the measured value of 39.4°.

The optical rotation of the slow and fast heparin are different. This is perhaps initially surprising since the published optical rotation for slow and fast heparin (Volpi et al 1993a), purified by precipitating the barium salts at room temperatures, were similar (approximately 50°). However the source of heparin was different. Pig intestinal mucosal heparin was used in this study compared to bovine intestinal mucosa for the published study. Since differences in the composition of heparin from different species and tissue sources are well known, particulary between beef

lung and pig mucosal heparin (Casu 1985), the difference in optical rotation are perhaps not surprising.

Table 2.4: Heparin fractionation

	Sample weight (mg)	$[\alpha]_D$
Heparin	500	39.4 (0.50)
Slow moving	172	46.5 (0.75)
Fast moving	192	29.9 (0.25)

Legend: Errors in optical rotation determinations are shown inside brackets

Figure 2.2: Electrophoretic analysis of GAG fractionation procedures

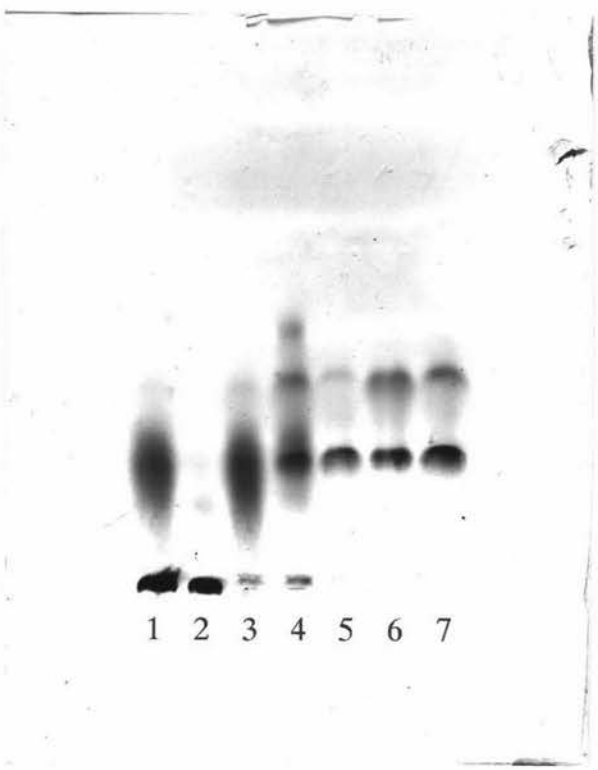

Legend: Lanes 1-3 Heparin fractionation: lane 1; NZP Heparin, lane 2; 2M KOAc ppt, lane 3; 2M KOAc supernatant
Lanes 4-7 Mucoid fractionation: lane 4; Mucoid, lane 5; 20% EtOH ppt, lane 6; 30% EtOH ppt, lane 7; 40% EtOH ppt. All samples were 20µg loadings.

2.3.4 Characterisation of GAG samples

2.3.4.1 Enzymatic digestion

The identity of the purified dermatan sulphate sample was confirmed by the examination of the enzymatic breakdown behaviour. Two assays were used to characterise the degradation of the two galactosaminoglycan samples (i.e. CS and DS) with the chondroitin lyases ABC and AC. These were:

- The progress of the digestion was monitored by measurement of the absorbtion of diluted aliquots of the reaction mixture at 232 nm.

- Final samples of the reaction mixture were subjected to cellulose acetate electrophoresis.

The products of the depolymerisation with chondroitinase ABC and AC lyase are typically disaccharides (if the reaction goes to completion) with 4,5-unsaturated uronic acid residues. These residues exhibit an intense absorbance maxima at 232 nm, allowing the reaction to be monitored spectrophotometrically. The specificity of the two enzymes is similar in that both attack the α 1,4- bond between N-acetyl galactosamine and uronic acid. Chondroitinase ABC lyase has a broad specificity and attacks this bond irrespective of the identity of the uronic acid.
However chondroitin AC lyase only attacks the α-1,4 linkages when the uronic acid is glucuronic acid. As a consequence of this it may partially degrade dermatan sulphate if it contains such linkages (i.e. if glucuronic acid are present). It is not known at present if sulphation of the disaccharides has any influence on the specificity of the enzymes.

In each digestion procedure positive and negative controls were used when examining the dermatan sulphate samples. Negative controls consisted of digestion mixtures with no enzyme added, whereas the positive controls consisted of chondroitin sulphate, which should be degraded by both enzymes. No significant

increase in the absorbance of the chondroitinase ABC lyase digestion blank was observed. Whereas the digestion of CS was complete within 2 hours (Figure 2.3a) as judged by the absorbance of the aliquots. Electrophoretic analysis of both the blank and enzymatic digestion of CS samples are shown in Figure 2.4 (Lanes 1 and 2) confirmed that the enzymatic digestion was complete at this stage. The digestion of DS by chondroitinase ABC lyase was complete within 4 hours (Figure 2.3b). Electrophoretic analysis of the reaction mixtures confirmed that degradation of DS was complete in the mixture containing enzyme (lanes 3 and 4 Figure 2.4).

Two sources of chondroitin AC lyase are available commercially. In each case the enzyme was extracted from a different microorganism: Flavobacterium heparium (ACI) and Anthrobacter aurecocus (ACII). Contrary to what is commonly believed, chondroitinase AC lyase can degrade dermatan sulphate, if dermatan sulphate contains glucuronic acid. The enzymatic activity of the two sources of AC lyase on dermatan sulphate has been studied (Gu et al 1993). However both of these lyases are inhibited by dermatan sulphate, particulary those rich in iduronic acid. This inhibition is sensitive to the buffer system selected, since inhibition is often reduced when salt is increased. For example chondroitinase ACII lyase from Anthrobacter aurecocus acts on C6S with a K_m of approximately 2 μM and is inhibited by dermatan sulphate with a K_i of 2 μM. Although full details about the optimum buffer system for AC lyase are not known, it was decided to use the same buffer system as was used for ABC lyase.

The situation with chondroitinase AC lyase digestion of the DS samples was more complex, than with the ABC lyase digestion. The enzyme was active since degradation of CS only occurred in the presence of enzyme. This degradation was complete within 3 hours (Figure 2.3b, lanes 5 and 7 Figure 2.4), as indicated by the time dependant increase in the absorbtion of the aliquots of the digestion. No significant increase of the absorbance of the diluted aliquots of the DS digestion mixture, was observed over the 4 hour course of the digestion (Figure 2.3b). Electrophoretic analysis indicated that the CS internal standard was not degraded (lanes 6 and 8 Figure 2.4) indicating that the activity of the AC lyase was possibly

being inhibited by dermatan sulphate. To minimize any inhibition the level of enzyme used in the depolymerisation reaction mixture was three times that used in a published study (Gu et al 1993). However the buffer system was different, Tris/acetate/NaCl versus sodium phosphate/ NaCl.

Figure 2.3a: Chondroitinase ABC lyase digestion

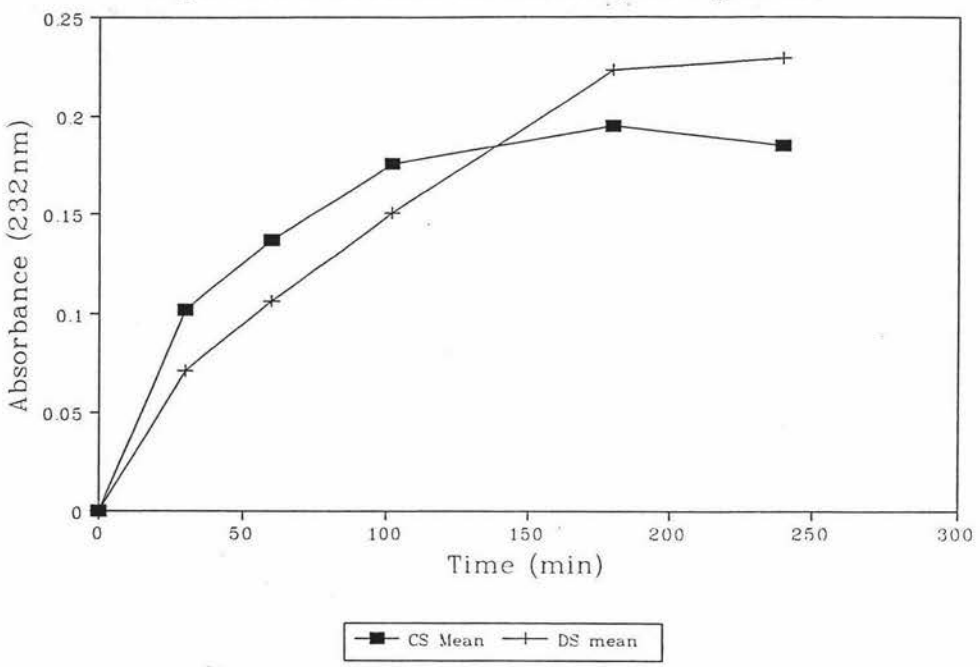

Figure 2.3b: Chondroitinase AC lyase digestion

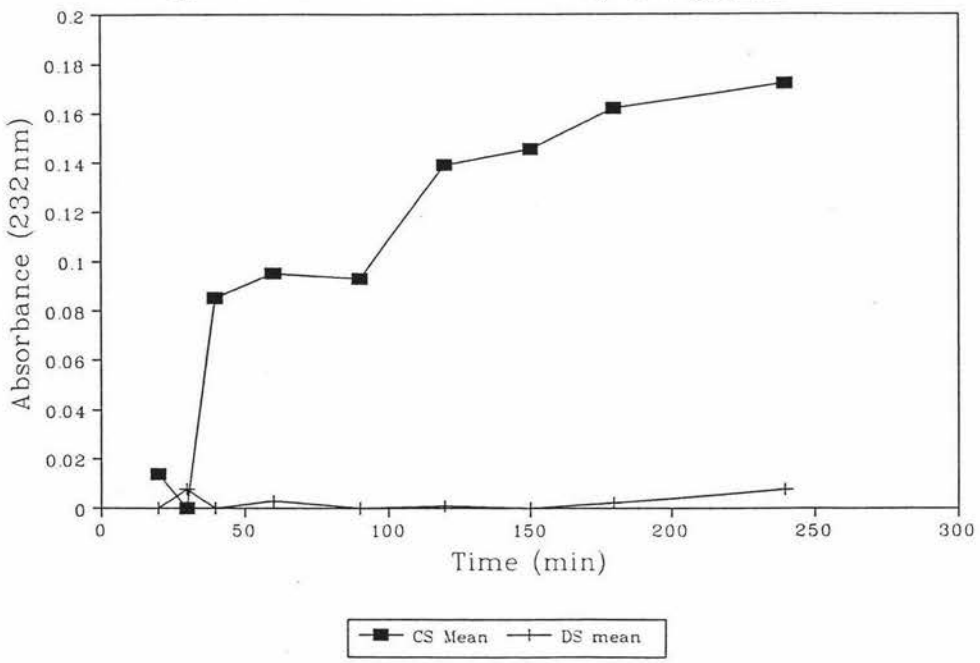

Taken together the results are consistent with the notion that the dermatan sulphate sample has a low level of glucuronic acid, less than 7%, the value established for the dermatan sulphate used in the comparative study (Gu et al 1993).

The identity of heparin samples was not established enzymatically since heparin lyases were unavailable to the writer. However the mobility of the heparin on cellulose acetate and the optical rotations were similar to literature values. The chondroitin sulphate sample used was a mixture of both chondroitin 4-sulphate and chondroitin 6-sulphate. Attempts to fractionate this sample into the separate classes were unnecessary under the terms of this study. This was because we were primarily interested in the binding behaviour of iduronic acid containing GAG's because of the important binding properties of these GAG's (Section 1.1.2).

Figure 2.4: Electrophoretic analysis of enzymatically degraded GAG standards

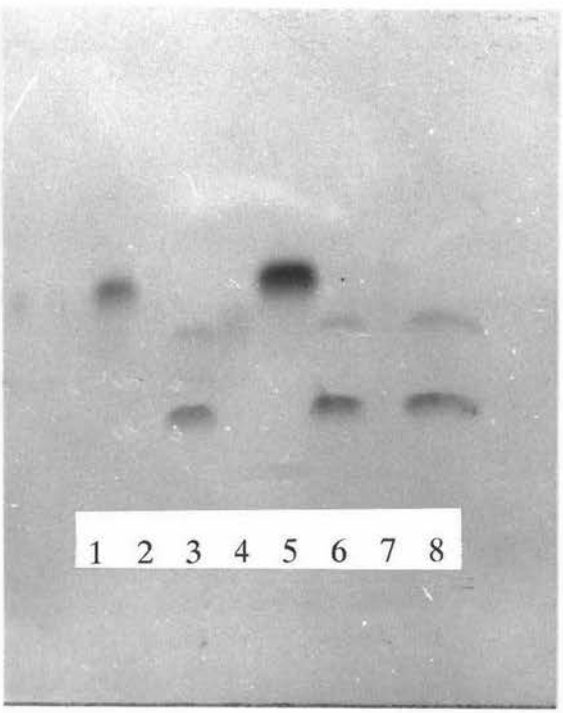

Lanes 1-4 Chondroitinase ABC lyase digestion: lane 1; CS blank, lane 2; CS enzyme degraded, lane 3; DS Blank, lane 4; DS Enzyme degraded. Lanes 5-8 Chondroitinase AC lyase digestion: lane 5; CS blank, lane 6; DS blank, lane 7; CS enzyme degraded, lane 8; DS Enzyme degraded.

2.3.4.2 C^{13} NMR Spectroscopy

C^{13} NMR spectroscopy provides an independent nondestructive method to examine the presence of individual GAG's within a sample. The spectral line widths are narrower when compared to proton NMR, allowing better resolution of the peaks. However it is only useful for identifying the major components of a mixture. The lower limit for detection of nonequivalent carbons is accepted as being 5% (Jenning and Smith 1980). C^{13} spectroscopy gives the number of nonequivalent carbon nuclei in a sample, since nonequivalent carbon nuclei give signals at different frequencies in C^{13} spectra. However under the conditions used in this study for measuring the C^{13} spectra of the GAG's can only be used to give qualitative data since the peak area cannot be used to estimate the ratio of the number of carbons for each peak. For quantitative work the spin lattice relaxation times must be measured and the spectra recorded with Nuclear Overhauser Effect (NOE) suppressed. It is well known that the spin lattice relaxation times of C^{13} nuclei at high temperatures may be sufficiently long enough to create difficulties in quantitative estimation (Gorin 1981). The main limitation of C^{13} NMR spectroscopy for GAG characterisation is that signal assignment often has to be made on the basis of chemical shift comparisons and the use of model compounds (Holme and Perlin 1989).

The 13 peaks observed in the C^{13} spectrum for the dermatan sulphate, purified in Section 2.3.2 (Figure 2.5a) sample were almost identical to published spectra for dermatan sulphate (Sanderson et al 1989 and Volpi et al 1992). Of the observed peaks, 12 were able to be assigned to known components of dermatan sulphate. The peak assignments are outlined in column 3 of Table 2.5. The thirteenth peak observed and the only difference from published spectra (65 ppm), was not assignable to any known component of dermatan sulphate. This peak was treated as an impurity in the deuterium oxide since the line width was greatly reduced compared to the other peaks observed so it could not be a component of the carbohydrate chain. The majority (i.e. >95%) of the uronic acid in this dermatan sulphate sample was judged to be present in the form of iduronic acid, since no peak corresponding to the carboxyl group of glucuronic acid (106.4 p.p.m.) was observed.

The prepared dermatan sulphate was intact since signals due to disaccharides with 4,5-unsaturated uronic acid residues with signals at 50.96 and 54.06 were absent (Sanderson et al 1989).

Since chondroitin 4-sulphate and chondroitin 6-sulphate differ only in the sulphation position on the N acetyl-galactosamine, the C^{13} signals from the glucuronic acid residue should be essentially identical. The different sulphation patterns of the N-acetyl-galactosamine may mean that the ring carbons of this residue will be in different environments. Up to twelve different signals can be observed for this sugar residue. Thus up to 20 different carbons will be observed for a mixture of chondroitin-4-sulphate and chondroitin-6-sulphate. In addition since the N-acetyl galactosamine residue of chondroitin-4-sulphate is essentially identical to the same residue in dermatan sulphate, 8 of the C^{13} peaks should be in common between the two spectra. These are outlined in column 1 of Table 2.5.

The spectrum of the chondroitin sulphate mixture contains 20 peaks indicating that there was no contamination of other GAG's in this sample. Of the peaks, 13 were able to be assigned, using published values (Bociek et al 1980). Overlap of the signals in the 74-80 ppm range of the spectra meant that 7 of the peaks could not be unequivocally assigned (column 5 in Table 2.5).

The C^{13} spectra of fast and slow heparin, purified in Section 2.3.3 (Figure 2.6) are noticeably more complex when compared to dermatan and chondroitin sulphate. A total of 25 and 40 different carbon signals were detected for slow and fast heparin respectively. The spectrum of slow heparin was typical of pig mucosal heparin (Casu 1985). The complexity of the two heparin spectra resulted in an inability to completely assign all of the peaks, particulary those in the 70-82 ppm range due, to extensive signal overlap in this region.

Figure 2.5: Chondroitin and Dermatan sulphate C^{13} NMR spectra

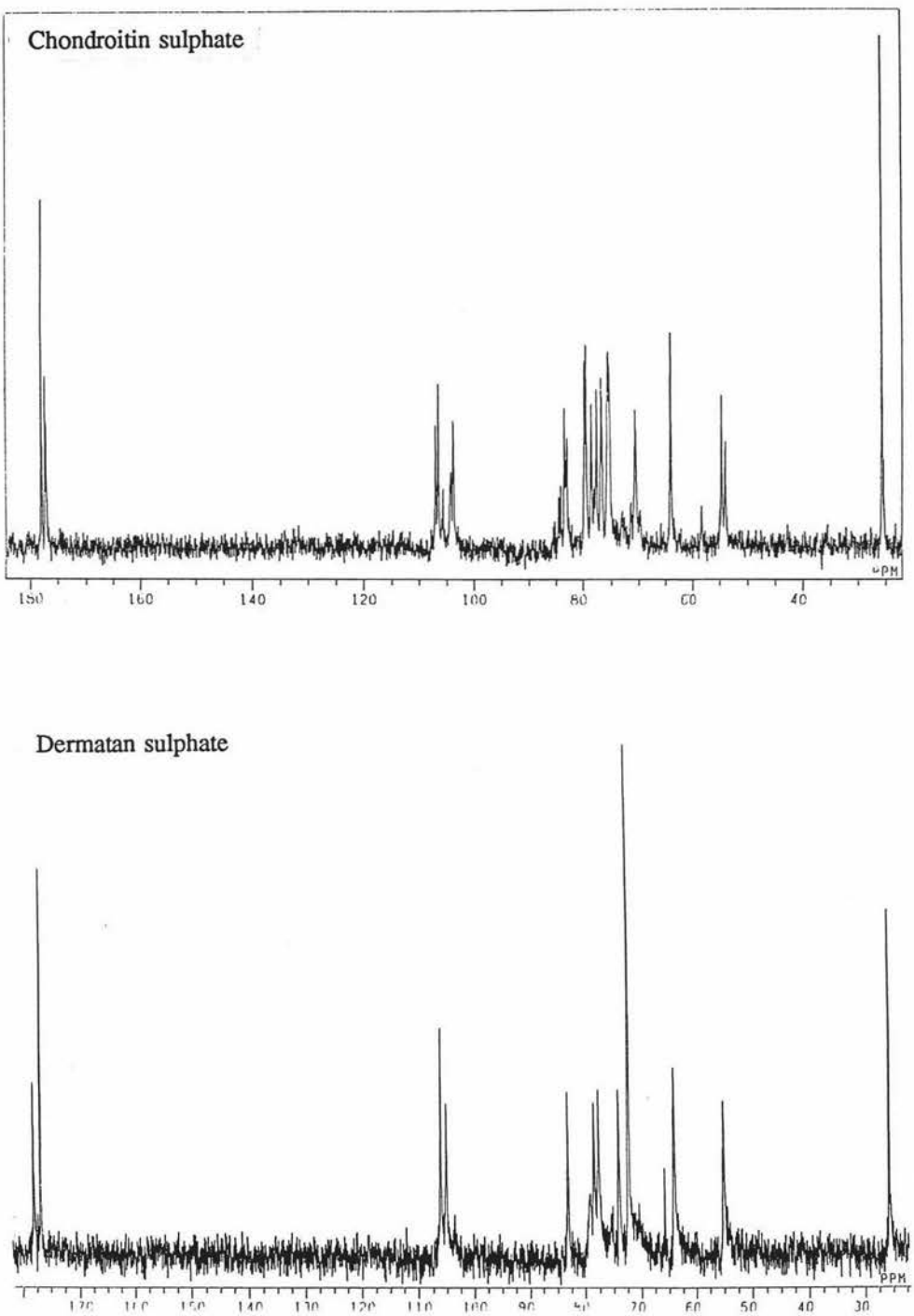

Conditions for C^{13} NMR spectra: Chondroitin sulphate; acquisition time 0.511 seconds, sensitivity enhancement 17, Dermatan sulphate; acquisition time 0..603 seconds, sensitivity enhancement 16

Table 2.5: Assignment of C^{13} Peaks for dermatan and chondroitin sulphate

Chemical shift	DS	Assignment for Dermatan sulphate	CS	Assignment for Chondroitin sulphate
178.105	+	Ac carboxyl		
177.993			+	Ac carboxyl
177.302			+	Carboyl
177.158			+	uronic
176.884	+	carboxyl IdoA		
107.153			+	C1 Hex A C6S
106.606			+	C1 HexA C4S
106.082	+	C1 IdoA		
105.056	+	C1 GalNAc		
103.927			+	C1 GalNAc C4S and C6S
83.511			+	C4 Uronic C4S
83.132	+	C4 IdoA		
83.021			+	C4 Uronic C6S and
79.767			+	C3 GalNAc of C4S
79.537			+	
78.615			+	C2,C3,and C5 GlcA
78.420	+	C3 GalNAc		of C4S and C6S
77.694			+	
77.590	+	C4 GalNAc		
76.743			+	C3 C6S GalNAc
75.649			+	C4 and C5 GalNAc
74.419			+	C4S and C6S
74.074	+	C3 IdoA and C5 GalNAc		
72.365	+	C2 and C5 IdoA		
70.581			+	C6 GalNAc C6S
65.700	+	Impurity		
64.102			+	C6 GalNAc C4S
64.040	+	C6 GalNAc		
55.031	+	C2 GalNAc		
54.656			+	C2 GalNAc
53.965			+	C4S and C6S
25.660	+	Methyl		
25.658			+	Methyl

Note: Signals in the C^{13} spectra of CS and DS that correspond to the same carbons are labelled in bold.

Four sources of chemical shift data were used in the assignment of the major signals for the fast and slow heparin. These were the C^{13} spectra for: pig mucosal heparin (Casu 1985), heparin and heparin derivatives (Fransson et al 1978), a highly sulphated heparan sulphate from rat liver (Kovensky and Cirrelli 1993) and the antithrombin III-binding sequence of heparin (Meyer et al 1981) was used for the assignment of minors signals. The assignment of the experimental resonances to the

published values was judged to be complete if they were within 0.2 ppm.

To facilitate the analysis of the C^{13} spectra of slow/fast heparin, the results were divided into six sections. These were: 20-30, 50-70, 71-82, 95-100, 102-110 and 175-185 ppm ranges respectively. Excluding the results in the 71-82 ppm range, assignment of the majority of the peaks was possible. The final assignments are shown in Table 2.6. In the 175-185 ppm range, 8 signals were observed in the spectra of both fast and slow heparin. Six of these signals were attributable to the carbonyl groups of N-acetyl and the carbonyl groups of the uronic acid residues. An extra signal at 184 ppm was observed in both spectra. It was not a component of the GAG chain because of the narrowness of the peak

Six signals were observed in the 100-110 ppm range, five of which were readily assignable (Table 2.6), however a peak at 102.315 ppm in the spectrum of slow heparin was not able to be assigned. There were four peaks in the 95-100 ppm range three were easily assigned. The remaining peak at 98.485 ppm in the spectrum of fast heparin was tentatively assigned to C1 of GlcNAc6OS (Meyers et al 1981).

The 50-70 ppm range consisted of 9 peaks. Most of the assignments were relatively simple. Two peaks at 60.616 and 60.848 ppm were assigned to C2 of $GlcNSO_3$6OS attached to different uronic acid residues (Meyer et al 1981). The peak at 60.646 ppm most probably corresponds to the Idu-$GlcNSO_3$6OS disaccharide, whereas the 60.846 ppm peak is GlcA-$GlcNSO_3$6OS since this peak only occurred in the spectra of fast heparin.

The 20-30 ppm region surprisingly contained 4 peaks. This region of the spectrum corresponds to the resonances of the carbon of the methyl group in the N-acetyl group or perhaps any acetate that may be present.

The final area of the spectrum the 71-81 ppm range was so complex, 10 and 20 peaks respectively for slow and fast heparin, that it proved impossible to make unequivocal peak assignments because of the number and overlap of the peaks. This

Figure 2.6: C^{13} NMR spectra of slow and fast heparin

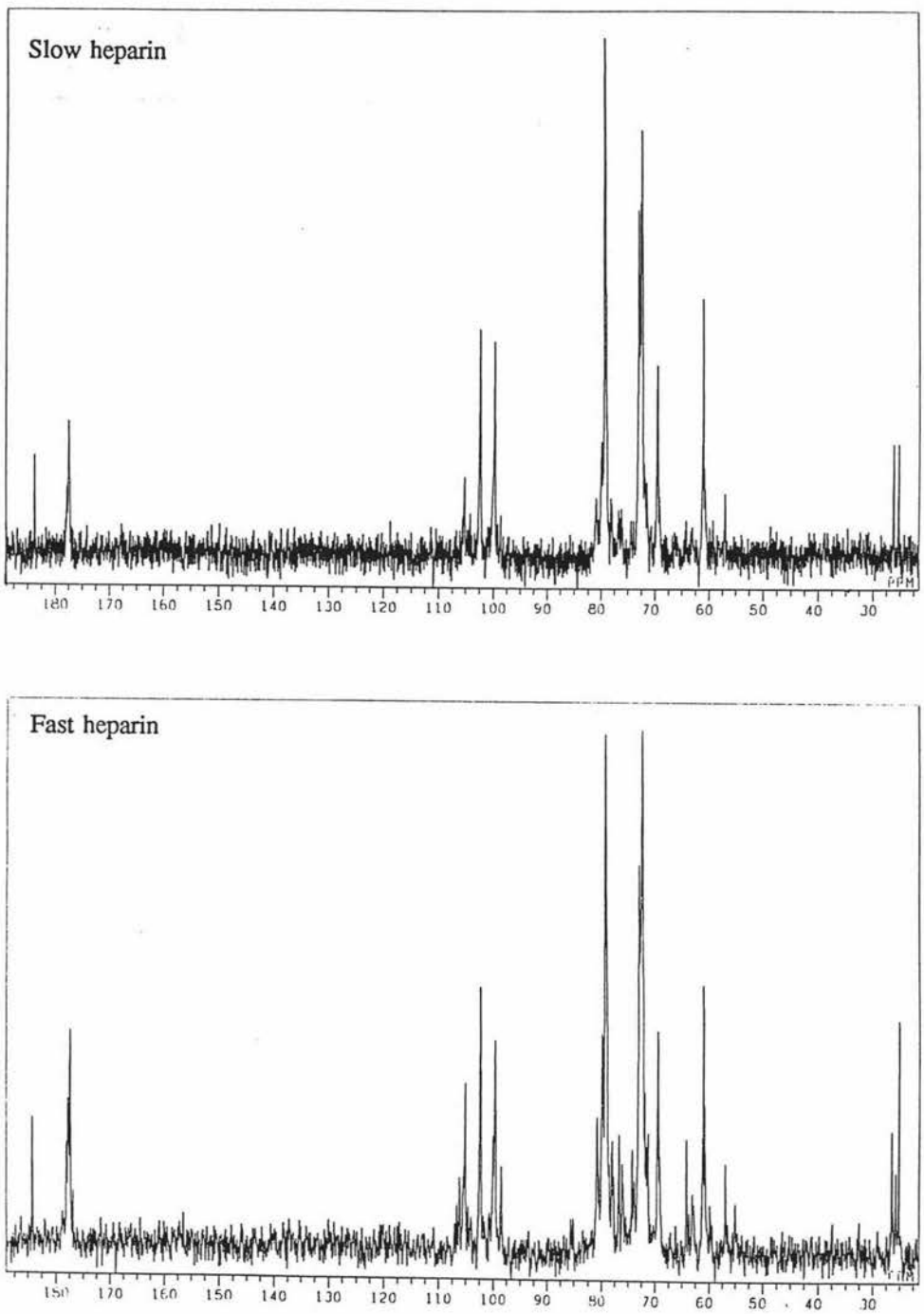

Condition for C^{13} NMR of slow and fast heparin; acquisition time 0.511 seconds with a sensitivity enhancement of 16.

region of the spectra corresponds to the resonances of the following carbons C2, C3, C4 of GlcA and IdoA C4, C5 of GlcN and C3 of GlcNS. The existence of more than 7 resonances for this region of the spectra is perhaps a reflection of the different sulphation position (that are normally rare) for these residues.

Several regions of the C^{13} spectra can be used as a diagnostic regions for the possible detection of GAG contamination (such as CS and DS) of heparin samples (Casu et al 1979). These are:

- The methyl resonances 25 ppm are slightly different for the different GAG classes (Holme and Perlin 1989).
- The C1 GlcA resonance at approximately 100 ppm.
- The C6 resonances of hexosamine residue 60-70 ppm.

Because of the procedures involved in the industrial purification of heparin, pharmaceutical heparin can contain up to 15% contamination of dermatan sulphate (Neville et al 1989). While conclusive proof of dermatan sulphate contamination in these samples cannot be ruled out solely on the basis of this C^{13} data, it was considered unlikely by the author that either of the heparin samples are contaminated with sizable amounts of dermatan sulphate. One peak in the 100-110 ppm range was unassignable (102.315), but it is highly unlikely that it corresponds to the C1 resonance of GalNAc of dermatan sulphate or C4S and C6S, since it is greatly different from their characteristic resonances, 105.066 and 103.93 ppm respectively. The C6 resonance of GalNAc for DS and CS are at approximately 64 ppm. One peak at 64 ppm observed in the spectrum of fast heparin was assigned to C6OH of GlcA. The absence of any confirmatory evidence in the 100-110 ppm region leads the writer to support by this assignment.

Definitive proof of the absence of contaminating GAG's (i.e. DS and/or CS) could be furnished by the following experiment. The fast and slow heparin samples could be subjected to a chondroitinase ABC lyase (Section 2.3.4.1) monitoring any increase in the absorbance at 232 nm. This would indicate that galactosaminoglycans (i.e. DS

and/or CS were present). In addition the C^{13} spectra of the treated samples after dialysis should then be undertaken. If degradation occurred and some of the C^{13} resonances in the spectrum of fast and slow heparin disappeared (particulary the resonance at 102.315 ppm) this would proof that DS or CS contaminants were present (Casu et al 1979). An additional test to rule out the existence of other contaminating GAG in the samples would be to perform two dimensional NMR spectra of the fast and slow heparin (Holme and Perlin 1989).

The complexity of the C^{13} spectra for fast heparin was unexpected. To the writer's knowledge this is the first demonstration of the complexity of this GAG type by C^{13} NMR spectroscopy. In addition it was apparent that there were large numbers of structural elements shared with heparan sulphate. It is difficult to understand why the complexity has not been observed before. An examination of the conditions used in the published C^{13} spectrum used similar conditions to this present analysis. The heparin used in this study is used by pharmaceutical companies as a raw material to produce clinical grade heparin. Because of commercial sensitivity the writer was unable to obtain any further processing and/or formulation information. However it is not entirely impossible that some or all of the fast heparin is removed from heparin before clinical formulation. Previously reported C^{13} NMR studies have predominately used clinical grade heparin.

2.3.4.3 Charge density of GAG standards

The charge density (i.e. the sulphate to carboxyl groups) of the GAG chain was measured. This ratio was determined by elemental analysis of dried GAG samples for sulphur and nitrogen. Assuming that all of the nitrogen in the sample is in the amino group on the GAG chain, the charge density was calculated by converting the percentage results to the respective molar values.

Table 2.6: Assignment of C^{13} Peaks for Fast and Slow heparin

Chemical shift	Fast heparin	Assignment	Slow heparin	Assignment
184.242	+	Impurity		
183.694			+	Impurity
178.050	+	Carbonyl NAc		
177.849			+	Carbonyl of NAc
177.791	+	C6 of GluNAc		
177.590			+	C6 of GluNAc
177.474			+	C6 of IduA
177.388	+	C6 of IduA		
106.145	+	C1 of GluA		
105.137			+	C1 Glc2OS
105.108	+	C1 of Glc2OS		
102.430			+	C1 of Ido2OS
102.401	+	C1 of IdoA2OS		
102.315			+	?
100.040	+	C1 of GluNS		
99.781			+	C1 of GlcNAc
99.723	+	C1 of GluNAc		
98.485	+	C1 of GlcNAc6OS		
80.804	+			
80.429	+			
79.825	+			
79.249			+	
79.220	+			
79.047	+		+	
78.874				
78.039	+			
77.895	+			
77.694	+			
76.657	+	C2, C3, C4 of		C2, C3, C4 of
76.081	+	GlcA and IdoA		GLcA and IdoA
74.152	+	C4, C5 of GLcN		C4, C5 of GlcN
73.777	+	and C3 of GLcNS		and C3 of GlcNS
72.971			+	
72.885			+	
72.856	+			
72.654			+	
72.510	+			
72.481			+	
72.337			+	
72.309	+			
71.905			+	
71.877	+			
71.704	+			
71.560	+			
71.416	+		+	
71.243	+			
69.515			+	
69.487	+	C6 of GlcN6OS		
69.055			+	C6 of GlcNOS
69.141	+	C6 of GlcN6OS		
64.102	+	C6OH of GlcA		
61.049	+	C2 of GlcNS	+	C2 of GlcNS
60.848	+	C2 GlcNS 6OS		
60.646	+	C2 GlcNS 6OS	+	?
56.816	+	C2 GlcNAc	+	C2 of GlcNAc
26.407	+			
26.061			+	?
25.687	+	?		
25.111	+	?	+	?

Note: Signals common to both fast and slow heparin are labelled in bold.

Table 2.7: Charge density and percentage sulphate and nitrogen of GAG's

GAG Sample	Charge density	% Sulphate	% Nitrogen
Heparin	2.25	22.2	1.73
Dermatan sulphate	1.20	13.4	1.96
Chondroitin sulphate	0.75	12.1	2.81

The charge densities of heparin and dermatan sulphate (Table 2.7) are within the normal range expected for GAG's of these classes (Table A1.3 in Appendix 1). The low value for chondroitin sulphate was initially surprising, but bovine trachea is known to contain a partially sulphated C4S, with only every third GalNAc being sulphated instead of every GalNAc residue (Charabarti and Park 1980). On the basis of the low charge density, it was considered likely that the CS samples examined may contain small amount of this undersulphated CS present.

2.4.4.4 Iduronic 2OS levels

The correlation published by Piani and coworkers (Piani et al 1993) provides a simple reproducible method to monitor the Idu2OS levels of heparin and heparan sulphates samples. The data shown in Table 2.8 clearly shows that the levels of Idu2OS are different in fast and slow heparin.

Table 2.8: Epoxidation reaction results

Sample	Assignment	Treatment	Optical rotation	Increment	%Idu2OS
2M KoAc ppt	Slow heparin	None Epoxidation	46.8 (0.8) 78.8 (0.5)	32.3 (1.3)	55.7 (2.2)
2M KOAc supernatant	Fast heparin	None Epoxidation	29.9 (0.25) 52.2 (0.8)	22.3 (1.0)	24.9 (1.8)

NOTE: Error of determination for each result are shown in brackets

Heparin and heparan sulphate differ in two important regards. N-sulphation typically occurs at a level of 60-80% in heparin and Idu2OS levels are high. In contrast in the case of heparan sulphate, the N-sulphation levels fall to 35-45% and Idu2OS levels are lower less than 20% (Piani et al 1993). To the knowledge of this writer this is the first time that the levels of Idu2OS in slow and fast heparin have been measured. On the basis of the low levels of Idu2OS in fast heparin, it is proposed that fast heparin may have large sections of heparan sulphate-like disaccharides sequences within the chain.

The level of HexA2OS in fast and slow heparin after digestion with heparin lyases (heparitinase I, II and III) have been measured by an HPLC assay (Volpi et al 1993b) as 60.6 and 86.5% respectively. This assay was unable to differentiate which of the two uronic acids were present because, the stereochemistry of the carboxyl group is destroyed as a result of the enzymatic cleavage reaction.

2.3.4.5 Molecular weight and molecular weight distribution

The molecular weight of each sample was determined by an empirical relationship between molecular weight and intrinsic viscosity (Equation 2.1 and Table 2.1). The viscosity results were converted to molecular weight after the GAG concentration had been determined by the uronic acid assay (Section 2.2.4.6). Samples results for dermatan sulphate are shown in Figure 2.7. The other GAG standards yielded similar results (Table 2.9). A sample calculation for dermatan sulphate is shown in Section A2.1 of Appendix 2. The average molecular weight of the disaccharide units of the CS, DS and heparin samples used in this study were calculated as 439, 472 and 557 respectively using the charge density figures measures in Section 2.3.4.3. This allowed the estimation of the average number of disaccharide units in each of the GAG chains (Column 5 Table 2.9).

2.4 SUMMARY OF CHAPTER

A summary of the properties of the GAG standards purified and/or characterised in this chapter is shown in Table 2.10. On the whole the properties examined were

similar to figures for each of these GAG classes isolated from a similar source (Casu et al 1980), with the possible exception of the chondroitin sulphate. The charge density of the CS sample was significantly lower than the figure of approximately one that was expected. However as has already been discussed this may be due to a partially sulphated species being present.

Figure 2.7: Intrinsic viscosity determination

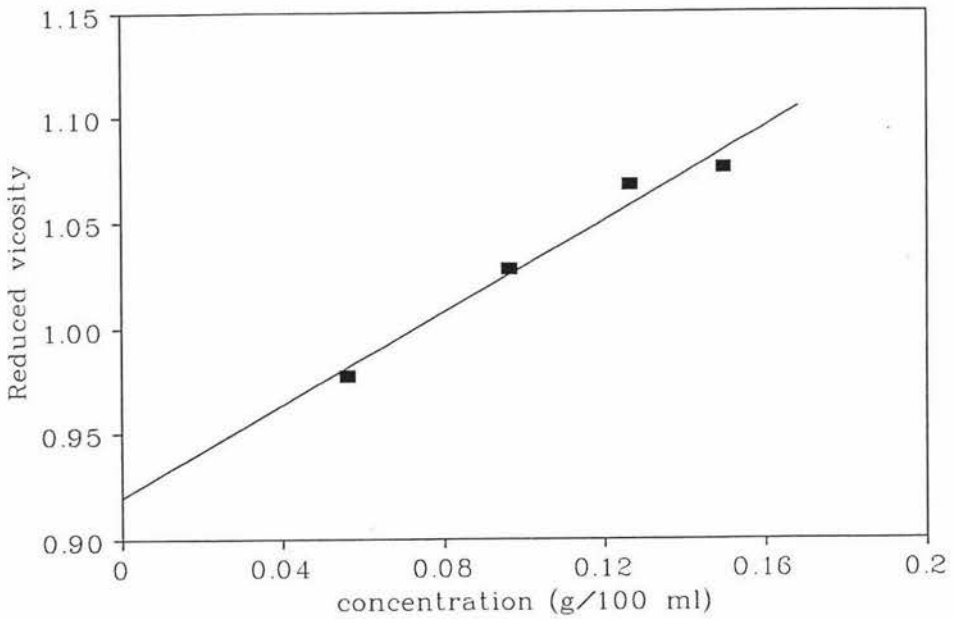

Table 2.9: Summary of viscosity results for GAG standards

GAG Sample	Intercept (SD)	Molecular weight	N	Number of disaccharide units
Unfractionated heparin	0.1893 (0.0017)	13840	4	25
Chondroitin sulphate	0.513 (0.080)	22370	4	51
Dermatan sulphate	0.9196 (0.0095)	49230	4	104

N is the number of observation used in the calculation of the intrinsic viscosity

Enzymatic and optical rotation characterisation of the purified DS sample suggested that the level of glucuronic acids residues within the GAG chains may be low (i.e. less than 10%). Analysis of the C^{13} NMR spectra indicated that the

level could not be greater than 5% of the total uronic acids.

Table 2.10: Summary of the properties of the GAG standards

	S (%)	Charge density	$[\alpha]_D$	n (dl/g)	Number of Disaccharides
CS	4.85	0.75	-20.6	0.51	51
DS	5.36	1.20	-51.8	0.92	104
Hep	8.86	2.25	39.4	0.19	25

The heparin used in this study was fractionated into slow and fast moving electrophoretic species using a selective precipitation protocol (utilizing 2M KOAc at pH 5.7). These species were partially characterised using two techniques (viz C^{13} NMR and quantification of iduronic-2-sulphate resides). The results of both assays were consistent with the idea that fast heparin had elements of heparan sulphate within its sequence. In particular the levels of Idu2OS residues (which are prevalent in heparin) in fast heparin were less than half the level of that in slow heparin.

The overall aim of this section of the experimental work of the thesis i.e. that representative samples of three GAG species: CS, DS and heparin that were pure and of known properties was successfully achieved. These samples aided the analysis of the binding behaviour of the GAG to the peptide resin (Chapter 4) and the solution binding studies (Chapter 5).

CHAPTER 3: PEPTIDE SYNTHESIS

3.1 INTRODUCTION

During this study six peptides were synthesized using solid phase peptide synthesis (SPPS) this technique has been recently reviewed (Barany et al 1987). SPPS was conceived by Merrifield in 1959. In 1984 he received the Nobel prize in chemistry in recognition to the impact the technique has had on the development of modern biochemistry. In brief outline SPPS involves the attachment of a suitably protected amino acid via its C terminus which has been suitability activated to an insoluble support. The amino group is then deprotected and an activated amino acid (AA) is added onto the immobilised AA. The process is continued until the desired peptide has been completed. Unlike in vivo peptide polypeptide synthesis, Merrifield peptide synthesis is performed in the reverse direction (i.e. C to N terminus). The advantage of the solid phase approach is that unreacted soluble reagents are removed by washing the resin in between the steps of the synthesis. Excess reagents for each step are added to drive the reactions to completion. The cyclic principle of SPPS also lends itself towards automation of the synthesis. Once synthesis of the peptide is complete, the peptide is cleaved from the resin, any side chain protecting groups on the peptide are removed, and the peptide is then purified.

The N terminal protecting group Fmoc (Fields and Noble 1990) has in many cases superseded Merrifield's original Boc group (Barany et al 1987). It offers several advantages, the main one being that it is removed by mild basic conditions, compared to its alternative which requires strong acid conditions for its removal. Traditionally SPPS has been performed on cross linked polystyrene supports and more recently polyamide/Kieselguhr supports (Barany et al 1987). Recent work by Englebretsen and Harding (Englebretsen and Harding 1992a, 1992b 1993, 1994a, 1994b, 1994c) has demonstrated that SPPS can be carried out on hydrophillic beaded cellulose based matrices. Peptide synthesis on such hydrophillic supports offers the potential for the synthesis of matrix bound peptide ligands for affinity work. This approach has been successively demonstrated with the synthesis of an affinity resin

for the extraction/purification of chymosin, a milk clotting protease (Englebretsen and Harding 1993) and the immobilisation of a luteinizing hormone releasing hormone (LHRH) peptide which bound LHRH antibodies (Englebretsen and Harding 1994c).

Three peptide resins (K_4G, K_8G, and $K_{12}G$) were synthesized in this study using the Fmoc approach described in the previous paragraph. These peptides were chosen as analogues of the polylysine used by Gelman and coworkers in their studies (Section 1.1.3.6). The varying lengths of the lysine chain were chosen in an attempt to probe what the minimum length required to the change the peptide conformation after binding the GAG chain. Glycine was added to the C terminus of the peptide chain to enable the integrity of the synthesis to be easily checked. Three criteria were enumerated to judge the success of the synthesis of the peptide ligand. The level of substitution of the final peptide resin can be calculated assuming all reactions have gone to completion. This can then be compared to experimentally determined values by amino acid analysis and picrate assay (Arad and Houghten 1990). In addition the ratio of amino acids determined by amino acid analysis of the peptide-resin should agree within experimental error to the theoretical values.

Three peptides (Table 1.6 for the sequences) were synthesized in their free form to enable solution binding studies of the peptides with GAG's to be performed. The integrity of the synthesis of these peptides was judged to have been successful if each of these peptides satisfied at least three of the following criteria.

1. Establishment of the correct amino acid ratios.
2. A single peak on analytical reverse phase HPLC.
3. A single peak on analytical capillary electrophoretic analysis.
4. The correct molecular weight by fast atom bombardment (FAB-MS).

Capillary electrophoresis (C.E.) is a relatively new analytical bioseparation technique (Li 1992 for a review). The technique involves electrophoresis of samples within a narrow bore silica capillary tube. CE offers several advantages over other analytical techniques such as: the speed of separation, the small sample volumes required and

finally the high efficiency of the separation (up to 1 million theoretical plates for some species). The mechanism of separation in CE is now well characterised. The inner wall of the capillary is negatively charged, due to acidic silanol groups. A boundary layer of buffer in contact with the wall has a net positive charge. When high voltage is applied to the capillary and the buffer, electroosmotic flow (EOF) moves the sample along the capillary as a result of the boundary layer moving. Charged molecular species also move in the electric field depending on their charge. Depending on the magnitude of the EOF, negatively charged species may have a net migration towards the cathode. This occurs particulary at pH's above 6. The principal disadvantage of CE is the interaction of highly basic peptides, such as those used in this study with negatively charged silanol groups. This results in low separation efficiencies for these peptides and in extreme cases no elution of peptides of this type. However a number of strategies have been used to bypass this problem. These are:

-The use of buffers with high or low pH

-Additives in the buffer which compete for wall absorption

-High ionic strength buffers

-The use of coated columns

The first two of the approaches outlined above were used for the characterisation of the peptides used in this study, to suppress the interaction of the basic peptides with the wall of the silica capillary. At low pH (eg pH 2.5) the majority of the silanol groups are unionized and this has two consequences. Firstly the walls of the capillary will not have a nett charge (basic peptides will not interact with the wall). Secondly the endosmotic flow will be very small. At higher pH's such as ph 6.2 the silanol groups would be expected to be fully ionized with the consequent increase in the endosmotic flow. However at this pH basic peptides such as the ones synthesized will interact with wall with a consequent decrease in separation efficiency. The buffer used in the analysis of this peptides contained an excess of amine groups (as in compounds like diaminopropane), which competes with the peptides for the silanol groups on the wall of the capillary, this results in an increase the efficiency of the separation.

3.2: MATERIALS AND METHODS

3.2.1 Equipment

The following equipment was used in this aspect of the project: 4175 Biolynx semi manual flow peptide synthesizer from Pharmacia (Uppsala, Sweden), ABI 430A automated vortexing batch synthesizer and 270A capillary electrophoresis system both from Applied Biosystems (Foster City, California, USA). Two C18 reverse phase HPLC columns from Vydac (Hesperia, California) were used: preparative C18 column (1 X 25 cm) and analytical C18 reverse phase column (dimensions 4.6 X 0.25 cm). Amino acid analysis was performed using the AA analyzer facility in the Chemistry and Biochemistry of Massey University. An Omni Scribe B-5000 strip chart recorder from Basch and Lomb (Houston, Texas, USA) was used to record the capillary electrophoresis results.

3.2.2 Chemicals

The following chemical were supplied by BDH (Palmerston North): Acetonitrile (HiPersol), phenol, piperidine, KCN and dimethylforamide (DMF). DMF was distilled under vacuum from calcium hydride prior to use. Drum grade dichloromethane (DCM) was dried over magnesium sulphate and distilled prior to use. Ninhydrin was supplied by Koch Light Chemicals (UK). Drum grade ethanol was used as supplied. Trifluroacetic acid (TFA) was supplied by Halocarbon (New Jersey, USA) and was distilled prior to use. Protected Nα-Fmoc-L-amino acids [Ala, Arg(Mtr), Asn, Asp(OtBu), Gln, Gly, His(Trt), Ile, Leu, Lys(Boc), Met, Phe, Pro, Ser(tBu), Thr(tBu), Trp, Tyr(tBu)] were supplied by Bachem (Torrance, California USA). Picric acid was supplied by Merck (Darmstadt, Federal Republic of Germany). 1-N-hydroxybenzoltriazole monohydrate ($HOBt.H_2O$), calcium hydride, diaminopropane and 1,3-diisopropyl-carbodiimide (DIC) were supplied by Aldrich (St Loius, USA). Diethyl ether (laboratory grade) by Ajax chemicals (Sydney). Mono sodium citrate was supplied by Spolek Chemicals (Prague, Czechoslovakia).

3.2.3 Quantitative ninhydrin procedure

A small quantity of resin is placed into a small sintered glass funnel and washed with 3 column volumes of 95% ethanol, then 2 column volumes of diethyl ether and dried at 110°C for ten minutes. A sample of this dried resin is weighed into a test tube (to the nearest 0.01 mg) after cooling in a desiccator. Using an automatic pipette the reagents were added in the following order:

-reagent 1: 80% phenol in ethanol 75µl
-reagent 2: 0.2 mM KCN in pyridine 100µl
-reagent 3: 0.28 M ninhydrin in ethanol 75µl

The tube was then incubated on a heating block at 110^0 C for 7 minutes. An aliquot of 50% ethanol (4.8 ml) was then added to the tube and the solution was then vortexed. After the resin has settled to the bottom of the tube the absorbance of the solution at 570 nm is measured. The amount of amine groups on the resin in µmol/g is then calculated (the extinction coefficient of ninhydrin 15000 M/cm).

3.2.4 Picrate titration of resin bound amine groups

Amine substituted Perloza resin was placed onto a dried preweighed sintered glass funnel and any dimethylforamide (DMF) was washed away with 50% aqueous ethanol. A saturated solution of picric acid in 50% ethanol was added to the resin. After standing for 5 min, excess picric acid was washed away with 50% aqueous ethanol. The bound picric acid was eluted with a 10% solution of triethylamine in 50% aqueous ethanol. The volume of the washing is then made up to 50 ml. The absorbance of this solution at 358 nm was recorded using 50% ethanol as a blank. The dry weight of the resin was determined by the standard procedure (Section 3.2.3). The amount of amine present was calculated using the extinction coefficient for picric acid as 14500 M/cm.

3.2.5 Synthesis of K_4G and K_8G peptide resins

K_4G and K_8G peptide resin were manually synthesized on an LKB Biolynx 4175 peptide synthesizer using amino substituted Perloza, with substitution levels of 0.56 and 0.31 mmol/g respectively, functionalised by a cyanoethylation/reduction procedure (Englebretsen and Harding 1992b, 1994a). Fmoc-glycine and α-Fmoc-ε-Boc-lysine were activated by the formation of HOBt active esters with four times excess of activated amino acids. The scale of the synthesis was 0.3 or 0.2 mmol respectively, single coupling were employed for each step.

3.2.5.1 Reaction of Perloza with FmocGLYOBt

The synthesis of the amino substituted Perloza has described (Englebretsen and Harding 1994). Fmoc-GLY was immobilised onto this resin using active esters formed by mixing Fmoc-GLY and HOBt. 1,3-Diisopropylcarbodiimide (DIC) was used as the condensing agent to couple the active ester to the amine groups on the resin.

Perloza 500 medium, 6.7 g was washed with ethanol and then DMF. The resin was then transferred to the Biolynx reaction column. Fmoc-GLY 0.297g (i.e. 3 molar excess) and HOBt.H_2O, 0.168 g (1.1 mmoles) were dissolved in 3 ml DMF. DIC 164 µl (1.05 mmole) was added to the DMF solution and the solution was stirred for 10 min.

3.2.5.2 Coupling of the aminoacids to the resin.

The standard LKB Biolynx 4175 peptide synthesis cycle was employed (LKB 1987) in the coupling of the subsequent amino acids. The protected amino acids were added in a three molar excess over the number of free amino groups on the resin. The synthesis cycle used to couple each amino acid is given in Table 3.1

Table 3.1: Biolynx continuous flow peptide synthesizer synthesis cycle

Function	Solvent/Reagent	Time	Flow rate (ml/min)
Load	Activated Fmoc aminoacid		2 ml/min
Recycle		1 hour	3 ml/min
Clean loader Wash	DMF	10 min	3 ml/min
Test ninhydrin (optional)	-	-	-
DeFmoc	20% piperidine/DMF	10 min	3 ml/min
Load	5 ml DMF		2 ml/min
Wash	DMF	10 min	3 ml/min

Adapted from: LKB 1987

3.2.5.3 Theoretical calculation of substitution levels

Every time an aminoacid is coupled to the resin the weight of the resin is increased. Assuming 100% coupling efficiency, the total amount of amine is constant throughout the synthesis, therefore the level of amino groups decreases as the synthesis proceeds, A sample calculation is shown in Section A2.2 of Appendix 2.

3.2.5.4 Amino acid analysis

A sample of peptide resin (or peptide) is weighed into a glass tube with a side arm and a threaded Teflon stopper. 0.5-1.0 ml of 6 M HCl containing 0.01% phenol was added to the tube. The tube was then evacuated briefly with a water pump and the stopper screwed down while the tube was still under vacuum. Digestion at 110^0 C was allowed to proceed for 24 hours. The HCl was then removed under vacuum. The sample was made up to known volume and submitted for analytical amino acid analysis.

3.2.5.5 Removal of protecting groups

Removal of the Boc protecting groups on the side chains of lysine was effected by the use of an acidic deprotection. The resin was solvent exchanged to dichloro-methane (DCM), by washing for 15 min at 3 ml/min. The cleavage reagent was comprised of: 90 ml DCM, 10 ml trifluoroacetic acid and 0.5 ml water which was washed through the resin for 15 min at 3 ml/min. After the cleavage had been performed the resin was washed with DCM and solvent exchanged to DMF in each case, both for 15 min at 3 ml/min. The extent of the deprotection reaction was monitored by use of the picrate reaction.

3.2.6 Automated synthesis of K_4G and $K_{12}G$ peptide resins

$K_{12}G$ Perloza was synthesized using a ABI 430A automated vortexing batch synthesizer on aminopropyl Perloza 200 fine (0.21 mmol/g amine substitution) at a 0.12 mmol scale. Standard SPPS protocols for the ABI 430A synthesizer were used throughout the synthesis. Deprotection of the final resin was achieved by the use of the cleavage reagent 20% TFA/80% DCM. The peptide resin was characterised by AA analysis and picrate titration. A second synthesis of K_4G-Perloza on a 0.2 mmol scale was also undertaken using the same protocol, but using amino Perloza with a lower amine substitution (0.53 mmol/g).

3.2.7 Synthesis of free peptides

The synthesis of the two peptides: protease C inhibitor (residues 264-283) and thrombospondin heparin binding peptide were performed on a ABI 430A peptide synthesizer using standard synthetic protocols. Deprotected peptides were purified and characterised using RP-HPLC as outlined below.

3.2.7.1 Purification of peptides

Peptides were purified using a preparative C18 reverse phase HPLC column, elution

of peptides was performed using a 0 to 60% acetonitrile gradient with 0.1 % TFA, over 60 min with a flow rate of 2 ml/min. The peptides were detected by absorbtion profiles at two wavelengths (214 and 280 nm).

3.2.8 Characterisation of purified peptides

3.2.8.1 Reverse phase HPLC

Solvent A: MilliQ water with 2% acetonitrile
Solvent B: Acetonitrile with 0.1% trifluoroacetic acid

Analytical RP-HPLC profiles of crude and purified peptides were performed to measure the purity of the peptide preparations. 150 µl of a 1 mg/ml solution of the crude peptides was injected onto an analytical C18 reverse phase column equilibrated with solvent A, at a flow rate of 1 ml/min. Bound peptides were eluted with a gradient of 0 to 60% solvent B in 60 min. The column output was monitored at two wavelengths (214 and 280 nm).

3.2.8.2 Capillary electrophoresis (C.E.)

Analytical capillary zone electrophoresis of the purified peptides was performed on an Applied Biosystems 270A electrophoresis system. Typically a 72 cm fused silica capillary, with a detector window 50 cm from the origin was used. Separation of the samples was performed using two different buffer systems

A. 20 mM sodium citrate pH 2.5: prepared by titrating a solution of monosodium citrate with 1M HCl to the required pH.
B. 60 mM diaminopropane, 20 mM NaCl pH 6.2: prepared by titrating a diaminopropane solution with 3M phosphoric acid to the required pH.

Separation parameters used for the two buffer system are outlined in Table 3.2

Table 3.2: Run parameters for Capillary electrophoresis

	20mM sodium citrate	60 mM diaminopropane
Voltage (kV)	30	18
Temperature	35	35
Risetime	5	5
Typical current (μA)	25	60

The output was followed by monitoring the detection window at 200 nm, the output being recorded on a chart recorder.

3.2.8.3 Fast atom bombardment (FAB)-mass spectrometry

Twenty μl of a 1mg/ml solution of the purified peptide was submitted for FAB-MS analysis to the analytical service unit of the Horticultural and Food Products C.R.I. Palmerston North. The samples were analyzed on a VG-70 350S mass spectrometer with a caesium ion gun (15 kV) source.

3.3 RESULTS AND DISCUSSION

3.3.1 K_xG Resins

Three K_xG resins were synthesized during this study with the lengths of the lysine chains being 4, 8, and 12. The success of the synthesis of all three resins was judged by four criteria. The efficiency of the coupling reaction for the manual syntheses (i.e. 4 and 8 lysine chain lengths) was monitored by the ninhydrin reaction, the efficiencies exceeded 95 % in both cases (Table 3.3). The substitution level of the completed peptide resins was measured by two methods (picrate and AA analysis).

Table 3.3: Analytical data on K_xG resins

Peptide resin	Coupling efficiency	Theoretical substitution (mmol/g)	AA determined substitution (mmol/g)	Picrate determined substitution (mmol/g)
K_4G	96.4	0.196	0.22	0.18
K_8G	95.9	0.166	0.19	0.18
$K_{12}G$	n.d.	0.13	0.10	0.13
K_4G	n.d.	0.32	0.30	0.34

n.d. : not determined. The last two resins were synthesized on the ABI 430A automatic peptide synthesizer.

As can be seen from the results in Table 3.3, the syntheses the peptide resin appeared to be successfully achieved, since the accuracy of AA analysis and the picrate titration is commonly accepted to be 5 and 10% respectively. The peptide resin synthesized must be completely deprotected before they can be used in resin binding experiment with the GAG classes prepared in Chapter 2. Removal of the Boc protecting groups on the ε-amino group on the side chain of lysine results in the appearance of more titratable amino groups on the resin. These new groups were monitored by the picrate assay, results are outlined in Table 3.4.

The final test of the integrity of the synthesis and the deprotection of the resins is the ratio of the amino acid glycine to lysine. This ratio was estimated by amino acid analysis and by the ratio of the picrate titration (before and after deprotection). The result for the 8 and 12 lysine chain lengths agreed with the theoretical values within experimental error, demonstrating the successful synthesis of these resins. However the results of the deprotection for the K_4G peptide resin were judged to be less than satisfactory. The synthesis of this resin was repeated on the ABI peptide synthesizer (Table 3.3 and 3.4). The results for this resin were within experimental error and the second synthesis of this resin was judged to be successful.

Table 3.4: Deprotection of K_xG Resins

Resin	Final amino group substitution (mmol/g)	Picrate substitution (mmol/g)	Glycine lysine ratio by picrate assay	Glycine lysine ratio by AA analysis
K_4G	2.00	1.52	1:3.00	1:4.64
K_8G	1.72	1.72	1:8.00	1:8.13
$K_{12}G$	2.00	2.01	1:12.00	1:11.30
K_4G	1.60	1.59	1:3.93	1:3.40

Three peptide resin with varying lysine chain lengths of 4, 8, and 12 have been successfully synthesized during this study. The advantage of the synthetic protocol used in the synthesis of these resins is that all of the lysine chain immobilised onto the resin are of a defined length and known orientation. The level of lysine on a particular resin are similar to each other. This should aid in the analysis of the GAG binding results (Chapter 4).

3.3.2 Synthesis of free peptides

Three peptides were synthesized in their free form during this study for use in solution binding assays. Two of these peptides were synthesized on the ABI 430A. K_8G was synthesized manually on the LKB Biolynx peptide synthesizer. Analytical data on the synthesis, purification and characterisation of these peptides are described below.

3.3.2.1 Protease C inhibitor peptide (residues 264-283)

The synthesis and purification of this peptide (sequence of PCI 264-283: SEKTLRKWLKMFKKRELEEY) was judged to have been successful since no evidence for deletion peptides could be found on HPLC and CE profiles (Figure 3.1 and 3.2). Aminoacid ratios were as follows: Ser 0.91 (1), Glu 3.75 (4), Thr 0.80 (1), Leu 2.68 (3), Arg 1.80 (2), Lys 4.75 (5), Met 0.99 (1), Phe 1 (1) and Tyr 0.94 (1), Trp n.d. (1). The majority of the amino acids agreed with the theoretical figures

within experimental error (5%). The values for serine and threonine were low, however the conditions used in the digestion are well known for destroying these amino acids. FAB-MS analysis of a solution of this peptide established the presence of a major $(M+H)^+$ peak at 2645 , which was very close to the expected molecular weight of 2644.16, confirming the presence of tryptophan. These results taken together with the CE and HPLC profiles, unequivocally demonstrate the purified peptide is the correct peptide and that no deletion peptides are present.

Figure 3.1: HPLC profiles of PCI peptide

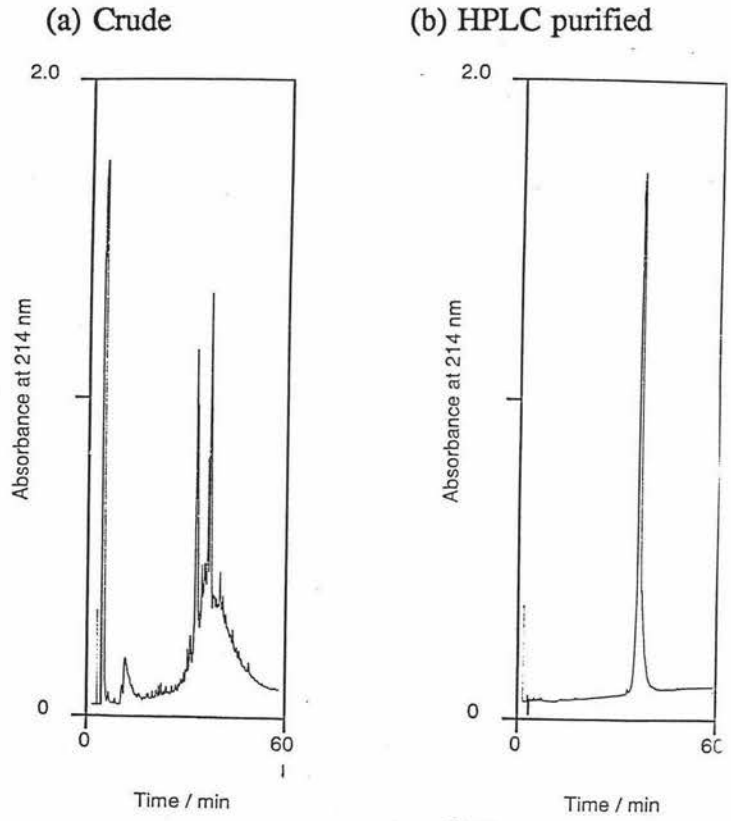

3.3.2.2 Thrombospondin peptide

The synthesis and purification of this peptide was successful (sequence SHWSPWSS) since no evidence for any deletion peptides was observed in both the HPLC and CE profiles (Figures 3.3 and 3.4 respectively). The ratio of amino acids (relative to proline) were identical to the theoretical expectation: Ser 4.00 (4), His 0.99 (1), and Pro 1 (1). The presence of tryptophan in the peptide was established by FAB-MS analysis, a peak corresponding to the MH^+ molecular ion was observed at 973.8 mass

units, the calculated figure being 974. These results unequivocally demonstrate the successful synthesis of this peptide.

Figure 3.2: CE profiles of purified PCI peptide

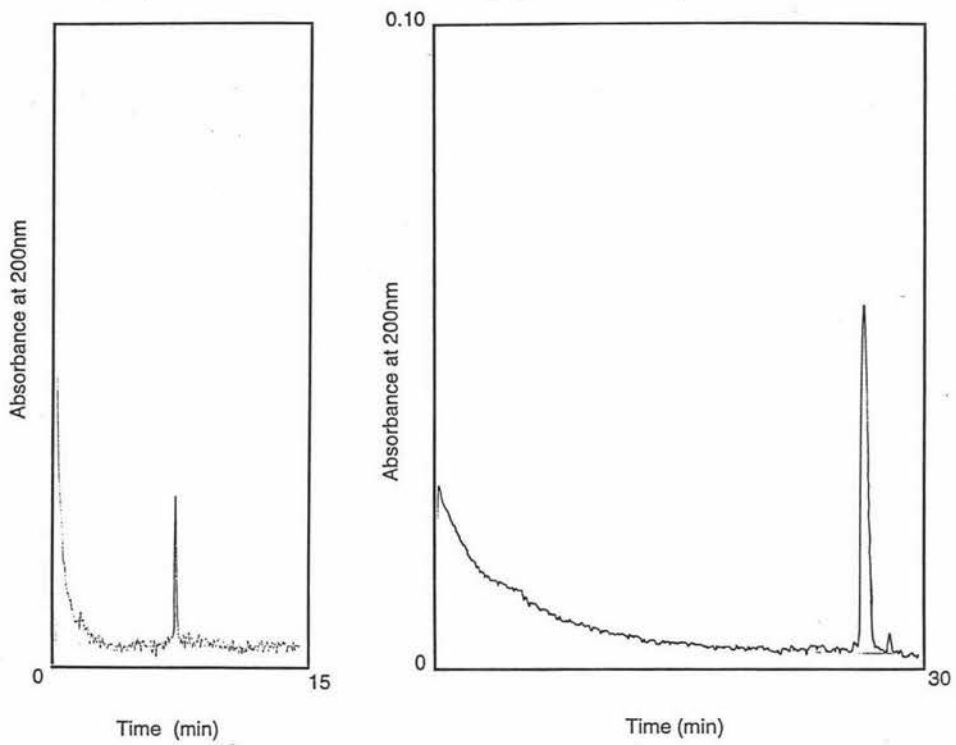

Figure 3.3: HPLC profiles of Thrombospondin peptide

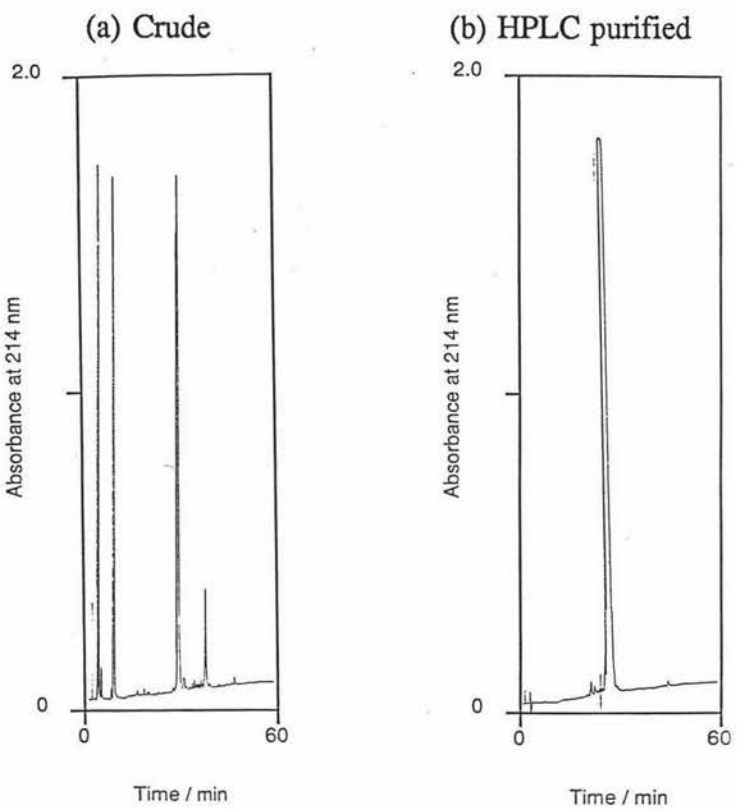

Figure 3.4: CE profiles of purified Thrombospondin peptide

(a) pH 2.5 (b) pH 6.2

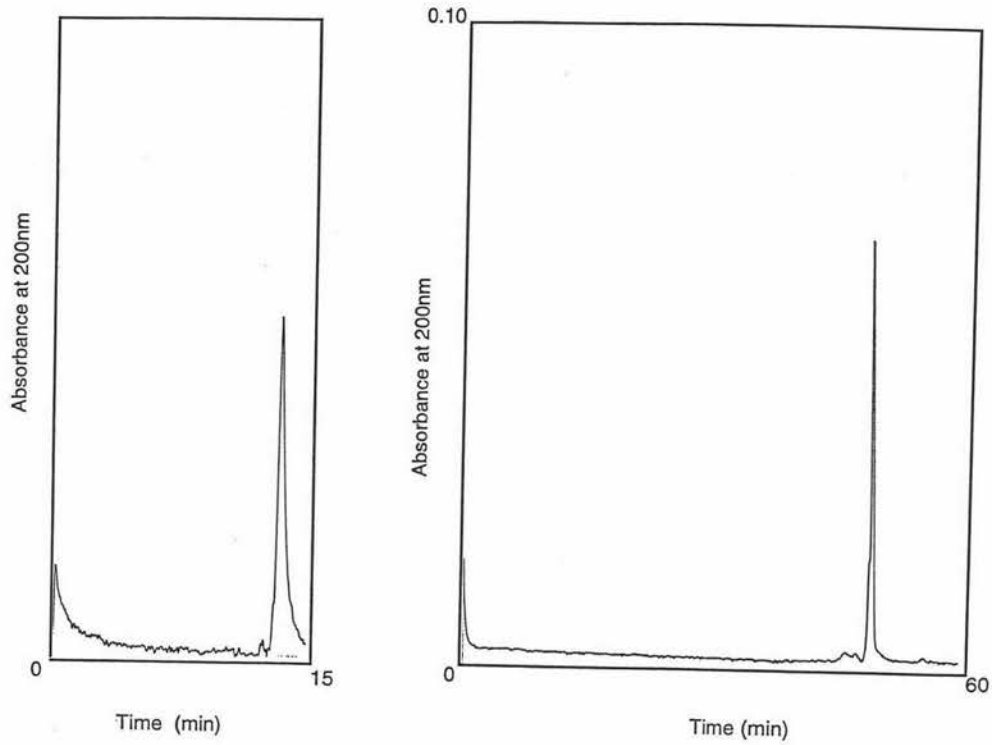

3.3.2.3 K_8G peptide

The K_8G peptide was manually synthesized on a Perloza resin with a cleavable linker (Englebretsen and Harding 1994a) in tandem with the non cleavable K_8G peptide resin. The synthesis of this peptide was monitored in a similar manner to the peptide resin, except that the deprotection of the resin results in the cleavage of the peptide from the resin.

Table 3.5: Analytical data for cleavable K_8G peptide

	Picrate substitution (mmol/g)	AA analysis substitution (mmol/g)	AA ratio
K_8G peptide	0.226	0.218	1:7.13

The synthesis of this peptide was successful since no evidence for any deletion peptides was observed in both the HPLC and CE profiles (Figures 3.6 and 3.7 respectively). The ratio of amino acids was close to theoretical expectation (Table 3.5). The ratio of the amino acids for the purified peptide was 1:8.42 which was within experimental error.

Figure 3.5: HPLC profiles of K_8G peptide

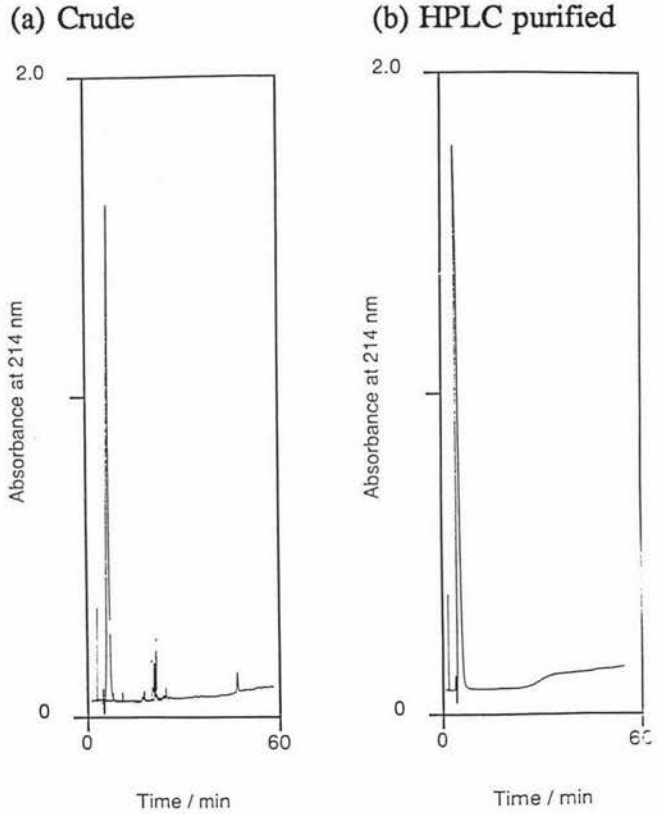

3.3.3 Capillary electrophoresis of free peptides

As can be seen from the results in Table 3.6, the use of the diaminopropane buffer increased the efficiency of the separation. The order of the mobility of the synthesized peptides increased with the charge to mass ratio of the peptides. The diaminopropane buffer (pH 6.2) had the greater efficiency of the two buffers tested by virtue of the fact that it contained a large excess of molecules (over the peptide concentration) that competed for the negative charges on the walls of the capillary.

Figure 3.6: CE profiles of purified K_8G peptide

(a) pH 2.5 (b) pH 6.2

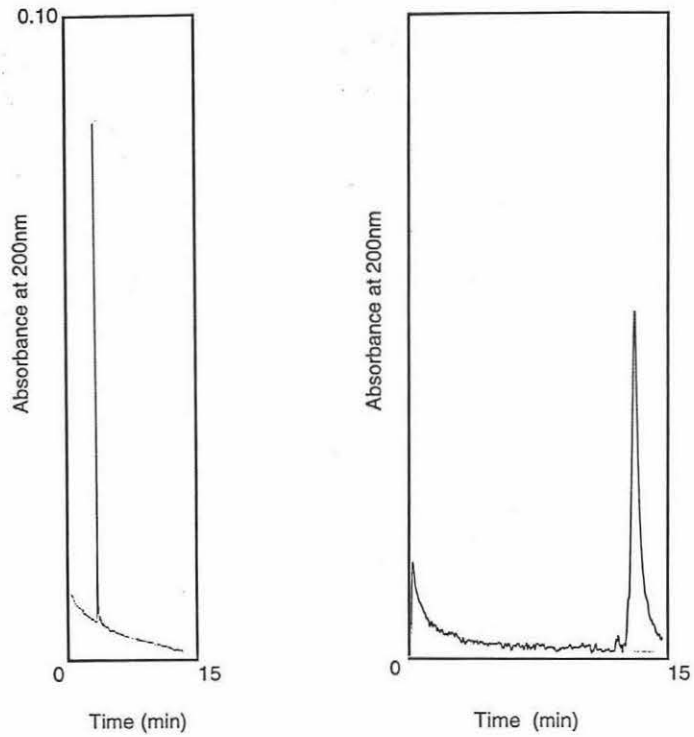

Table 3.6: Comparison of the CE buffers performance

Peptide	C.E. Buffer			
	pH 2.5		pH 6.2	
	t_R (min)	N_{eff}	t_R (min)	N_{eff}
Thrombospondin	10.15	3900	48.9	41210
PCI	7.40	9380	26.5	13300
K_8G	5.00	2400	12.9	3960

3.4 SUMMARY

The synthesis of three short polylysine resin of the form K_xG (where x= 4, 8 and 12), with the polypeptide chain being immobilised in a defined orientation i.e. through the C terminus, was successfully achieved. The success of the synthesis was judged by two criteria. These were:

1. Establishment of the correct ratio's of lysine to glycine i.e. 4, 8 and 12 (for K_4G, K_8G, and $K_{12}G$ respectively).

2. Measurement of the amine level of the final resin by two assays and comparison to the expected value if all coupling reactions have gone to completion.

In addition three short peptides (thrombospondin peptide, PCI 264-283 and K_8G) were prepared. The peptide was judged to be free of peptide impurities (i.e. deletion peptides) on the basis of three criteria. These were: a single peak on RP-HPLC and CE analysis (proving purity), and the correct molecular weight as measured by FAB-MS (confirming correct sequence). Additional criteria of both purity and synthesis integrity was the measurement of the correct amino acid ratios.

Chapter 4: BINDING OF GAG's TO IMMOBILISED PEPTIDE RESINS

4.1 INTRODUCTION

A large body of work by Gelman and coworkers exists on the interaction of polybasic amino acids, i.e. lysine, arginine and ornithine with GAG's (outlined in Section 1.1.3.6). Three properties of this binding that make the interaction of GAG's with polylysine chains in solution attractive as a potential novel separation technique are as follows:

1. The interaction between polylysine and the GAG's is not solely related to the charge density of the GAG class, since heparan sulphate is bound more strongly than the chondroitin sulphates, and dermatan sulphate binds more strongly than heparin (Table A1.2 in Appendix 1).

2. The interaction for some of the GAG's is quite strong (e.g. dermatan sulphate requires greater than 2M salt to inhibit binding).

3. The distribution of charges on the GAG chain also seems to play a role in the strength of the binding. For example chondroitin-4-sulphate is bound more tightly than chondroitin-6-sulphate even though they have the same charge density.

To highlight these properties, a comparison of the binding behaviour of PLL in solution to typical chromatographic techniques used in GAG purification is outlined below. Two reports (Bohn and Kalbhen 1971a and 1971b) compare the efficiency of some of the most frequently used column chromatographic techniques for the separation of GAG's in the early 1970's. Little has been reported since on studies of this type. Cetylpyridinium chloride and the ion exchanger DE-52 were found to be superior to all other ion exchange supports. "*However, in no case was a complete separation of a mixture containing hyaluronic acid, chondroitin-4-sulphate, chondroitin-6-sulphate, dermatan sulphate, heparan sulphate and heparin achieved*".

Bohn and Kalbhen used step gradients for the elution of their GAG samples. For two of the resins they examined, it is possible to estimate the salt strength required for 50% elution and from these figures calculate the relative binding strength of the resin (Section A3.1 of Appendix 3). As can be seen from the Table 4.1, and data in Appendix 3, while some ion exchange resins may have one or more of the listed properties associated with the PLL/GAG interaction, no ion exchange resin had all three. Dowex 1X2 (a strong-base ion exchanger) and ECTEOLA resin both bind GAG strongly, but dermatan sulphate appears to bind the Dowex 1X2 resin to a greater extent than heparin. In both cases the GAG classes elute in overlapping salt fractions. The ion exchange resin (DE-52) that was the best in separating the GAG samples still gave an overlapping fraction for dermatan and heparan sulphate, with some heparin also being eluted with this fraction.

Table 4.1: Binding behaviour of GAG's on ion exchange resin.

GAG Class	Charge density	Dowex 1X2 R.B.S	ECTEOLA R.B.S
CS	1.00	1.00	1.00
HS	0.99	<0.84	-
DS	1.40	1.18	1.14
Hep	-	1.11	1.59

Source: Bohn and Kalbhen 1971

Key: R.B.S; relative binding strength the salt concentration required for 50% elution of the GAG divided by the equivalent concentration for chondroitin sulphate. CS: chondroitin sulphate, HS: Heparan sulphate, DS: dermatan sulphate, Hep: heparin.

The fractionation of GAG's on polylysine resins has been reported (Suzuki and Koide 1984a and 1984b). This has been discussed in Section 1.2.3. However there were some large discrepancies between the Suzuki and Koide paper and Gelman's work. These are be outlined below. A summary of the elution behaviour of the GAG samples tested for immobilised polylysine compared to the binding strength found by Gelman and coworkers is outlined in Table A1.3 of Appendix 1. The first fact that is apparent is that the immobilised polylysine made by Suzuki no longer binds chondroitin-6-sulphate more strongly but now binds chondroitin-4-sulphate to the same extent. The binding of dermatan sulphate is weaker when compared to the

solution studies. This could be due to the fact that the dermatan sulphate used in their study had a lower charge density. The final fact is that the PLL column binds heparin more strongly than dermatan sulphate. This is probably as a result of the weakened binding of dermatan sulphate.

The immobilisation procedure used by Suzuki and Koide may not be the correct one to use because the polylysine chains they used (the exact length is not stated) may result in the attachment of a single poly-L-lysine at more than one point on the chain. If multiple attachments did occur, the flexibility of the chain would be restricted so the transition for charged coil conformation to alpha helix may be hindered and thus affect the strength of the binding of the GAG.

To further examine the use of polylysine column as a method to fractionate GAG mixtures, small amounts of resin with polylysine chains of defined length and immobilised in a known orientation were synthesized (Chapter 3). The point of attachment was a the carboxyl terminus of the peptide.

The binding of chondroitin sulphates, dermatan sulphate and heparin to polylysine in solution results in the polypeptide chain adopting an alpha helical conformation (Section 1.1.3.6). It was decided to see if there was a minimum chain length for this effect to occur. For this reason three peptide resins with chain length of 4, 8, and 12 lysines were synthesized. These chain lengths were chosen because it was thought that four lysines would be unlikely to be able to adopt a complete alpha helical conformation whereas 8 and 12 may be able to adopt such a conformation. As a control a full length polylysine chain (633 residues) of similar length to that used in the solution binding studies (500 residues) was immobilised onto a resin.

The binding behaviour and salt elution patterns of each of these resins was examined using the GAG standards purified and characterised in Chapter 2. The binding behaviour of the resin for the GAG standards was examined to see if any differential GAG binding ability comparable to Gelman group's solution binding experiment were present.

4.2 MATERIALS AND METHODS

4.2.1 Chemicals

The following chemicals were used in this study: laboratory grade acetone and pyridine, analytical grade sodium chloride from Ajax chemicals (Auburn, Australia). Poly-L-lysine (with an average of 633 residues per polypeptide chain) as the hydrobromide salt and p-toluenesulphonyl chloride (tosyl chloride), and norleucine were supplied by Sigma (St Louis, Missouri, USA). Perloza was supplied by ICS (Prague, Czechoslovakia). Buffer grade tris-(hydroxylmethyl) aminomethane (TRIS) and laboratory grade glycerol were supplied by US Biochemical Cooperation (Cleveland, Ohio) and Scientific Supplies Ltd (Auckland NZ). Molecular sieves (type 4Å) was supplied by Union Carbide (USA).

4.2.2 Equipment

The following equipment was used in this study: low pressure liquid chromatography systems: ECONO system from Biorad (Hercules, California USA), FPLC and a Frac-200 fraction collector from Pharmacia (Uppsala, Sweden). Disposable polystyrene columns (2ml) from Pierce (Rockford, Illinois, USA). A glass column (5cm length, 0.9cm id) was used to contain the resin when connected to the FPLC/Econo system. A CDM 83 conductivity meter from Radiometer (Copenhagen, Denmark) was also used in this study. Data analysis was performed on a Quattro Pro spreadsheet supplied by Borland International (Greens Hills, CA).

4.2.3 Preparation of immobilised polylysine resin

Full length polylysine resin was immobilised onto a Perloza matrix using the p-toluenesulfonyl chloride method for activating agarose (Nilsson and Mosbach 1980). Acetone and pyridine were dried and stored over molecular sieves (grade 4Å) before use. Perloza was solvent exchanged to dry acetone by washing the resin in four steps of increasing acetone concentration (30, 60, 80 and 100%) and finally by

washing three times with dried acetone. Dried Perloza (10 grams) was mixed with 2 g of tosyl chloride dissolved in 10 ml of dry acetone. Dry pyridine (2 mls) was then added to this solution. The mixture was then mixed by repeated inversion at room temperature for 1 hr. At the end of this time the resin was solvent exchanged to 1 mM HCl in four steps (30, 50, 70, 100% 1 mM HCl).

To quantify the amount of tosyl chloride on the matrix approximately 50 mg of the resin was suspended in 3 ml of 87% glycerol and the absorbtion spectra between 250 to 300 nm was measured using unmodified Perloza as a blank. The extinction coefficient of the tosyl group on the resin at 261nm was taken as 480 M/cm.

The tosylated resin (7 grams) was suspended in 5 ml of coupling buffer (0.1 M phosphate buffer pH 7.5) and 62 mg of polylysine was then added. The mixture was then mixed by inversion at room temperature for 48 hours. At the end of the procedure, the resin was washed with 20 gel volumes of each the following solutions: 0.1 M $NaHCO_3$, 0.5 M NaCl and 1 mM HCl.

The amount of polylysine immobilised the resin was assessed by three tests: ninhydrin (Section 3.2.3), picrate (Section 3.1.2.4) and quantitative aminoacid analysis (Section 3.2.5.4). For the quantitative amino acid analysis an internal standard (norleucine) was included in the digestion stage. All tests were performed in duplicate.

4.2.4 Binding of GAG standards to polylysine resins

4.2.4.1 Binding and elution experiments

Each resin (1 ml) was loaded into a glass minicolumn and the column fitted to an FPLC. The resin was then equilibrated to a 20 mM Tris.HCl buffer at pH 7.5. An aliquot of pure GAG standard was loaded onto the column (typically 100 µl of 10 mg/ml). Unbound GAG was removed by washing the resin with loading buffer. Bound GAG was eluted with a linear salt gradient (Figure 4.1 and Table 4.1), the

flow rate was 1.5 ml/min. Fractions were taken at 2 minute intervals with a fraction collector. To study the effect of the slope of the salt gradient on the elution of the different GAG classes from the K_4G resin, two salt gradients were investigated (column 2 and 3 of Table 4.2). Each resin was examined for its ability to bind each of the GAG standards characterised in Chapter 2.

Figure 4.1: Shape of gradients used in resin binding experiments

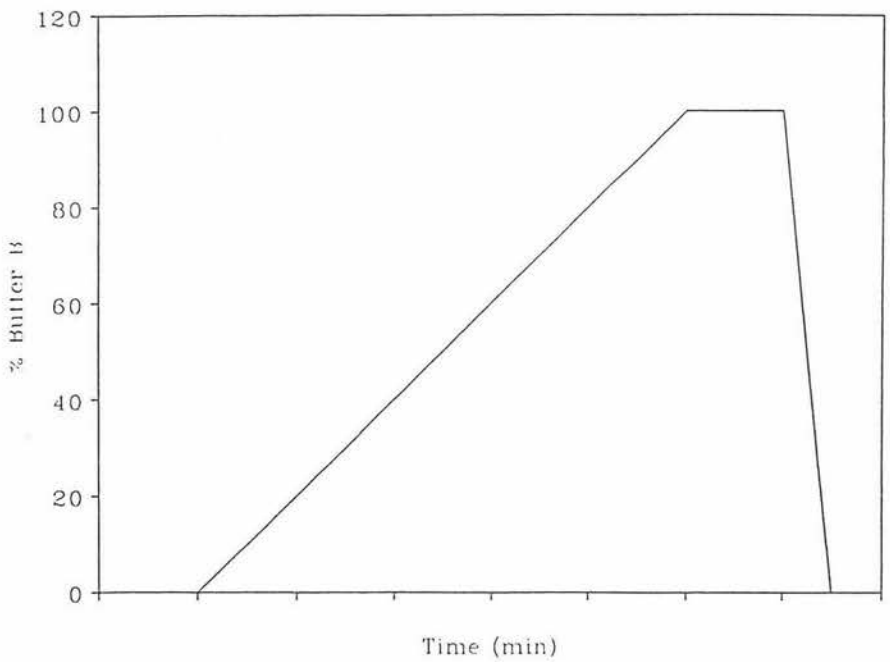

The relative salt concentration of each of the fraction was determined by measurement of the conductivity of the fractions. Relative GAG concentrations were measured by the dimethylmethene blue dye binding assay (Section 2.2.4.7). Fractions having absorbances above the background were pooled and retained for quantitative analysis of the amount of the GAG in the sample.

4.2.4.2 Data analysis

To facilitate the comparison of the GAG binding ability of the peptide resins and the full length polylysine resin, the relative binding strength of each resin for each GAG standard was calculated. The method of the calculation is outlined below. The elution curves for each GAG standard were analyzed using Quattro Pro spreadsheet software. Absorbances of adjacent fractions having an absorbance above the background were added obtaining cumulative absorbances for eluted GAG at each fraction. These were used to calculate the percent elution of GAG at each fraction, and were plotted versus the salt concentration. The salt concentration required to elute 25, 50 and 75% of the bound GAG was determined by interpolation. The relative binding strength of each resin for a particular GAG was determined by dividing the salt concentration required to elute 50% of the bound GAG by the salt concentration required to elute the same proportion of bound chondroitin sulphate.

Table 4.2: Details of gradients used in resin binding experiments

	Resin				
	K_4G	K_4G	K_8G	$K_{12}G$	PLL
A (min)	10	10	10	15	15
B (min)	60	30	30	45	60
C (min)	10	10	10	10	10
D (min)	5	5	5	5	5
Maximum Concentration of NaCl (M)	2.00	2.00	2.00	3.00	3.00
Gradient slope (M/min)	0.033	0.066	0.066	0.066	0.05

4.2.5 GAG binding capacities of the peptide resins

A known weight of each peptide resin (typically 0.4 g) was loaded into a disposable polystyrene minicolumns. Each column was then equilibrated to loading buffer. The

column was then overloaded with GAG standards (typically 1.5 ml of 10 mg/ml GAG) and washed with loading buffer to remove any unbound GAG. Bound GAG was then eluted by washing with the elution buffer until no more GAG eluted. Washings were pooled and made up to 25 ml. The eluted GAG were then measured quantitatively using the dimethylmethene blue dye binding assay (Section 2.2.4.7). The amount of bound GAG was then related to the amount of wet resin in the minicolumn. GAG capacity experiments were typically performed in triplicate.

4.2.6 Ligand displacement chromatography on PLL-resin

A mucopolysaccharide solution (150 µl at 26 mg/ml) was injected onto the PLL column. The column was washed with loading buffer (20mM Tris.HCl pH 7.5) for 10 min at 1.5 ml/min. The procedure was repeated with a second injection (150 µl at 26 mg/ml) of the mucopolysaccharide solution. Bound GAG was eluted with a 60 min gradient from 0 to 3 M NaCl gradient run, at 1.5 ml/min, and with 2 min fractions being taken. Data analysis was the same as in Section 4.2.4.2. After elution the bound and unbound GAG's were concentrated and dialysed four times by ultrafiltration and the identity of the GAG fraction was examined by cellulose acetate electrophoresis (Section 2.2.4.1).

4.3 RESULTS AND DISCUSSION

4.3.1 Immobilisation of polylysine (PLL)

Polylysine was immobilised onto Perloza to a low but measurable level (Table 4.3). All three assay methods agreed within experimental error. The level of lysine immobilised (2.2 mg/g) was comparable to the level used by Suzuki and Koide, 2.8 mg lysine/ml. It is thought that the displacement of tosyl chloride from the resin by polylysine requires that the amino groups be uncharged. Under the condition used in the coupling (i.e. pH 7.5) more than 99.9% of the ε-amino group will be charged, whereas 50% of the α-amino group is uncharged, since the pK_a of the α-amino and ε-amino groups of lysine are 7.7 and 10.3 respectively (Richard et al 1991). The

immobilisation conditions should favour single point attachment i.e. at the α-amino group at the end of the polypeptide chain. However it should be pointed out that while every effort was made to ensure that single point attachment occurred, low levels of multiple attachment may be still possible.

Table 4.3: Substitution level of PLL resin

Assay Method	Amine Substitution (µmol/g dry resin)	Error (µmol/g)
Picrate	17.0	6.0
Ninhydrin	18.4	0.5
Amino acid analysis	16.6	0.7

4.3.2 Validation of relative binding strength

The GAG elution data was examined to determine if a method to measure the relative GAG binding ability of the peptide resin (that was independent of the gradient used for elution) could be formulated. The relative binding strength was defined as the salt concentration required for 50% elution for a GAG divided by the concentration of salt required for 50% elution of the bound chondroitin sulphate to the same column. This parameter was required to enable comparisons of the peptide and polylysine resin GAG binding data with the published GAG binding data of Gelman and Suzuki (Sections 1.1.3.6 and 1.2.3 respectively). The elution of bound dermatan sulphate and heparin from K_4G resin under two conditions, with similar column geometries but different gradient slopes were examined the results are outlined in Table 4.4, full details are shown in Table A3.1 and A3.2 of Appendix 3.

As can be seen from the results in Table 4.4 the slope of the gradient affects the position of the elution of the respective GAG standards. However the relative binding strength appears to be independent of the slope of the gradient and column geometry within the limits of this study. The results for heparin were similar under the two different conditions used for elution (mean relative binding strength of 1.50 with and error of 0.12.

4.3.3 Binding of GAG standards to PLL-resin

The immobilised polylysine resin binds the GAG standards to different extents as can be seen in Figure 4.2. The average salt strengths for 25, 50 and 75 % elution of each of the GAG standards are shown in Table 4.5 (full details in Table A3.6 of Appendix 3). The relative binding strengths of the individual GAG classes examined increases with the increasing charge density of the GAG chain.

Table 4.4: Validation of relative binding strength for K_4G resin

GAG	Number of runs	Gradient slope	$M_{0.50}$	R.B.S.	Instrument used
CS	2	Shallow	1.29(0.08)		Econo system
Hep	2		1.74(0.02)	1.41 (0.10)	
CS	1		1.16		FPLC
DS	1		1.64	1.41	
CS	1	Steep	1.04		
DS	1		1.49	1.43	
Hep	2		1.66(0.02)	1.59 (0.02)	

Key: CS, Chondroitin sulphate, DS dermatan sulphate, Hep heparin, $M_{0.5}$ molarity of salt required to elute 50% of the bound GAG, percentage error shown in brackets. Shallow and steep gradients were 0.033 and 0.066 M/min respectively, see Figure 4.1.
RBS; Relative binding strength.

The range over which the GAG standards were eluted was broad. As can be seen from the table, 50% of the bound GAG (i.e. 25 to 75% cumulative elution) was typically over a 0.5 M salt concentration range. As a result the elution of a GAG mixture will only result in an enrichment of a particular GAG rather than a single step purification.

4.3.4 Binding and elution of GAG standard from K_xG peptide resins

A summary of the salt concentration required for 25, 50 and 75% of the bound GAG for each of the K_xG peptide resins synthesized are displayed in Table 4.6. Full data

on all runs are displayed Section A3.2 of Appendix 3. As can be seen from the results the relative binding strength for both dermatan sulphate and heparin did not significantly change with the increasing length of the lysine chain (over the range examined).

Table 4.5: Elution of GAG standards from PLL-resin

GAG	$M_{0.50}$	Range	R.B.S (error)	GAG capacity mg/g
CS	0.56	0.46		14 (0.6)
DS	0.79	0.49	1.41 (0.18)	18 (1.0)
Hep	1.10	0.50	1.96 (0.30)	13 (2.0)

KEY: CS; Chondroitin sulphate, DS; Dermatan sulphate, Hep; Heparin. RBS; Relative binding strength; salt concentration for 50% elution for a GAG divided by the concentration for 50% elution of the bound chondroitin sulphate. The error in the GAG capacity determination for each K_xG-resin is within the brackets. $M_{0.50}$: salt strength required for elution of 50% of the bound GAG. Range is the salt concentration range over which the elution of 25 to 75% of bound GAG occurs.

Table 4.6: Summary of elution experiment on peptide resins

Resin	GAG	$M_{0.50}$	Range	GAG capacity (mg/g)	R.B.S
K_4G	CS	1.04	0.58	36 (5)	1.00
	DS	1.49	0.40	44 (4)	1.43 (0.02)
	Hep	1.56	0.52	58 (1)	1.50 (0.12)
K_8G	CS	1.16	0.65	42 (7)	1.00
	DS	1.61	0.44	31 (3)	1.39 (0.03)
	Hep	1.69	0.53	39 (4)	1.46 (0.06)
$K_{12}G$	CS	1.68	0.39	39 (2)	1.00
	DS	2.24	0.28	38 (1)	1.33 (0.13)
	Hep	2.26	0.30	41 (3)	1.34 (0.10)

KEY: CS; Chondroitin sulphate, DS; Dermatan sulphate, Hep; Heparin. R.B.S: relative binding strength; salt concentration for 50% elution for a GAG divided by the concentration for 50% elution of the bound chondroitin sulphate. The error in the GAG capacity determination for each K_xG-resin is within the brackets. $M_{0.50}$: salt strength required for elution of 50% of the bound GAG. Range is the salt concentration range over which the elution of 25 to 75% of bound GAG occurs.

Figure 4.2: Elution of GAG standards from PLL-resin

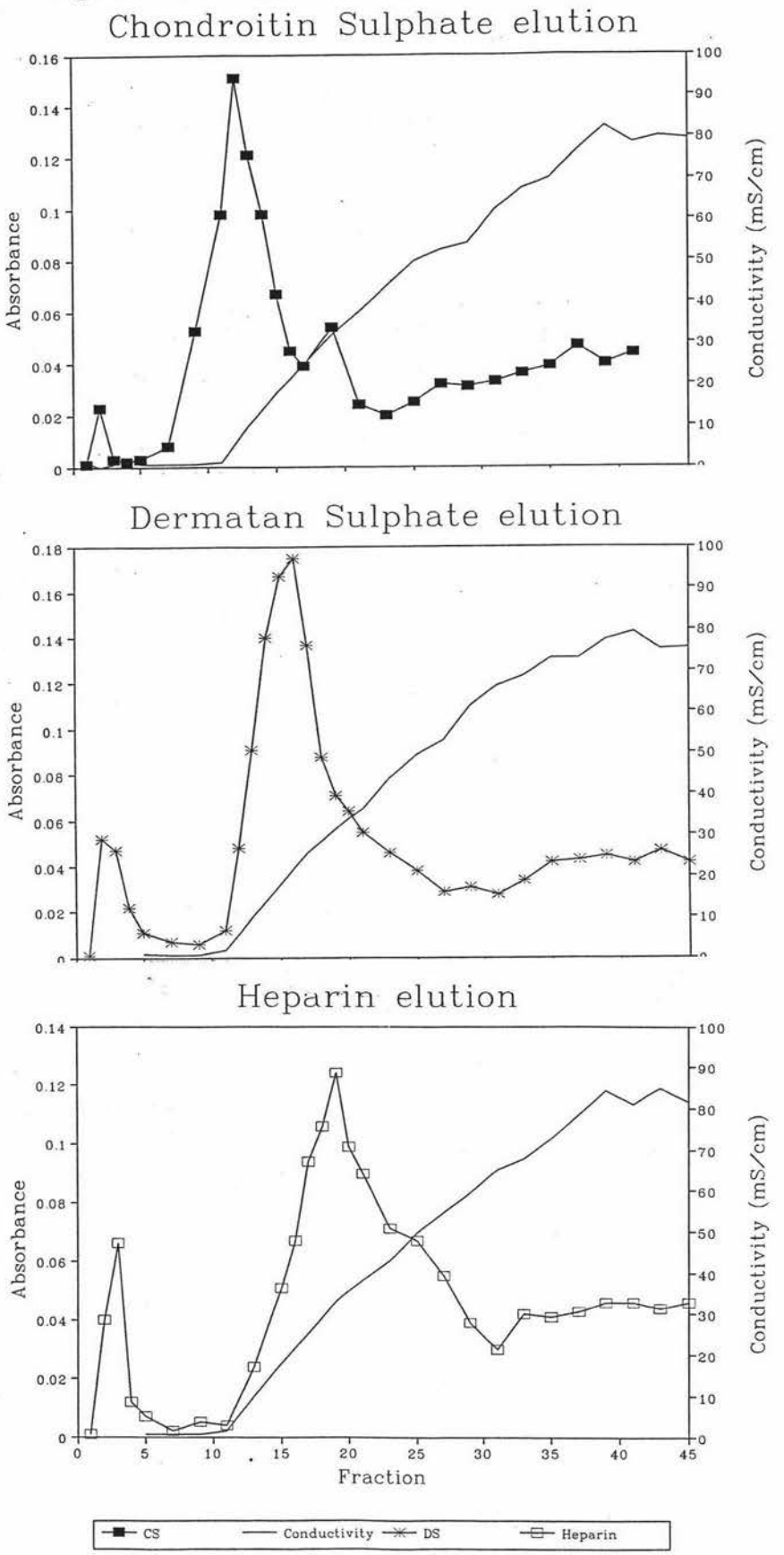

In addition the relative binding strength of the three resins of the K_xG series for the different GAG standard is identical within experimental error. The maximum binding capacity for these peptide resins for each of the GAG standards (column 5, Table 4.6) was measured by overloading the columns with the respective GAG samples and then measuring the amount of GAG eluted by 3M salt.

4.3.5 Comparison of the binding behaviour of the PLL-resin and K_xG resins

The main difference between the K_xG-resins and the polylysine resins synthesized by Suzuki and Koide (1984a and 1984b) is that the K_xG-resins bind dermatan sulphate to a different extents. A comparison of the relative binding for dermatan sulphate for polylysine in solution and bound to a solid support is shown in Table 4.7. All three K_XG-resins that were synthesized did not bind dermatan sulphate more strongly than heparin, as expected on the basis of Gelman's studies (Section 1.1.3.6). In addition the binding behaviour of dermatan sulphate on the PLL-resin and K_xG-resins were identical (within experimental error), and the mean of the relative binding strengths for all of the K_xG series of resins was between that of Suzuki and Koide's PLL resin and Gelman's solution binding experiments. The charge density of the dermatan sulphate used in this study differed for the dermatan sulphates in the published work: 1.2 versus 1.0 and 1.4 respectively. The relative binding strength of heparin on the PLL-resin synthesized was significantly different from the K_xG series of resins (1.96 versus 1.46), and was similar to the published resin binding data, despite the fact that the charge density of the heparin was significantly less (2.25 versus 2.80).

A number of explanations can be invoked to rationalise the differences in the binding of dermatan sulphate between the solution binding data (Section 1.1.3.6) and resin bound PLL, both in the case of the published work (Suzuki and Koide 1984) and this thesis. These include:

- The binding of the dermatan sulphate could be dependant on the charge density of

the GAG chain which can vary for samples from different sources/isolation methods.

- The mode of the binding of GAG to the polylysine chain in solution may be different to the situation with resin bound polylysine chains.
- The differences in the binding of heparin to K_xG and PLL resins could be dependant to a chain length dependence, and the K_xG studied could all be too short.

Table 4.7: Comparison of GAG binding

	Dermatan sulphate charge density	R.B.S.	Heparin charge density	R.B.S
Suzuki's	1.00	1.05	2.80	1.57
Gelman's	1.40	>2.50	2.30	1.88
PLL-resin	1.20	1.4 (0.17)	2.25	1.96 (0.30)
K_4G-resin		1.42 (0.02)		1.50 (0.12)
K_8G-resin		1.39 (0.03)		1.46 (0.06)
$K_{12}G$-resin		1.33 (0.13)		1.34 (0.10)

Note: The error in the RBS (relative binding strength) determination is shown within the brackets.

The charge density of a GAG class has been related to the binding affinity of that class in particular situations. For example the binding of chemically modified chondroitin sulphate, dermatan sulphate and heparin to low density lipoproteins has been studied (Gigli et al 1992, 1993). Within each GAG class in this application a linear correlation between the charge density and the binding affinity was found. In the case of dermatan sulphate when the charge density was increased form 1 to 2, the binding affinity increased by 2 orders of magnitude, while chondroitin sulphate under the same conditions increased its binding by only 1 order of magnitude. Similarly for heparin when the charge density was increased from 2 to 3 the binding affinity increased by 1 order of magnitude. It is possible that the different charge densities of dermatan sulphate used in this study (1.2) when compared to those used in the published studies (1.4 and 1.0) could explain the differences in the relative binding strength results of dermatan sulphate and heparin. It is considered by the writer however unlikely that the low relative binding strengths were low solely due to the

above effect.

The alternative explanations for the differences in the binding strengths of dermatan sulphate and heparin can be examined experimentally. To examine the mode of binding of the resin bound polylysine chains, the stoichiometry of binding can be compared to the solution binding experiment. If the mode of binding is radically different, the stoichiometry of binding would be expected to change. Using the GAG binding capacities of the resins along with the lysine substitution levels, the stoichiometry of the GAG/polylysine interaction, in terms of the number of lysines in the polylysine chain bound per disaccharide unit can be calculated. A sample calculation is shown in Section A3.2 of Appendix 3. The results of these calculations are shown in Table 4.8.

Gelman's group expressed the stoichiometry of the GAG/PLL interaction in terms of the number of lysines bound per disaccharide unit. The binding of the GAG standards to the K_xG series resins is of the same order of magnitude as the original solution binding studies (Column 6 Table 4.8), whereas the PLL resin bound less than one twentieth of the levels expected on the basis of the solution binding results. As can be seen from the results in Table 4.8, there are fundamental differences between the two types of resin synthesized (K_xG series and PLL-resin). The binding stoichiometry results do not follow the same trend as the solution binding results with an increasing number of disaccharides are bound as the charge density of the GAG is increased (i.e. Hep > DS > CS).

The CS standard used in this study bound to the short PLL chains at a higher level than the solution binding studies (Blackwell et al 1977). The situation with DS was such that the K_8G and $K_{12}G$ also bound to a greater amount, whereas the K_4G result was within experimental error. A similar situation exists for the binding of heparin by the K_xG series resins, with the K_4G resin binding to a significantly different level from the remaining two resins.

Table 4.8: Stoichiometry of GAG binding to polylysine resins

GAG Class	Resin				Solution binding (Gelman et al)
	K_4G	K_8G	$K_{12}G$	PLL	
CS	1.55 (0.22)	1.44 (0.24)	1.81 (0.09)	0.040 (0.002)	1
DS	1.36 (0.12)	2.1 (0.2)	2.00 (0.05)	0.036 (0.002)	1.4
Hep	1.2 (0.02)	1.96 (0.21)	2.18 (0.34)	0.056 (0.010)	2.3

NOTE: The relative error for each figure in the Table is recorded within the brackets

The binding of more lysine per disaccharide unit to the K_xG series resins compared to the earlier solution binding studies can be explained in two ways. Firstly the binding of the short PLL chains could occur in such a manner that more than one PLL chain could bind to the same GAG chain, at different points on the GAG chain. If this did occur the remaining sections of the GAG will be immobilised so that any further binding of the short K_xG chains will be hindered. An alternative explanation could be that the PLL chain in the K_xG series resin, may be unable to adopt an α-helical conformation upon binding GAG's. If the binding was associated with in the extended chain form or ß-strand conformation of the peptide, the lysine chain would bind over a greater contour length of the PLL chain.

The rise per residue for a polypeptide chain folded into an α-helical or a ß-strand conformations are 1.5 and 3.3 Å respectively (Schulz and Schrimer 1979). If the short K_xG chains adopt a ß-strand conformation on binding CS and DS, the stoichiometry would be expected to be approximately double i.e. for CS, DS and Hep the values should be 1.8, 2.6 and 4.2 respectively. The results for the K_8G and $K_{12}G$ resins are slightly lower than this prediction. This suggests that any differences in the mode of binding between the solid phase and the earlier solution binding studies could explain the increased results of the binding stoichiometry.

4.3.6 PLL-resin: Ligand displacement chromatography

The GAG binding behaviour of the synthesized PLL-resin was examined further by ligand displacement chromatography to see if the resin was able to separate dermatan sulphate and chondroitin sulphate mixtures. Ligand displacement chromatography is used when the different ligands bind to an affinity resin to different extents. If the column is deliberately overloaded, the ligand with a higher affinity is able to displace the ligand with a lower affinity. After loading, the resin is washed with loading buffer to remove any unbound ligand. Bound ligand is then eluted by increasing the ionic strength. Ligand displacement chromatography has been used for separation of heparan sulphate and chondroitin sulphate proteoglycans on an immobilised lipoprotein lipase affinity column (Section 1.2.5). The results of the example discussed in Section 1.2.5 (Klinger et al 1985) can be explained in two ways. The behaviour may be due to preferential binding of heparan sulphate proteoglycans (HSPG's) compared to the chondroitin sulphate proteoglycans (CSPG's), or the HSPG's may be able to displace any bound CSPG's. From the results presented by the authors in this paper, it is impossible to differentiate these two possibilities. However the inability to rationalise the exact results is unimportant since the column is able to effect separation that are impossible by conventional means.

In the examples being presented in this thesis the two ligands are CS and DS, the two major components of the mucopolysaccharide mixture. After overloading the column (as described in Section 4.2.6) the bound GAG's were eluted with salt (Figure 4.3) and characterised in two ways. The mean relative binding strength was calculated for the results of four experimental runs as being 1.48 (with an uncertainty of 0.1). The result was identical to the relative binding strength of dermatan sulphate, suggesting that under these conditions dermatan sulphate was preferentially bound. As an additional test electrophoretic analysis of the bound GAG fraction (data not shown) indicated that this fraction was pure dermatan sulphate (no visible chondroitin sulphate bands with a 5 ug loading). The PLL-resin synthesized was able to separate CS and DS from a mixture, however the separation of the components may also be achieved by classical ion exchange technology.

4.3.7 CHAPTER SUMMARY

The GAG binding results for both the K_xG series and the PLL resin synthesized and characterised in this thesis were different from the earlier reported solution binding studies of GAG binding to PLL. The behaviour of immobilised PLL resin was similar to the behaviour of the previously published PLL column work (Suzuki and Koide 1984a and 1984b). In both cases the binding of dermatan sulphate was between the results between the earlier solution and resin bound PLL chains. The binding of heparin by these resin was more complicated, in that the K_xG series resins had the same relative binding strength for both heparin and dermatan sulphate. The PLL-resin synthesized had a relative binding strength for heparin that was identical to the earlier solution binding studies. The relative binding strength for dermatan sulphate result was less than heparin's, which is similar to the behaviour exhibited by Suzuki and Koide's PLL resin.

Figure 4.3: Typical profile for PLL-resin with ligand displacement chromatography

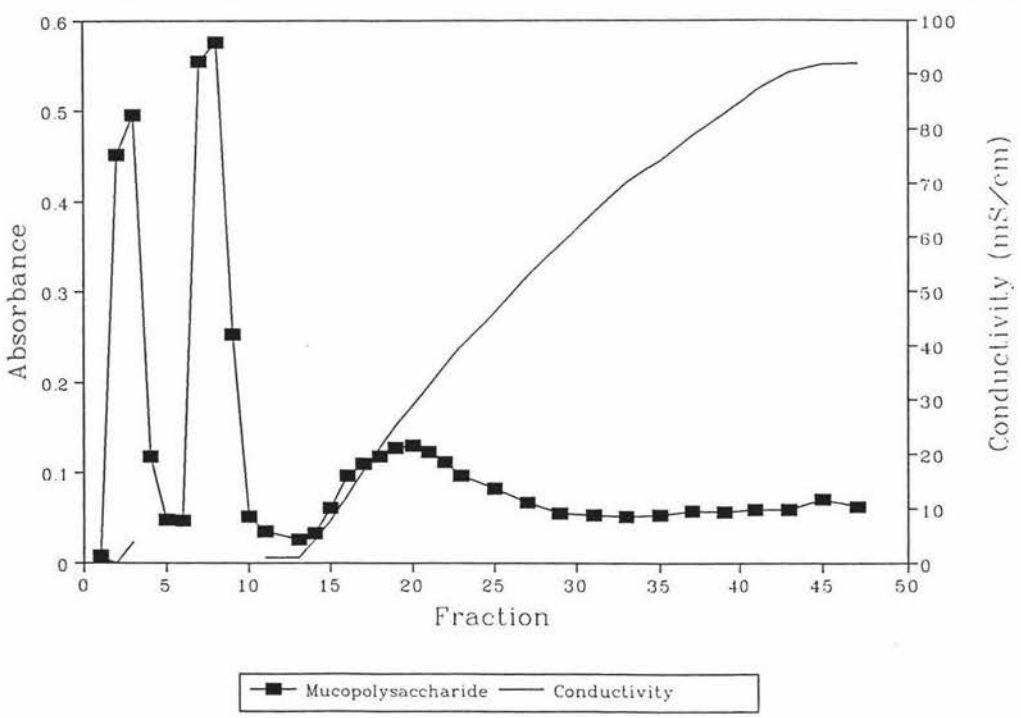

The failure of this study to reproduce the earlier solution binding interaction with resin bound polylysine chains could be due to a number of reason. These include:

- The binding of the dermatan sulphate could be dependant on the charge density of the GAG chain.
- The mode of the binding of GAG to the polylysine chain in solution may be different to the situation with resin bound polylysine chains.
- The differences in the binding of heparin to K_xG and PLL resins could be dependant to a chain length dependence, and the K_xG studied could all be too short.

The stoichiometry of the interaction between the GAG chains and the immobilised polylysine chains for the K_xG series of resins was measured and found to be significantly different to the earlier work. These results suggest that the mode of binding may indeed be different with short polylysine chains. To understand the reason for the differences in the behaviour of the polylysine resin when compared to solution binding data, the interaction of the GAG standard with polylysine (both the full length PLL chains and the K_8G) in solution was undertaken in Chapter 5.

Chapter 5: SOLUTION BINDING OF GAG'S TO PEPTIDES

5.1 INTRODUCTION

The binding of GAG's to proteins has been divided into two types: cooperative electrostatic binding and sequence specific binding (Section 1.3). It is important for a variety of reasons to be able to differentiate these two kinds of binding. Is the binding of the GAG to the peptide, sequence specific or is it occurring thorough cooperative electrostatic binding?. If the binding constants of GAG's to peptides are able to be measured, they may be able to answer this question. Other questions that **must** be answered to aid in the selection of peptides for use in immobilised peptide chromatography are as follows:

- Is the binding of the peptide just a function of the charge density of the GAG chain (i.e. cooperative electrostatic binding) ?

- Does the molecular weight of the GAG have any effect on the binding behaviour of a particular GAG class (i.e. cooperative electrostatic binding) ?

- Is their a single binding constant for a particular GAG type (i.e. implies cooperative electrostatic binding)?

A positive answer to these questions implies that the specificity of the peptide/GAG interaction is not very high. Immobilization of peptides of this type, for the fractionation of GAG would probably serve no useful purpose i.e. will probably be no better than other separation protocols that are available at present. If the peptide has more than one binding constant for a particular GAG class, this implies that sequence specific binding is probable. Sequence specific binding would probably also be of limited use for the fractionation of GAG mixtures since the peptide would probably only bind a subset of the chains of a particular GAG class. This would be particulary true for infrequent sequences in the GAG chain e.g. ATIII high affinity pentasaccharide binding sequence which occurs in only 30% of heparin chains

(Section 1.3.1).

Two techniques were used to study the interaction of the GAG's standards with the peptides synthesized in solution. These were as follows:

- A circular dichroism (C.D.) study to determine the solution conformation of the peptides when complexed to the different GAG standards (characterised in Chapter 2).
- The stoichiometry of the GAG binding to the peptide after forming the complex was also examined using a previously published assay (Stone and Epstein 1977).

Cardin and Weintraub suggested in their initial paper on consensus sequences in protein for GAG binding (Cardin and Weintraub 1989) that the consensus sequences of GAG/heparin binding sites were expressed on amphipathic helices or amphipathic beta strands. The existence of amphipathic helices has long been known and are probably common, since approximately 50% of helices in a sample of 115 helices with more than seven residues (from 21 proteins) were found to be amphipathic (Cornette et al 1987). Periodicity in the amino acid sequence for hydrophobic and hydrophillic amino acids is reflected in amphipathic helices (and ß-strands) when they fold into an α-helix (or ß-strand).

Eisenberg and coworkers (Eisenberg et al 1984) have treated the hydrophobicities of the amino acids as vector quantities. A periodic structure of a polypeptide chain can be specified by m, the number of residues per turn (equation 5.1). The vectors of the hydrophobicity for each amino acid along a section of a polypeptide chain in a defined secondary structure can be added to yield the hydrophobic moment of the section of polypeptide in this secondary structure.

Equation 5.1:

$$\delta = \frac{2\pi}{m}$$

where δ is the angle in radians at which successive side chains emerge from the

backbone. In an α-helix δ is 100° and m is 3.6, whereas in a ß-strand δ is in the range 160 to 180° and m is in the range of 2.0 to 2.3.

The different secondary structures, in both model peptides and in sections of secondary structure identified from X-ray structures of proteins, display characteristic hydrophobic moment profiles (Eisenberg et al 1984). The periodicity of the hydrophobicity within a sequence matches the periodicity of the secondary structure. For α-helical sections the maximum in the hydrophobic moment profile is at (or near) 100 degrees. Similarly for ß-strands the maximum is at (or near 160 degrees) and finally with a polypeptide folding into a 3_{10} helix (a secondary structure with a 3 residue repeat) the profile has a maximum near 120 degrees.

The widely used method of helical wheels (Schiffer and Edmundson 1967) to demonstrate the partitioning of polar and nonpolar residues onto different sides of the α-helix has been criticized on statistical grounds (Flinta et al 1983). The authors tested the significance of the idea of amphipathic helices by generating peptide sequences by computer stimulation (all with 18 residues). The number of polar residues was varied from 2 to 9, and for each number of polar residues 10,000 random sequences were generated. Partitioning of the polar residues was examined by two methods. The first is the helical wheel method where the helix was cut along its length to maximise the hydrophobicity difference between the sides. Helical hydrophobic moment analysis at 100° was also performed. Surprisingly **only** 6% of the randomly generated helices with 2 polar residues were of the unbiased kind. Even with 7 polar residues there is still a 2% probability that the seven polar residues could occur on the same side of the helix by chance. These stimulations demonstrated that the helical wheel method is a **poor** method for detecting amphipathic helices, as it has a strong bias for the attribute it sets out to measure. The hydrophobic moment at 100° was considered to be a better method to detect partitioning of the polar residues, as it was able to detect amphipathic helices with 4 or more basic residues. The use of hydrophobic profiles in the characterisation of amphipathic secondary structures (Eisenberg et al 1984), particulary in the calculation of amphipathic indexes for α-helices and ß-strands has been used in many

applications.

Hydrophobic moment profiles for each sequences of the peptides synthesized is this study were examined in an effort to predict the preferred secondary structure of the peptide.

5.2 MATERIALS AND METHODS

5.2.1 Chemicals

The following chemicals were supplied by Sigma (St Louis, USA): two lengths of polylysine (with 126 and 633 residues) as the hydrobromide salt, norleucine and tricine buffer (N-tris[hydroxymethyl]methyl glycine). Methylthene blue, certification grade 90% was supplied by BDH chemicals (Palmerston North, NZ). Analytical grade ammonium hydroxide was supplied by JT Baker chemical Co (Phillipsburg, New Jersey, USA). All solution unless otherwise indicated were made up in Milli Q water.

5.2.2 Equipment

A Jasco J-270 spectropolarimeter supplied by the Japan Spectroscopic Co Ltd (Tokyo, Japan) was used to measure the C.D. spectra of solution of peptides and peptide/GAG complexes examined during this study. Two spectrophotometers were used in this phase of the study; a Shimadzu UV-160 recording spectrophotometer supplied by Shimadzu corporation (Kyoto, Japan) and a Pye Unicam PU8610 kinetics spectrophotometer supplied by Pye Unicam (Cambridge, England). Cuvette stirrers (cell spinbars) were supplied by BioLab Scientific Ltd (Auckland, NZ). A 25µl microsyringe was supplied by Hamilton Company (Reno, Nevada, USA). Quattro Pro 4.0 spreadsheet data package was supplied by Borland International (Green Hills, California, USA). Eppendorf tubes (1.5 ml) were supplied by Scientific Supplies (Auckalnd, NZ).

5.2.3 Stoichiometry of GAG/peptide interaction

To establish the stoichiometry of the binding between the polylysine and the synthesized peptides with the GAG standards, a dye binding technique used for the measurement of the stoichiometry of the binding of cationic peptides to heparin (Stone and Esptein 1977) was modified slightly.

5.2.3.1 Purification of methylene blue

A common impurity of methylene blue is a demethylated compound having only three methylene groups instead of four. This impurity can be removed by solvent extraction of the methylene blue solution in dilute ammonium hydroxide as described (Bergmann and O'Konski 1963), with one modification: the solvent extraction was performed with toluene instead of benzene.

The purity of the product can be estimated from the ratio of the height d and e of the peak (typically 662 nm) and the inflection point (typically 683 nm) respectively obtained from the absorbtion spectra. Since all demethylation products of methylene blue have lambda maximum less than 665 nm, contamination with these demethylation products will results in lower R values.
Equation 5.2

$$R=\frac{d}{e}$$

The R vaules typically increase from 1.7 to 2.00 during the purification procedure.

5.2.3.2 Methylene blue titration

When free GAG's are added to a dilute solution of the cationic dye methylene blue (blue-green colour), a large metachromic spectral shift to the familiar purple-blue complex occurs. If the polypeptide (K_8G or PLL chains) binds to the GAG chain the

formation of the GAG-dye complex is blocked by the interaction of the GAG chain with peptide. Peptides were complexed with the relevant GAG in an incubation mixture in an Eppendorf tube (1.5 ml), typical mixtures consisted of:

20µl peptide solution (typically 5 mg/ml)
80µl Milli-Q water
400µl GAG solution (typically 10mg/ml)
500 µl 20 mM tricine buffer pH 7.4

A aliquot of a diluted methylene blue solution in 10 mM tricine buffer pH 7.4 (2.5 ml) was added to a 3 ml quartz cuvette and stirred with a micro cuvette stirrer. To establish the time taken for the complex to reach equilibrium, the peptide complex solution was titrated at 1, 2, 4 and 12 hours, in the manner described below. Small volumes (typically 2-20 µl) of the peptide complex solution were added to the cuvette with a micro-syringe. After each addition the solution was stirred for 5 seconds and the absorbance at 662 nm was measured. The time for equilibrium to be established is determined as a result of this experiments. The solution are allowed to stand for this time before the titration was performed, when determining the stoichiometry of the interaction.

5.2.3.3 Data Analysis

The absorbance of the solution at each stage was plotted versus the cumulative volume. The resulting curve was typically hyperbolic with two linear arms. The results for each arm were fitted to lines by linear regression. The intersection point of these two lines was taken as the end point of the titration. To obtain the end point for the blank complex mixture, the titration was repeated with an incubation mixture containing no peptide. The difference between the blank and complex end points allows the calculation of the amount of GAG complexed by a known amount of peptide (Section A4.3 of Appendix 4). To measure the time taken for the complex to reach equilibrium the amount of GAG complex per milligram of peptide at the various time intervals was calculated. Once the time taken to reach

equilibrium was established the assay was repeated using this time interval at various peptide loadings and the mean results calculated. Titrations were repeated with different peptide loadings until the stoichiometry of binding was measured to an acceptable level of uncertainty. The concentration of the peptide solution was determined by quantitative amino acid analysis (Section 3.2.5.4) with the addition of a known amount of norleucine in the hydrolysis mixture as a internal standard.

5.2.4 Secondary structure determination

To establish the secondary structure of the peptides, circular dichroism (C.D.) spectra of the peptides and peptide/GAG complexes were measured using quartz cuvettes with a 1 mm pathlength. In all cases far UV (185 to 250nm) spectra for the samples were measured using the parameters as outlined in Table 5.1.

The calibration of the instrument was checked by examining the spectrum of a 9 µg/ml solution of ammonium d-10-camphorsulfonate. All CD spectra scans were performed in 10 mM tricine buffer pH 7.5, since Tris buffer absorbs appreciably in the far UV wavelength range.

The effect of three GAG standards on the conformation of peptides in solution were examined. These were CS, DS and heparin. The preparations and/or characterisations of the GAG standards were described in Chapter 2. As a positive control the effect of binding of these GAG standards to two lengths of PLL (with 126 and 633 residues respectively) was measured. The characterisation of the binding of K_8G, PCI (residues 264-283) and thrombospondin peptide using the technique of CD to the GAG standards (prepared in Chapter 2) was also performed.

Stock solutions of the peptides synthesized for CD work were in the range of 1.7-7.1 mg/ml. The exact concentration used was dependant on the peptide used. To ensure the maximum possible binding of the peptide to the GAG, peptides were mixed with an excess of the respective GAG (exact excess dependant on the peptide used). A blank solution for each peptide/GAG combination was prepared containing all of the

relevant additions except that of the peptide. To obtain the CD spectra of the complex the spectra of the GAG blank was subtracted from the complex spectra.

Table 5.1: Set up parameters for CD analysis

Parameter	Value
Band width	1 nm
Slit width	Auto
Sensitivity	10 mdeg
Response	2 sec
Scan speed	20 nm/min
Step resolution	0.2 nm

After CD spectral analysis the solutions were concentrated to six times the level used in the CD analysis by rotary evaporation. The concentrated peptide solutions were subjected to quantitative amino acid analysis, using norleucine as an internal standard (Section 3.2.5.4).

The measured CD spectra were converted to mean residue ellipticities using the peptide concentration measured by quantitative amino acid analysis. The percentage of each secondary structure element (α-helix, ß-sheet, ß-turn, random/other) was estimated by using the Yang predictive protocol that was included on the software of the CD instrument (Yang 1985) with two constraints. These were that the proportion of each secondary structure element was greater than or equal to zero, and that the total of all the secondary structure elements was equal to one.

The salt strength required to dissociate the complex between PCI and DS or heparin was measured by the addition of aliquots of 3M sodium chloride to the incubation mixture. For the heparin complex the salt concentration range of 0 to 1 M was examined, whereas for dermatan sulphate the concentration range was 0 to 0.5 M. Because sodium chloride absorbs strongly at wavelengths less than 190 nm and gives rise to considerable noise in this region of the spectra. The complexes were only

scanned from 190 to 250 nm. Peptide concentrations were determined by quantitative amino acid analysis and the final spectra were displayed as elipticities.

5.2.5. Secondary structure prediction

The hydrophobic moment for each secondary structure (i.e. a particular δ angle) is able to be calculated by using the Fourier transform (equation 5.3), by substituting in the relevant amino acid sequence into the equation. The method of calculation of the hydrophobic moment used in this study was that of Eisenberg and coworkers (Eisenberg et al 1984) with two modifications (outlined below).

Equation 5.3:

$$\mu(\delta)=\sqrt{([\sum_{n=1}^{N} H_n \sin(\delta n)]^2+[\sum_{n=1}^{N} H_n \cos(\delta n)]^2)}$$

To examine the potential secondary structures of the peptides synthesized during this study the hydrophobic moment was calculated for a variety of angles over the range 0 to 180°. The hydrophobicity scale used in this analysis was the consensus scale of Eisenberg's group (Eisenberg et al 1984).

The two modification of the standard procedure for hydrophobic moment analysis (Eisenberg et al 1984) were made. These were as follows:

1. To ensure that the hydrophobic moment at 0° was zero, following the data treatment method of Cornette (Cornette et al 1987), the periodicity of the sequence was examined in terms of H_n-H (where H_n is the hydrophobicity of the amino acid at position n in the sequence and H is the mean hydrophobicity of the sequence). This was performed for two reasons:

   - Without this correction the graph of the hydrophobic moment versus the angle will have a large value at 0° and this may mask important periodicities.
   - It will disrupt the evaluation of the amphipathic indexes (defined in next

section).

2. To measure the tendency of a sequence to fold in either an alpha helix or beta strand, amphipathic periodicity indexes (AI) for each secondary structure were measured from the hydrophobic moment plot of the sequence over the 0-180°. The AI for alpha helixes and beta strands are defined below in equations 5.4 and 5.5 respectively.

Equation 5.4:

$$AI(\alpha)=\frac{(1/30)\int_{90}^{120}P(w).dw}{(1/180)\int_{0}^{180}P(w).dw}$$

Equation 5.5:

$$AI(\beta)=\frac{(1/20)\int_{160}^{180}P(w).dw}{(1/180)\int_{0}^{180}P(w).dw}$$

The alpha amphipathic index can vary from 0 (i.e. no peak) to 6 (all in α-helix region i.e. 90° to 120° range). Similarly the beta amphipathic index can vary from 0 (i.e. no peak) to 9 (all in ß-strand region i.e. 160° to 180° range). Amphipathic indices in either the α-helical or ß-strand regions are significant when the measured values exceed 2 i.e twice the value that would be expected if the peptide exhibited no preference for any secondary structure.

The hydrophobic moment for each angle was calculated on a Quattro Pro spreadsheet after substituting the relevant sine and cosine values for each angle into the spreadsheet. A sample calculation for one angle of one peptide is shown in Section A4.1 of Appendix 4. Because of the complexity of the calculation the analysis of all angles between 0 and 180° was not attempted. Rather the hydrophobic moments were calculated at 20 angles between 0 to 180°, viz 0,10,20...180 and 85,95,145 degrees respectively. The amphipathic indexes for alpha helix and beta strand were measured by quantifying the area under the plots of μ(δ) versus δ using equation 5.4 and 5.5.

5.3 RESULTS AND DISCUSSION

5.3.1 Hydrophobic profiles

This periodicity of hydrophobicity intrinsic in the amino acid sequence can be detected by hydrophobic moment analysis (Eisenberg et al 1984), using the Fourier transform. In an effort to quantify the relative tendencies of the peptide to fold into an alpha helix or beta sheet, the proportion of the area under the curve in the alpha helical and beta strand region of the curve was measured (Donnelly et al 1993 and Cornette et al 1987 respectively).

The hydrophobic moment profile over the range of 0° to 180° of the three free peptides synthesized during this study i.e K_8G, PCI (264-283) and thrombospondin are shown in Figure 5.1. To aid in the comparison of the hydrophobic moment of the peptides synthesized, the results are reported on a per residue basis. As can be seen from Figure 5.1, only one of the peptides [viz PCI (264-283)] had a prominent peak in the α-helical region. The lack of periodicity in the K_8G peptide was not surprising since the sequence is essentially a repeat of lysine. Polypeptides composed of the same residues (e.g PLL chains) have no distinct peak in their hydrophobic moment profiles. The thrombospodin peptide has a broad peak centred at 120^0, signifying a possible periodic structure with a three residue repeat.

To further characterise the hydrophobic moment profiles of the peptides used in this study, the amphipathic indices of each of these peptides in an α-helical and ß-strand conformation was measured. The results are shown in Table 5.2. Amphipathic indexes for five additional peptides known to bind GAG's, and for which the solution conformation of the unbound peptide is known are also shown. As can be seen from the Table, two of the peptides [thrombospondin and PCI (residues 264-283)] have amphipathic indices for the beta region less than one, indicating that ß-strand structures would not be expected to be dominant. In addition the AI(α) for all three peptides is less than 2 suggesting that all three peptides have no distinct tendency for α-helical conformation.

The conformation of the ATIII 123-139 fragment and a randomised version of the peptide with the same amino acid composition has been characterised by CD spectroscopy (Lellouch and Landsbury 1992). Both peptides had spectra that were typical of random conformations. The conformation of the two peptides when bound to heparin was also characterised. ATIII 123-139 had a ß-strand conformation whereas the randomised version exhibited no change in conformation.

Figure 5.1: Hydrophobic moment profiles for the peptides

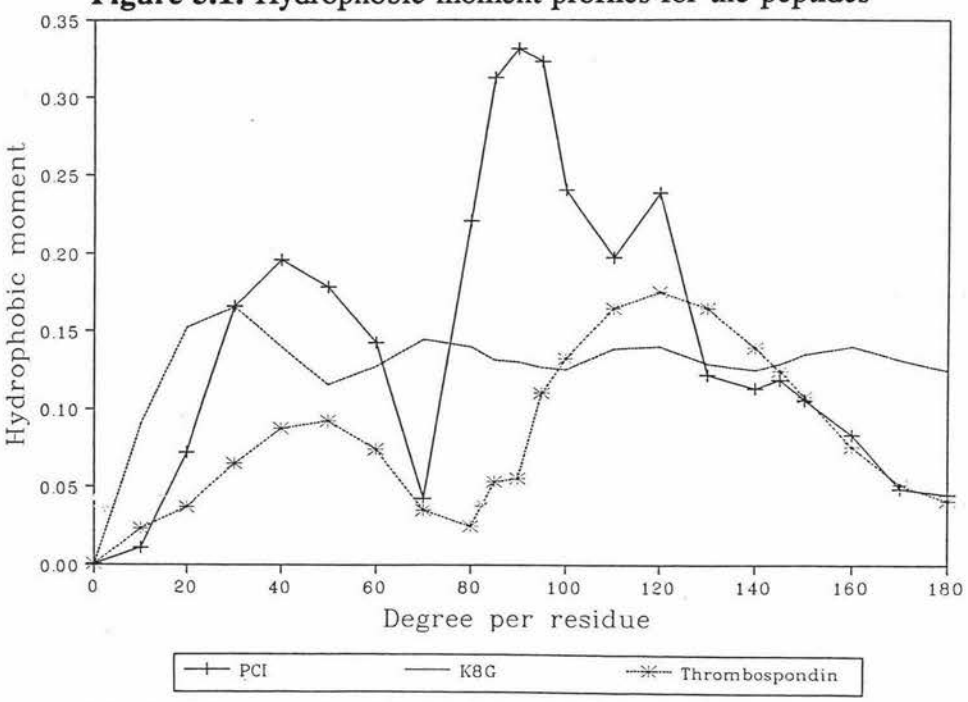

Table 5.2: Amphipathic indexes of GAG binding peptides

Peptide	AI(α)	AI(ß)	Source
Thrombospondin	1.955	0.662	This study
PCI	1.898	0.415	
K_8G	1.215	1.022	
ATIII 123-139	2.055	1.423	Lellouch and
AT III random	1.139	0.966	Landsbury 1992
FN-C/HII	0.854	0.498	Drake et al 1993
F9	1.466	1.378	Burke et al 1991
PF4	2.549	0.433	Pratt and Church 1992b

The platelet factor 4 peptide (residues 74-85) has a significant amphipathic index for the α-helical region. The C-terminal residues of the platelet factor 4 protein have been demonstrated to be in a α-helical conformation from X-ray crystallographic analysis (St Charles et al 1989). The molecule exists in a tetrameric form in its native state. Molecular modelling studies of the interaction of heparin with PF4 have been reported (Stuckey et al 1992). In this model the heparin binds to the α-helix at right angles, wrapping around the tetramer along a ring of positive charges, linked to all four lysines on the α-helix.

The conformation of a 15 residue fragment of fibronectin (FN-C/HII) has been characterised by H^1-NMR spectroscopy (Drake et al 1993). The analysis suggests the existence of multiple turns or helix in the C-terminal residues of the peptide. The conformation of the cell adhesion promoting peptide F9 (derived from laminin) has been characterised by both CD and H^1-NMR spectroscopy (Burke et al 1992). CD analysis indicated the existence of the secondary structures ß-strand, ß-turn and α-helix (in the ratios 30, 22 and 6%). NMR analysis supported these figures. The F9 peptide has been implicated in the binding of HS chains on the cell surface.

Amphipathic indexes for α-helix and ß-strand seem to have some value in rationalising the conformation of the peptide, since with the PF4 peptide which binds in an α-helical manner, the AI(α) is high. The ATIII random peptide has a decreased AI(ß) compared to ATIII 123-139, the latter peptide binding in a ß-strand conformation, whereas the former binds in a random conformation.

5.3.2 CD conformational study

5.3.2.1 Calibration of the technique

The calibration of the CD spectropolarimeter was judged to be satisfactory since the observed lambda maximum for d-10-camphorsulphonic acid (290.2 nm, error 0.2), was identical the published value. The molar ellipticities were also measured and were well within experimental error (2%) to the published values of (7910 and 7800

respectively).

The spectra of PLL when complexed to dermatan sulphate is different from the sum of the individual spectra of PLL and dermatan sulphate alone (data not shown). This indicates that some form of conformational change has occurred on the PLL chain and/or dermatan sulphate as a result of the binding. The assumption used by all authors to date when the discussing conformation of peptides upon binding GAG using CD is that all of the changes detected by CD are those associated to the peptide. It is thought that the CD spectra of GAG's (Figure 5.2) is essentially independent of the GAG conformation. This assumption allows the spectra of the protein/peptide component of the complex to be calculated by subtraction of the spectra of the GAG blank spectra from the complex spectra. Some experimental evidence for this assumption was found in the CD spectra of dermatan sulphate and heparin. The rotation of the DS and heparin samples was found to be essentially independent of the salt concentration (Table 5.3)

Table 5.3: Optical rotation of Dermatan sulphate and Heparin at 222 nm

Salt concentration (M)	DS rotation	Salt Concentration (M)	Heparin Rotation
0.00	-1.427	0.00	-1.009
0.05	-1.484	0.20	-1.143
0.10	-1.449	0.40	-0.989
0.15	-1.301	0.60	-0.947
0.20	-1.357	1.00	-1.090
0.50	-1.320		

Dermatan sulphate results: mean 1.39 (SD 0.074), coefficient of variation 5.3%
Heparin results: mean 1.026 (SD 0.079), coefficient of variation 7.7%

While there is some variation in the heparin results the overall the variation is within experimental error. The situation with dermatan sulphate is slightly more complex since the trend for a modest (12%) decrease in the rotation results was apparent over the salt range examined. It is thought that for dermatan sulphate to a first approximation the conformation is independent of the salt concentration, since the

variation is less than that encountered for heparin. These results are in agreement with the published experimental work that demonstrated that the CD spectra of heparin and C6S were insensitive to changes in ionic strength (Lellouch and Landsbury 1992).

Figure 5.2: CD spectra of GAG standards

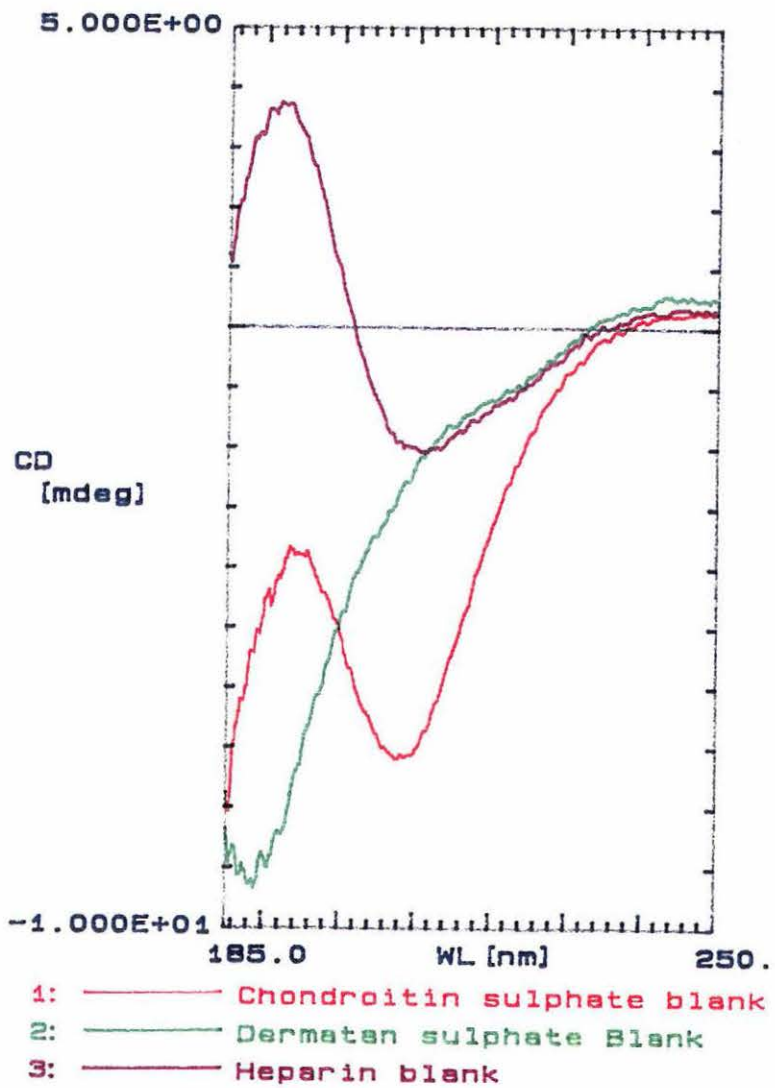

GAG concentration (mg/ml): 0.525, 0.493, 0.489, for CS, DS and Heparin respectively

The conformation of a section of a given polypeptide backbone exists in one of four different possible states: α-helical, ß-strand, ß-turn and random coil. The first three states are well known for their hydrogen bonding patterns, and the arrangement of the peptide backbone in three dimensions. The final state, the random coil is perceived as the conformation adopted by a polypeptide having no secondary structure at all. However it is not clear what this means exactly. Two extra points about the random coil clarify this however. Firstly it can be thought of as a range of conformational states with similar energy that are rapidly interconverting. Secondly NMR evidence supports the idea that the random coil exist 95% of the time in the ß strand region of the Ramachandran plot and most of the remaining time in the α-helical region (Williamson and Watts 1992).

5.3.2.2 Polylysine/ GAG interaction

As a check on the behaviour of the K_xG series resins the conformation of K_8G in solution and when complexed to the GAG standards was undertaken. As positive controls two lengths of polylysine (126 and 633 residues) were complexed to the GAG's and the results compared to Gelman's study (Section 1.1.3.6). Gelman's group used PLL with 500 residues is their studies. The PLL samples used in this study are either side of this value. The results for the two lengths of PLL binding to CS, DS and heparin are shown in Figures 5.3, 5.4 and Tables 5.4 and 5.5, respectively.

Both lengths of PLL displayed measurable amounts of secondary structure in the absence of GAG being complexed to them (29.3% α-helix and 28.4% ß-turn respectively). These results are not surprising by themselves because it is well known that the solution conformation of PLL at neutral pH is ordered. The electrostatic repulsion between the charged side chains forces the polypeptide chain into an extended helical conformation with 2.5 residues per turn.

Figure 5.3: CD spectra of long PLL/GAG complexes

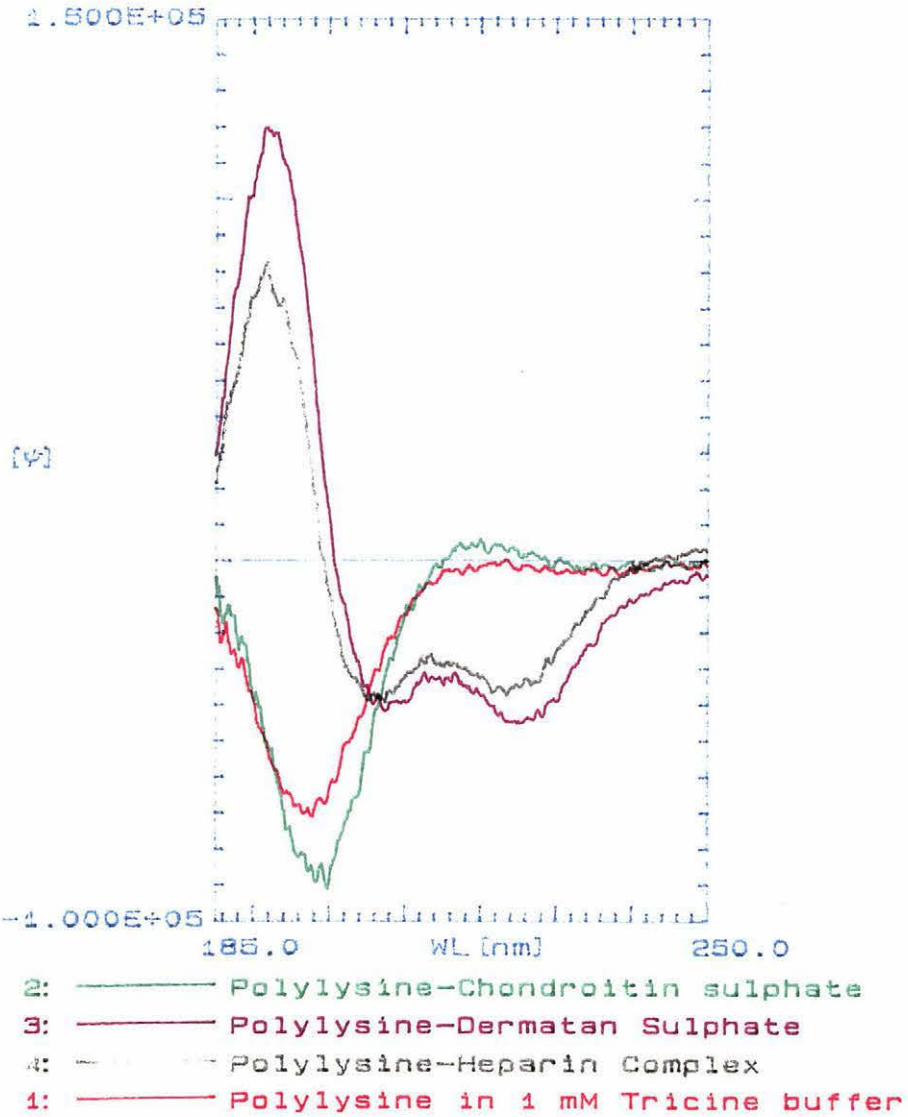

PLL concentration 0.057 mg/ml, peptide/GAG weight ratio(mg GAG/mg PLL): CS 3.5, DS 1.3, Hep 4

Table 5.4: Secondary structure elements for long PLL/GAG complexes

PLL (long) complex	% α-Helix	% ß-Turn	% ß- Strand	% Random	R.M.S.
PLL alone	0	28.4	8.9	62.8	23.9
CS	0	0	34.2	65.8	68.3
DS	69.7	0	0	30.3	13.1
Heparin	74.4	25.6	0	0.0	30.9

Figure 5.4: CD spectra of short PLL/GAG complexes

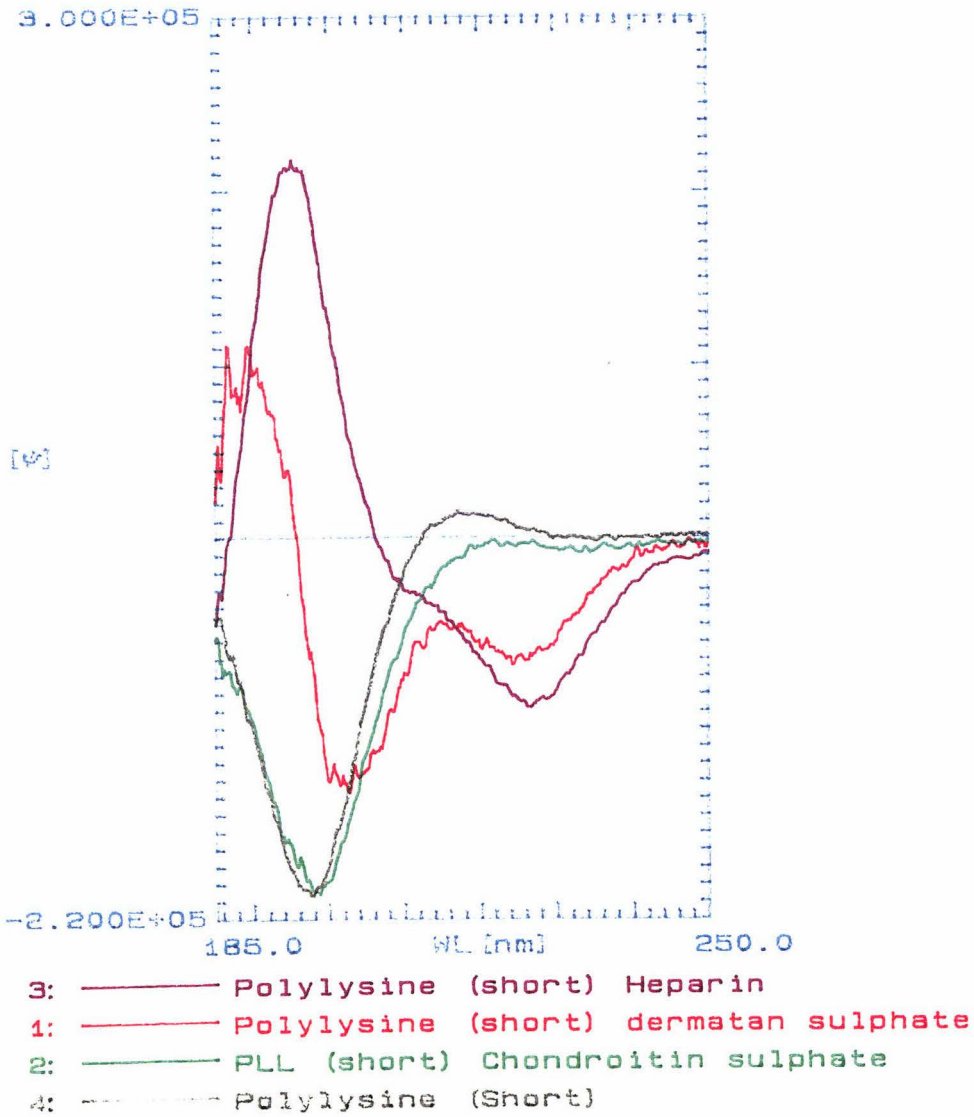

PLL concentration 0.041 mg/ml, peptide/GAG weight ratio(mg GAG/mg PLL): CS 3.3, DS 3.3, Hep 6

Table 5.5: Secondary structure elements for short PLL/GAG complexes

PLL (short) complex	% α-Helix	% ß-Strand	% ß-Turn	% Random	R.M.S.
PLL alone	29.3	0	0	70.7	75.6
CS	0	48.1	0	51.1	65.8
DS	9.8	33.1	0	57.1	25.7
Heparin	47.6	0	5.7	46.7	13.9

The percentage of helix induced by binding GAG's for the two lengths of PLL are compared to the earlier published work in Table 5.6. The results for PLL with 126 and 633 residues have a broad similarity to the published work. There are however two differences. The binding of dermatan sulphate to PLL seems to be related to the length of the polypeptide chain. Short lengths of PLL (126 residues) are associated with ß-strand being the major secondary structural element, whereas when the length is increased (to 500 or 633 residues) helix is the dominant secondary structure. A similar situation exists with the heparin/PLL interaction i.e. the length of the polypeptide chain has some effect on the preferred secondary structure. In this case however while long chain lengths agree with the published results, the results for the short chain length are markedly different.

Table 5.6: Comparison of induced helix for PLL GAG binding

GAG Type	Number of lysine residues		
	126	633	500
CS	0	34.2	20
DS	9.8	70	60
Heparin	47.6	74.4	>80
Source	This Study		Gelman et al

The relevant CD spectra for K_8G are displayed in Figure 5.5 and the results in Table 5.7. The range of secondary structures displayed by K_8G in the free and bound forms were restricted to one of two secondary structures: ß-turn or ß-strand. The amount of ß-strand induced upon binding GAG was essentially identical for chondroitin and dermatan sulphate. Heparin induced a slightly higher amount of ß-strand. The conformation of K_8G when bound to the GAG's standards is fundamentally different to longer PLL chains (with greater than 126 residues). This confirms the suspicion from the resin binding results (Section 4.3.5), that the binding of GAG's to short PLL chains (i.e K_xG series where x was 4,8, or 12) was different to that of longer PLL chains.

Figure 5.5: CD spectra for K_8G/GAG complexes

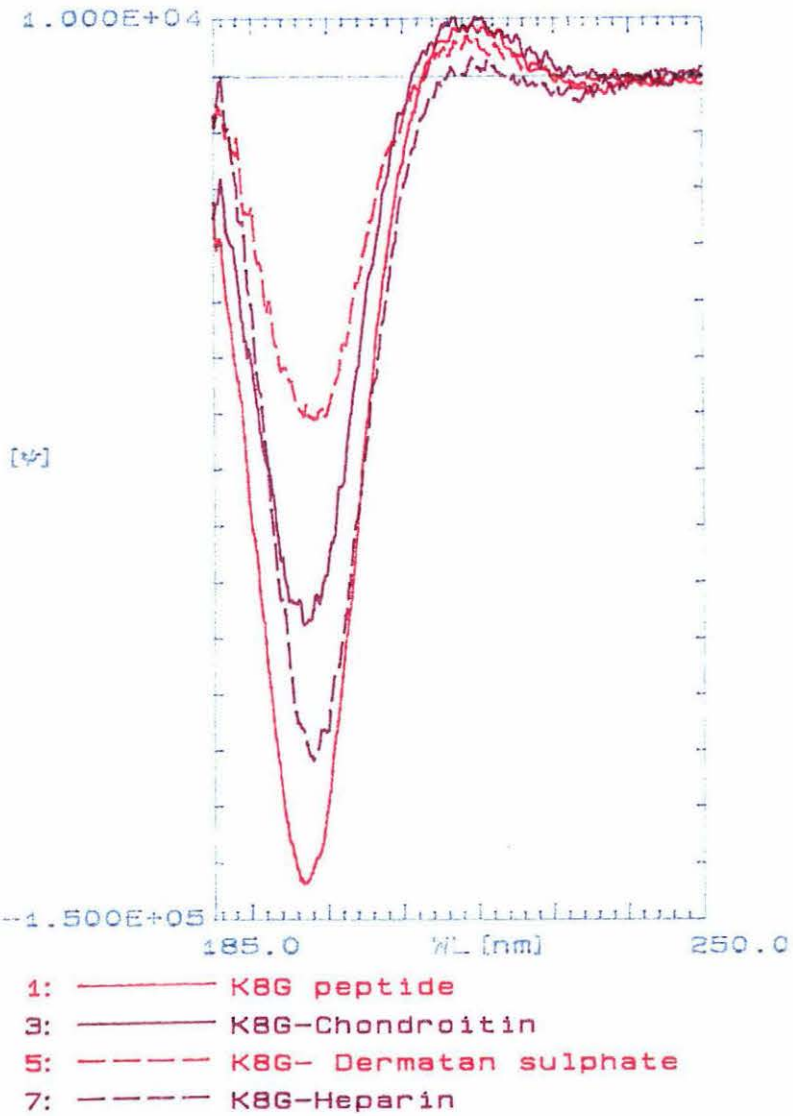

K_8G concentration 0.058 mg/ml, peptide/GAG weight ratio(mg GAG/mg peptide): CS 3.5, DS 2.3, Hep 8.6

Table 5.7: Secondary structure elements for K_8G/GAG complexes

K_8G Complex	% ß-Turn	% ß-strand	%Random	R.M.S.
Peptide alone	33.9	0	66.1	27.9
CS	0	19.9	80.1	78.3
DS	0	22.4	77.6	73.1
Heparin	0	32.0	68.8	66.4

5.3.2.3 Thrombospondin peptide

The solution conformation of the thrombospondin peptide in the free and bound forms was studied the results are shown in Figure 5.6 and in Table 5.8. The free form of the peptide were composed of two structural elements, ß-strand and beta turn, in the ratio of 2:1 respectively. This ratio did not change significantly upon binding the different GAG standards. While changes in the CD spectra are indicative of GAG's binding to peptides the conserve is not necessarily true (Lellouch and Landsbury 1992, Tyler-Cross et al 1993).

Figure 5.6: CD spectra of Thrombospondin/GAG complexes

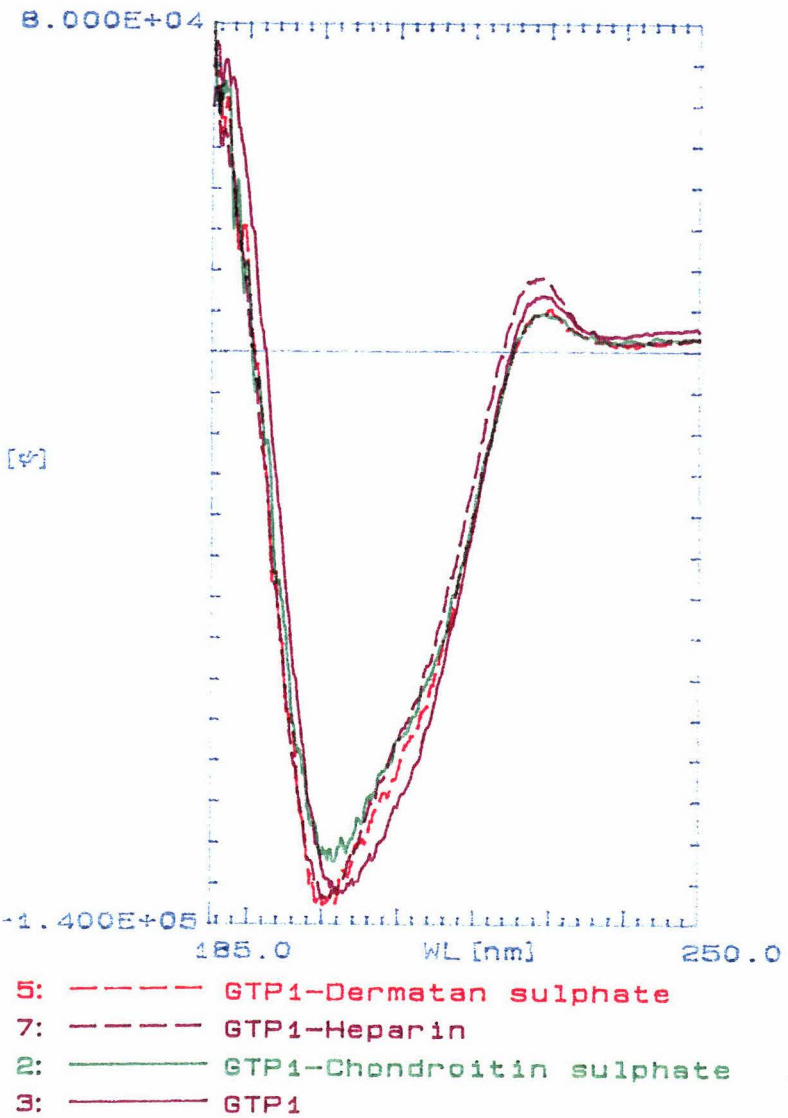

Thrombospondin concentration 0.126 mg/ml, peptide/GAG weight ratio(mg GAG/mg peptide): CS 4, DS 4, Hep 4

Table 5.8: Secondary structure elements of Thrombospondin/GAG complexes

Thrombospondin complex	% ß-Strand	% ß-Turn	R.M.S.
Peptide alone	61.9	38.1	39.8
CS	60.6	39.4	40.8
DS	60.5	39.5	46.4
Heparin	62.1	37.9	42.4

5.3.2.4.1: PCI peptide

The CD spectra of the PCI peptide both in the free form and complexed by the GAG standards are shown in Figure 5.7 and Table 5.9. The free peptide did possess some secondary structure by itself (principally ß-Strand). The different GAG standards clearly induced widely different secondary structure on the basis of the different CD spectra of the complexes. Dermatan sulphate and heparin have almost double the amount of ordered secondary structure when compared to chondroitin sulphate (59, 64 and 35% respectively). The dominant ordered secondary structure for each complex depends on the class of GAG, for chondroitin sulphate and heparin, α-helix is dominant, whereas for dermatan sulphate the ß-strand conformation dominates.

The peptide PCI(264-283) is a 20 residue fragment of protease C inhibitor. A variety of experimental techniques have been used to prove that this peptide is the main binding site for heparin on this protein (Pratt and Church 1992a and 1992b). In common with heparin cofactor II and antithrombin III, PCI inhibits a variety of proteases, and GAG's accelerate this inactivation process by acting as a template for the binding of the protease inhibitor and proteases thus accelerating the inhibition.

The specificity of the GAG acceleration of protease inhibition by PCI has been examined (Pratt and Church 1992a). While heparin is the most effective GAG for this function other GAG's can substitute for this effect (Table 5.10). The authors attributed the activation of PCI inhibition of protein C (and thrombin) by chondroitin

Figure 5.7: CD spectra of PCI peptide/GAG complexes

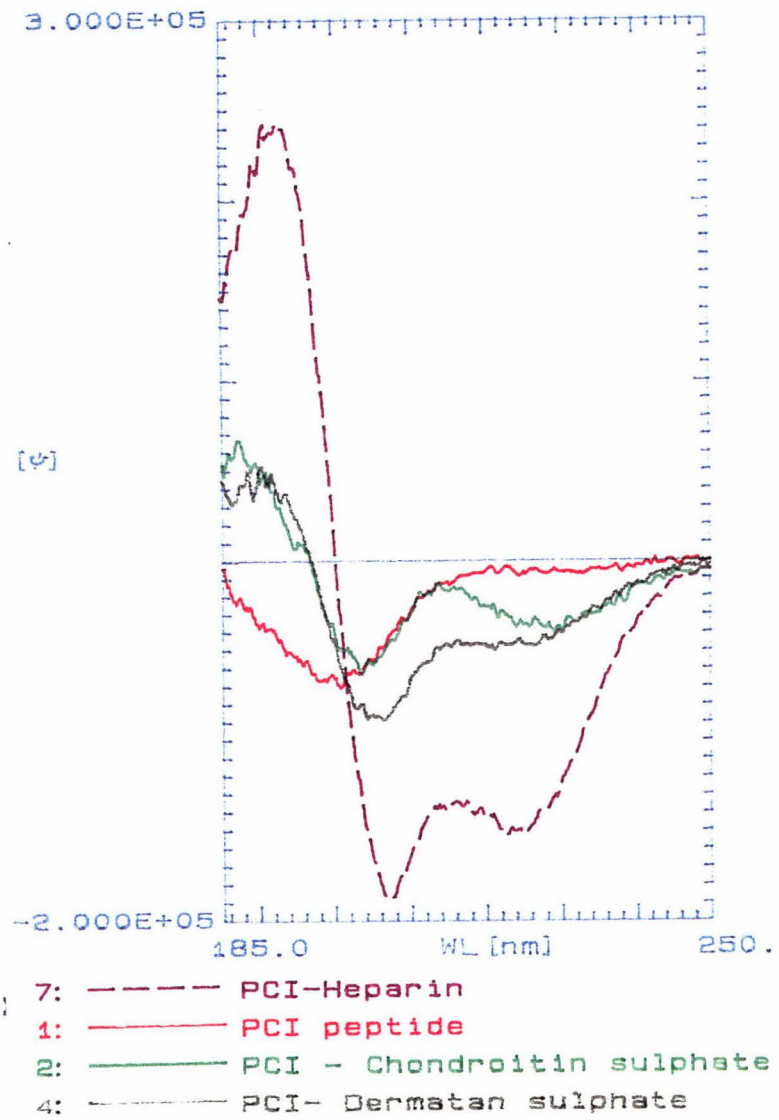

PCI concentration 0.033 mg/ml, peptide/GAG weight ratio(mg GAG/mg peptide): CS 3, DS 3.3, Hep 7.6

Table 5.9: Secondary structure elements of PCI peptide/GAG complexes

PCI complex	% Helix	% Turn	% Beta strand	% Random	R.M.S.
Peptide alone	0	15.2	34.2	50.6	30.8
CS	22.9	12.4	0	64.7	35.1
DS	13.6	6.2	39.3	40.9	26.5
Heparin	34.5	12.6	17.0	35.9	15.3

sulphate to a possible contamination of heparan sulphate in the chondroitin sulphate preparation used. However the chondroitin sulphate used by the writer in the CD conformational studies is free from any HS contamination (Chapter 2). The inhibition of another protease, urokinase, by PCI has also been studied. In this case however dermatan sulphate from three sources (kidney cells, porcine skin and beef mucosa) have been shown to activate the process (Geiger et al 1991).

Table 5.10: Relative rate increase of GAG for PCI inhibition

GAG	Thrombin	Activated Protein C
Heparin	9.4	52
HS	1.9	3.1
C4S	1.7	4.1
C6S	nd	nd
DS	nd	4.6

Adapted from Pratt and Church 1992,
nd: none detected

The order of increasing induced secondary structure in the PCI peptide after binding GAG's parallels the ability of the GAG class to accelerate the inhibition of thrombin and activated protein C by the PCI protein.

The strength of the interaction between the PCI peptide and the GAGs, dermatan sulphate and heparin was monitored by increasing the salt concentration in the incubation mixture and monitoring the elipticity of the peptide component of the complex at 222 nm. Both complexes displayed an S shaped curve that was high at low salt concentrations. The curve then decreased with increasing salt (Figure 5.8). The strength of the complex was then quantified by determining the salt concentration required to inhibit 50% of the secondary structure. These were measured to be 0.1 and 0.3 M for dermatan sulphate and heparin respectively. The strength of the interaction of this peptide with heparin has previously been measured using a solid phase assay, with salt elution from heparin Sepharose columns (Pratt

and Church 1992b), as 0.8 M. Demonstrating that In the solid phase interaction the strength of the interaction is more than 2.5 times that of the solution phase. Two possible reasons for this apparent discrepancy are outlined below:

- The two assays are measuring different properties. Inhibition of secondary structure may not necessarily mean the inhibition of binding.

- It is conceivable that the heparin used in the published study is different from the one used in this study, which could result in different binding strengths.

Figure 5.8: Salt dissociation curves for PCI peptide/GAG complexes

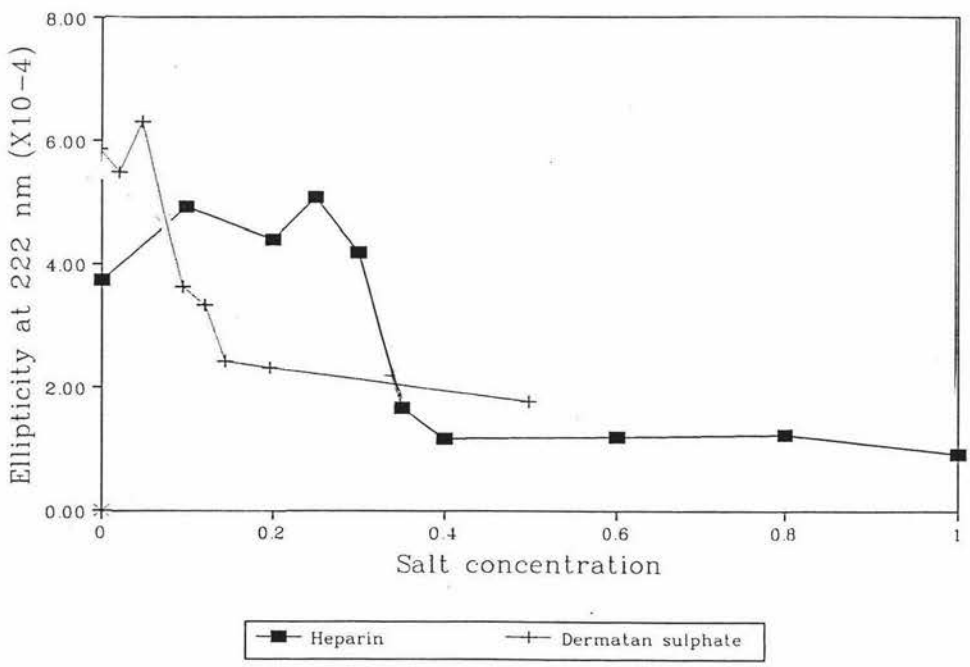

PCI concentration 0.033 mg/ml, peptide/GAG weight ratio(mg GAG/mg peptide): DS 3.3 and Hep 7.6

5.3.2.4.2 Fine structure of heparin

There is some experimental evidence to support the first statement, since the interaction of a ATIII peptide, residues 123-139 (sequence FAKLNCRLYRKANKS SK) with heparin has been characterised (Lellouch and Landsbury 1992). Binding of

this peptide to heparin induced a ß-strand structure, 0.6 M salt was required to inhibit 50% of the secondary structure. A similar ATIII peptide, residues 124 to 140 (sequence AKLNCRLYRKANKSSK) has been synthesized and its interaction with heparin Sepharose characterised (Pratt and Church 1992), only 0.3 M salt was required to inhibit the interaction. However the figures for the PCI peptide occur in the reverse order indicating that this may not be the correct explanation for the discrepancy.

The heparin used in this study is different from that used by Gelman in the PLL/GAG interaction study. The properties of the heparin used by Pratt and Church (Pratt and Church 1992b) in their study of the interaction of the PCI peptide with heparin were not reported. Heparin has been shown to inhibit the proliferation of vascular smooth muscle cell. In addition this effect is dependant on the source of the heparin used, since the extent of the inhibition for 10 commercial sources of heparin have been shown to be different (Castellot et al 1986).

A recent article has demonstrated that the fine structure of heparan sulphate chains on identical proteoglycan core proteins can be different (Sanderson et al 1994). These differences correlated with the ability of this HSPG to bind to type I collagen. The differences for high affinity binding to type I collagen were high levels of N-sulphation and 2Osulphation, lower levels of 6Osulphation and different heparitinase cleavage patterns (i.e. different cleavage sites). The distribution of this high affinity HSPG was examined in three different cell lines. It was found to be present in 2 cell lines, demonstrating that the properties of heparan sulphate can be dependant on the source (i.e. tissue) from which it is extracted.

It is impossible from the data obtained by the writer for the PCI/heparin interaction to be able to differentiate the exact reason for the difference in the binding strength between the solution binding study by the writer and the published solid phase binding assay (Pratt and Church 1992b). However the writer considers that the most probable reason is that the strength of the interaction may be dependant on the source of the heparin.

5.3.3.1 Stoichiometry of GAG- peptide binding

As can be seen from Figure 5.9 the addition of heparin to dilute methylene blue solutions brings about a decrease in the absorbance of the solution at 662 nm. The titration curve follows a hyperbolic shape, and regression lines can be fitted to the two arms of the curve. The end point of the titration is marked by the intersection of these two lines.

Figure 5.9: Methylene Blue titration curve

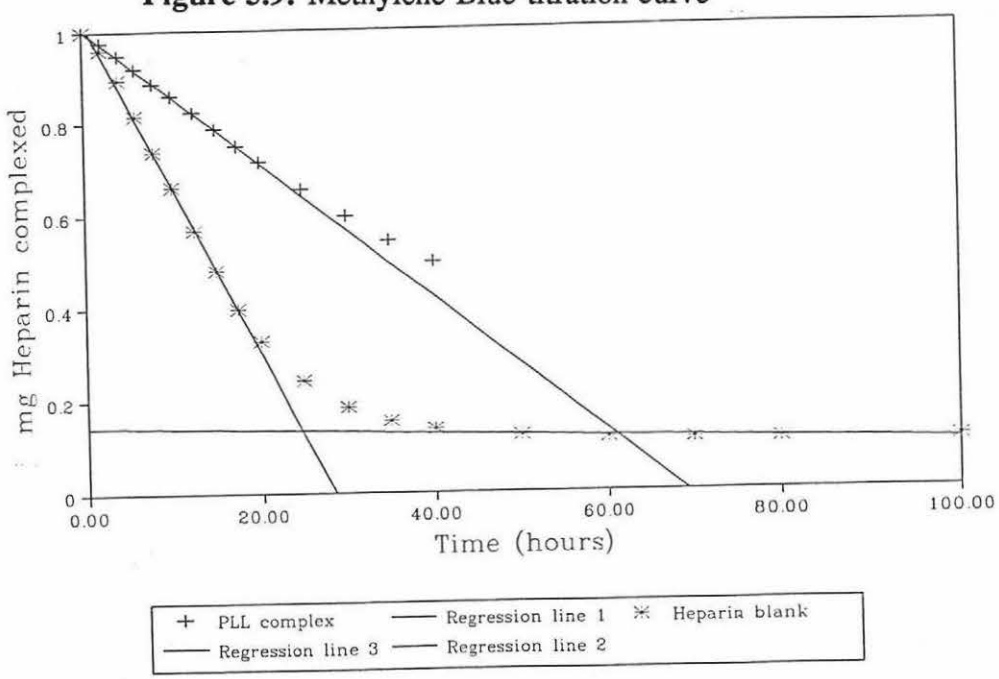

Complex regression Line 1: Constant 1.0034, slope -0.0145. Blank regression Line 2: Constant 1.0222, slope -0.359 Blank regression Line 3: Constant 0.143, slope -0.00042

When PLL is mixed with heparin in excess some of the heparin is complexed to the PLL and is unavailable to complex with methylene blue during the titration. Using the endpoints of the blank and complex solutions the weight of heparin complexed by the PLL can be calculated. A worked example of this procedure is outlined in Appendix 4 (Section A4.3). Thus the stoichiometry of binding i.e. number of lysines bound per disaccharide unit can be measured. As a control the stoichiometry of the PLL/heparin complex was measured at various time intervals to establish the time taken to reach equilibrium. The results as shown in Table 5.11.

Table 5.11: Time course of heparin binding

Time (hours)	mg PLL complexed/ mg heparin
1	1.33
2	0.98
4	1.01
12	0.99

As can be seen from Table 5.11 the complex reached equilibrium after two hours after the initial mixing. Similar results were obtained with the other GAG's viz CS and DS (data not shown). To standardize the measurement of the formation of the complexes for PLL and the other peptides, complex formation was allowed to proceed for 3 hours at room temperature before the methylene blue titration was performed.

5.3.3.2 Stoichiometry of GAG/lysine interaction

The stoichiometry of binding of three lengths of PLL chains (8, 126 and 633 residues respectively) to the GAG standard are shown in Table 5.12. For comparison the published data of Gelman's group are also displayed in Table 5.12. The stoichiometry of binding of the short and long PLL chains to the GAG standards is broadly similar to the previously published work (Section 1.1.3.6) in that increasing number of lysine residues in the PLL chain are bound by the GAG classes as the charge density increases. However there appears to be two significant differences in the binding of GAG's to short PLL chains (with 126 residues). These are:

- The binding of chondroitin sulphate is elevated slightly.
- The binding of heparin is greatly elevated 4.59, cf 2.77 and 2.3 for long and medium PLL chains respectively.

These differences in the binding stoichiometry for the different GAG standards is ever more predominant with the K_8G peptide. The binding of CS is significantly elevated (1.88 versus 1), whereas the binding of DS and heparin is decreased.

Table 5.12: A comparison of the stoichiometry of the GAG/polylysine interaction.

			Polylysine	Chain length		Gelman's	Results
GAG	Charge density	K_8G	Short	Long		Medium	Charge density
CS	0.75	1.88 (0.17)	1.15 (0.03)	1.00 (0.07)		1	1
DS	1.2	1.25 (0.02)	1.58 (0.07)	1.55 (0.17)		1.4	1.4
Hep	2.25	1.71 (0.11)	4.59 (0.32)	2.77 (0.17)		2.3	2.3
Source	This Study					Blackwell et al	1977

A number of questions concerning the stoichiometry of binding can be formulated from the information in Table 5.12. These are:

- What determines the stoichiometry of GAG binding to the PLL chain?
- What effect does the induced conformation of the PLL chain after binding have on the stoichiometry of binding?

Gelman's group (Blackwell et al 1977) suggested that the charge density of the GAG gives some indication of the final stoichiometry of binding. The results for the two lengths of PLL in this study (126 and 633 residues) to heparin are not identical to the charge density of heparin. However the binding of both dermatan and chondroitin sulphate matches the charge density of the GAG chain. These results taken together suggest that the stoichiometry of the PLL/GAG interaction is not determined solely on the basis of the charge density of the GAG chain. The results in Table 5.12 also confirm the conclusion from the CD study of K_8G (Section 5.3.2.1), that the mode of binding of GAG's for short PLL chains is fundamentally different. Because as the PLL chain length decreases the stoichiometry of the binding becomes perturbed when compared to the published results.

5.3.3.3 A comparison of binding stoichiometry: solution versus solid phase

A comparison of the binding behaviour of the polylysine chains on the solution phase and bound to the resin (Chapter 4 results) is shown in Table 5.13. For the short PLL chain with 8 lysines, with the exception of the binding of DS, the binding behaviour between solution and resin bound agree within experimental error. In the situation for the long PLL chain (with 633 lysines), the binding results are drastically different.

Table 5.13: PLL chain binding behaviour solution and resin bound

	K_8G	Results		PLL	Results
GAG	Solution	Resin bound		Solution	Resin bound
CS	1.88 (0.17)	1.44 (0.24)		1.00 (0.07)	0.040 (0.002)
DS	1.25 (0.02)	2.10 (0.20)		1.55 (0.17)	0.036 (0.002)
Hep	1.71 (0.11)	1.96 (0.21)		2.77 (0.17)	0.056 (0.010)

Error of the determinations are shown within the brackets

5.4 CHAPTER SUMMARY

5.4.1 PLL/GAG interaction

The interaction of three lengths of polylysine (with 8, 126 and 633 residues) with the GAG standards was characterised using two assays. The first being a CD spectral study to measure the conformation induced upon binding the relevant GAG. The stoichiometry of the binding interaction was also measured using a dye binding assay. The results were compared for the published material for PLL chains (with 500 residues) binding to GAG's.

There are indications from the CD results of the binding of the GAG standard (i.e. CS, DS and heparin) that the chain length influenced the degree of the dominant secondary structure. For PLL with more than 126 residues all the GAG's induced some α-helix, and the amount of helix increased with increasing chain length. The binding of GAG's to short PLL chains i.e. K_8G and 126 residues (when CS binds) results in a radically different mode of binding with ß-strand structures being induced instead of the α-helix expected on the basis of Gelman's results. The stoichiometry of the binding interaction reinforces the above conclusion, since the number of disaccharide residues bound per lysine residue was significantly different from the longer PLL chains (with 500 and 633 residues).

5.4.2 GAG/peptide interaction

The interaction of the PCI (residues 264-283) peptide with the three GAG standard's, clearly demonstrated that the different GAG's can induce different secondary structures upon binding. For CS and heparin α-helix dominates, whereas ß-strand is dominant for DS, however heparin and DS have approximately twice the amount of secondary structure compared to CS. The strength of the interaction for DS and heparin was measured by the concentration of salt required to inhibit 50% of the interaction as 0.1 and 0.3 M respectively. The interaction of the thrombospondin peptide with the GAG standards demonstrated that there was no change of conformation associated with binding.

The results in this chapter, have not been able to answer the question as to why the different GAG should induce different secondary structures upon binding the same peptide. In an effort to answer this question the results of a number of articles on GAG/peptide interactions were examined in the following chapter (Chapter 6).

Chapter 6: A REEXAMINATION OF PUBLISHED WORK

6.0 INTRODUCTION

A large body of experimental data on the binding of GAG's to peptides and proteins (principally heparin) exists in the biochemical literature (Jackson et al 1992, for a review). Despite of this voluminous literature a number of key questions remain unanswered. These are:

1. At present there are five different consensus sequences for the binding of GAG's (Section 1.3.2). Why are there so many?

2. Typically the conformation of a synthetic GAG binding peptide changes on the binding of GAG's (Section 1.3.3). What causes this change in the peptide conformation, the sugars on the GAG chain, or the peptide sequence, or a combination of the two?

3. The binding strength for a number of synthetic peptides to heparin has been measured. What determines the strength of the interaction?

4. How does the specificity of some GAG/peptide (Section 1.3.1)interactions arise?

5. How common is sequence specific binding? Is it the exception or the rule in GAG/protein interactions?

Vigourous attempts have been made throughout the writing this thesis to answer some of these questions, using the available published data. As a result two complementary model's concerning the conformation of the peptide and strength of the binding of GAG's to short peptides have been developed. For the reader's convenience each of the above questions have been addressed in order.

6.1 GAG binding sites on proteins

The GAG binding sites on protein and/or peptides can be broadly classified into two types: continuous and discontinuous. In the first type the binding site is contained within the primary structure (i.e. sequence) of the protein. With discontinuous binding sites the residues making up the binding site are not adjacent in the primary sequence, but they are in the final three dimensional structure of the protein. Examples of the former type form the basis of the majority of the published work on GAG binding sites, since synthetic peptides of these sites may be synthesized. The use of synthetic peptides has several advantages in the experimental study of GAG/ protein interactions.

- Competition experiments between a GAG, putative GAG binding site and intact protein can be performed to identify the true GAG binding site on the protein.
- The interaction between peptides and GAG can be more easily be studied

To date four different groups have published papers on five consensus sequences, which have been used to identify continuous GAG binding sites on proteins (Section 1.3.2). It is puzzling to the writer as to why there are so many consensus sequences. These consensus sequences were critically examined to find any patterns within these sequences that were missed by the authors in the initial description of these sequences.

6.1.1 Chi squared test

The observed distribution of the types of residues (basic, acidic and aromatic) within the consensus sequences was compared to the known average distribution of these residues in eukaryotic proteins (Flinta et al 1986) using the Chi-squared test (Equation 6.1).

Equation 6.1:

$$\chi^2 = \Sigma \frac{(O-E)^2}{E}$$

The degree's of freedom for the table = (C-1)(R-1)
Where O is the observed results, E is the expected results predicted from the null hypothesis, C are the number of columns in the Table and R is the number of rows in the Table.

In all cases a null hypothesis was formulated, to predict the distribution of the residues at positions in the consensus sequence, and this was compared to the observed distribution. The three basic amino acids (lysine, arginine and histidine) occur in the ratio of 50, 36 and 14% respectively of the total basic amino acids in an average eukaryotic protein. The general form of the null hypothesis was that the observed distribution of each residue was identical to that encountered in an average eukaryotic protein (Flinta et al 1986). Using statistical tables the observed Chi squared value was examined to see if it exceeded the tabulated value (at the 1% level of significance). If it did the null hypothesis was rejected.

6.1.2 Cardin and Weintraub's consensus sequences

Two GAG binding consensus sequences were proposed in the original paper (Cardin and Weintraub, 1989), using 12 known heparin binding sequences in 4 proteins. Two search strings were formulate for the identification of heparin binding sequences in other proteins (Section 1.3.2 and Tables 6.1 and 6.2). Using these search strings, 45 regions in 21 heparin binding proteins were identified. A number of key points about these consensus sequences need to be elaborated: firstly certain positions within these sequences do not have basic residues present in them 100% of the time, secondly the frequency of aromatic and acidic residues within the consensus sequences is also variable. The distribution of basic, aromatic and acidic residues within each of Cardin's consensus sequences was critically examined, and a number a points about the sequences were elucidated (full details in Sections A5.1.1 and A5.1.2 in Appendix 5).

Cardin identified 28 sequences that conformed to the first type of consensus sequence. The overall proportions of types of basic residues (i.e. lys, his and arg) in

type I sequences at positions 2,3,4, and 7 is a reflection of the relative frequencies of these amino acids in an average eukaryotic protein. However positions 2 and 4 seem to have distinct preferences for basic residues, these are;

- Position 2: K ~ R >> H
- Position 4: K >> R >> H

It is perhaps significant that these positions have also been identified as not being having basic residues present all of the time (i.e. basic 57 and 61% of the time respectively).

Table 6.1: Cardin's Type I consensus sequence

Sequence	X	B	B	B	X	X	B	X
Position	1	2	3	4	5	6	7	8
% Basic	14	57	100	61	0	0	100	21
% Acidic	3	0	0	0	3	7	0	3
% Aromatic	6	11	0	11	11	3	0	3

Where: B is a basic residue and, X is a hydrophobic residue
Source: Cardin and Weintraub 1989

There is a tendency against acidic residues at positions 1, 5, and 8, but at position 6 the levels match those expected in an average eukaryotic protein. In addition aromatic residues seem to be neither required or discriminated against in the consensus sequence on the basis of the statistical analysis. Finally at position 2,3, and 4 there are four possible variants of the consensus sequences. These are: BBB, XBB, BBX, and XBX. In the sequences described by Cardin and Weintraub there are no sequences of the XBX type and XBB and BBX seem to be preferred over the BBB type.

Cardin identified 19 sequences corresponding to type II consensus sequence (Table 6.2). As in the case of the type I sequences the overall proportion of the basic residues in type II sequences matches the expected distribution of these residues in proteins. However at position 5 there appears to be a significant preference for types

of basic residues (i.e. R >> K > H). Acidic residues within this consensus sequence are disallowed at position 1 and 4, but seem to be preferred at position 6. Aromatic residues seem to be required at position 1 some of the time.

Table 6.2: Cardin's type II consensus sequence

Sequence	X	B	B	X	B	X
Position	1	2	3	4	5	6
% Basic	25	94.7	100	0	100	10.5
% Acidic	0	0	0	0	0	25
% Aromatic	25	0	0	12.5	0	5.3

Where: B is a basic residue and X is a hydrophobic residue.
Source: Cardin and Weintraub 1989.

The tendency for particular basic amino acids at positions 2 and 4 of type I, position 5 of Type II of Cardin's consensus sequence was surprising, but it must be stressed that the majority of the sequences examined were putative GAG binding sites. The appearance of significant levels of acidic residues at position 6 of type II sequences (25%) was also both puzzling and unexpected. In addition on the basis of the statistical analysis, acidic residues at position 6 of type I consensus sequences are neither preferred or disallowed i.e. the frequency matches the level expected in an average eukaryotic protein. There is good experimental evidence that this is real (for type I consensus sequences) and perhaps functionally important in the GAG binding sites of some proteins. A recent paper describes the binding of heparin to the chemokines: PF4, IL8, NAP-2 and GROα (Witt and Lander 1994). All four chemokines have the heparin binding site at the C-terminus of the polypeptide. Two of these proteins (NAP-2 and GROα) have binding sites corresponding to Cardin type I. The GROα has a acidic residue at position 6, and the binding strength of these two proteins was identical, demonstrating that acidic amino acids at this position do not hinder GAG binding, in addition the specificity of the binding increased.

6.1.3 Sobel's consensus sequence

A third putative consensus sequence (Sobel et al 1992) has been identified from a small sample (9) of plasma proteins that bind heparin (Table 6.3). The evidence for this sequence in the writer's opinion seems to be weak for two reasons. These are:

- It is based on a very small number of sequences
- While the sequence is palindromic the frequency of basic amino acids at the two ends of the sequence (i.e. positions 2,3 and 11,12) seems very low.

Table 6.3: Distribution of basic residues in Sobel's consensus sequence

Position	1	2	3	4	5	6	7	8	9	10	11	12	13
	X	B	B	X	X	B	B	B	X	X	B	B	X
%Basic		50	25			89	100	89			62.5	28	
R		1	1			5	1	5			1	0	
K		3	1			3	4	2			4	1	
H		0	0			0	4	1			0	1	
Total AA		4	8			9	9	8			8	7	

As with Cardin and Weintraub's consensus sequences the overall frequency of the basic residues is the same as what would be expected on the frequency of these residues in proteins. Full details of the analysis are in Section A5.1.3 in Appendix 5. Despite the small number of sequences used in the analysis the proportion of basic residues at position 6,7, and 8 was examined, and in all three cases preferences for the type of basic residue seem to be apparent. These were;

- Position 6 R > K >> H
- Position 7 H ~ K > R
- Position 8 R >> K > H

Given the small number of sequences these tendencies for particular basic amino acids at these position are provisional. It is considered possible by the writer that the

Sobel's consensus sequence may be a combination of Cardins and Weintraub's type I consensus sequence, with an inverted Cardin and Weintraub's type I consensus sequence (as shown in Figure 6.1).

Figure 6.1: Proposed origin of Sobel's consensus sequence

Cardin type I					X	B	B	B	X	X	B	X*	X	
Iverted Cardin type I	X	X*	B	X	X	B	B	B	X					
Sobel	X	B	B	X	X	B	B	B	X	X	B	B	X	X
						↑		↑						

The asterisked sites on the Cardin's type 1 sequence are basic 21% of the time, so the combination of two sequences of this type in the above manner can reproduce Sobel's sequence. The tendency for kinds of basic residues at the arrowed positions differ between the two consensus sequences however (Table 6.4), but this could just be a reflection of the small number of sequences used in this analysis of Sobel's sequence.

Table 6.4: Comparison of basic amino acid tendencies

Position	Cardin Type I	Position	Sobel's
2	K ~ R >> H	6	R > K >> H
3	K, R, H	7	H ~ K > R
4	K >> R >> H	8	R >> K > H

A test of the above hypothesis (i.e. that Sobel's consensus sequence is a combination of 2 forms of Cardin and Weintraub's consensus sequence) would be to do a sequence search in one of the protein sequence data bases to obtain more putative GAG binding sequences. If the above hypothesis is correct three predictions can be tested, these are:

1. That sequences of the reverse of Cardin and Weintraub's type I consensus sequence should be identified ie XBXXBBBX (I').
2. The tendency of the various basic amino acids at position 2 and 3 (For Cardin type I) should be identical to position 6,7 and 8 of Sobel's sequence.

3. Sequences such as XBXXBBBXXBX (truncated version of Sobel's consensus sequence) should also occur at a higher frequency than XBBXXBBBXXBBX (Sobel's consensus sequence).

The examination of this hypothesis awaits the identification of more continuous GAG binding sites on protein/peptides.

6.1.4 Margalit et al's GAG binding consensus sequence

An article has challenged the validity of the Cardin and Weintraub consensus sequences on three grounds (Margalit et al 1993). These were that:

- That the known heparin binding sites of ATIII (124-145), platelet factor 4 (66-70) and bFGF (28-46) do not correspond to either consensus sequence.
- Short consensus sequence such as BBXB seem incompatible with the requirement for a pentasaccharide as the unique minimum functional unit of heparin.
- Finally in the analysis of the consensus sequences putative heparin binding sequences were used.

After the examination of 18 known heparin binding sites with **known** structure a distinct spatial distribution of basic residues was identified. When the binding site folds into an α-helix, the motif is 2 basic residues 20 Å apart on opposite sides of the helix (i.e. 13 residues apart). Similarly for a ß strand conformation it has the residues 23 Å apart on opposite sides of the ß-strand (i.e. 5 residues apart).

However rather than being a rebuttal of the Cardin and Weintraub consensus sequences, it seems more likely that this a corollary of it. Since the sequences cited above, **do conform** to the consensus sequences, once it is appreciated that some positions in the sequences do not have to be basic 100% of the time (i.e. position 2 and 4 of type I and position 2 in type II). Cardin and Weintraub's consensus sequences could perhaps be regarded as modules from which the full GAG binding site can be built up.

6.1.5 Hyaluronan binding site

A motif for hyaluronic acid binding site on three proteins (RHAMM, CD44 and the link protein) has also been proposed with 2 basic residues, 7 residues apart with no acidic and at least one basic residue in the intervening section (Yang et al 1994). It has been shown to occur in all hyaluronic acid binding proteins sequenced to date. All of the sequences used by the Yang's group to formulate this consensus sequence, contained Cardin and Weintraub consensus sequences. In addition the distance between the 2 basic residues corresponds to the distance proposed by Margalit, if the binding site folds into a ß-strand (23.1 Å). In contrast if the motif is in an α-helix, the distance corresponds to a shorter distance (10.5 Å).

6.1.6 Ligands for sulphate binding

Two reports describing the binding sites of sulphates and phosphates in the X-ray crystal structures have been reported (Chakrabarti 1993, Copley and Barton 1994). The types and number of amino acids which act as ligands for both sulphate and phosphate are described by both of these authors. The data in both of these papers was reanalysed by the writer after removing protein structures that were duplicated in both reports (5 in all) and phosphate binding proteins, the binding sites of 98 sulphates in 58 proteins remained (Table A5.5 in Appendix 5). Four amino acids (Arg, Lys, His and Ser) acted as ligands in 68% of the cases, despite the fact that they occur with a frequency of 21% in the average eukaryotic protein. Among the basic amino acids, arginine is the most common ligand (full details in Section A5.2 in Appendix 5), despite it occurring at a lower frequency than lysine in an average eukaryotic protein (Flinta et al 1986). The reason for the differential preference for particular basic amino acids (i.e. Arg) as ligands for sulphate is that the different amino acids have different H-bonding patterns and stereochemistries for the binding of sulphate (Chakrabarti 1993).

As demonstrated in Section 6.1.1 and Table 6.4, some of the positions in Cardin and Weintraub's consensus sequences have preferences for particular basic amino acids

that seem to match the above data. These positions are:

- Position 2 of the Type I consensus sequence, with the order K ~ R >> H
- Position 5 of the Type II consensus sequence, with the order R >> K > H

It is tempting to speculate that these two positions are the more important determinants for sulphate binding within each of these consensus sequences for the binding of GAG's. The levels of serine within sequences conforming to Cardin and Weintraub consensus sequences were examined and it was found (data not shown) that the level matched the frequency in the average eukaryotic protein.

There is some evidence to support the idea that the different basic amino acids can influence the behaviour of GAG binding peptides. The binding of the ßA4 peptide (the major peptide of the amyloid deposits in Alzheimer disease) to heparan sulphate has been implicated in the formation of these deposits (Section 1.1.2 and Section A1.2 of Appendix 1). The mutagenesis of histidine 13 to arginine, in vivo experiment with rodents, demonstrated that the formation of mature amyloid deposits did not occur (Talafous et al 1994). To the writer's knowledge this is the first and only experimental evidence indicating that the exact identity of the basic amino acid involved in the binding of GAG chains can influence the peptides behaviour.

6.1.7 Summary of consensus sequences

The five different putative consensus sequences proposed for GAG binding sites on protein/peptides can easily been condensed into 2 (possibly 3, if Sobel's sequence is unique). These consensus sequences can be combined in a modular fashion to form complete GAG binding sites with the extra constraints that have been formulated by some groups (ie Margalit et al 1993 and Yang et al 1994).

A comparison of the frequency of occurrence of acidic, aromatic and basic residues within each of Cardin's and Weintraub's consensus sequences (Cardin and Weintraub 1989) to the levels found in the average eukaryotic protein revealed a number of

trends. Three positions within these consensus sequences had defined tendencies for particular basic amino acids, these positions were 2, 4 of type I and position 5 of type II. Position 1,5 and 8 of type I and 1 and 4 of type II had a distinct tendency against acidic residues. However at position 6 of the type II consensus sequence acidics seems to be preferred.

The reason as to why there are 2 (possibly three) modular components of the GAG binding site is not known but some plausible explanations can be invoked. These are:

- They may bind different GAG classes (Section 1.1.1.1)
- They could be binding to the same GAG but with the modules folded into different secondary structures.
- They could be motifs for different types of GAG binding functions (e.g coagulation function, growth factor binding).

Insufficient data exists in the literature at present to answer this question.

6.2 Conformational change of peptide on binding GAG's

The binding of heparin to peptides/proteins is often accompanied by a conformational change (Section 1.3.3). The obvious question is what drives the conformational change? Is it the GAG acting as a template or is it some property intrinsic in the peptide sequence?

6.2.1 Importance of the conformational change

The change of conformation of the peptide is thought to be operationally important in the strength of the binding. There is some experimental evidence to support this idea. A variety of peptides from transforming growth factor ß1 have been synthesized (McCaffery et al 1992). The strength of binding to immobilised heparin was measured in the presence and absence of 6M urea, which was postulated to

disrupt the induced secondary structure. For 4 of the 5 peptides synthesized, urea decreased the strength of the ionic interaction between heparin and the peptide, indicating that secondary structure was important for binding.

6.2.2 PLL/GAG interaction

A reexamination of the proportion of induced helix in poly-L-lysine (PLL) after binding GAG's (Section 1.1.3.6) revealed an interesting trend. There is extensive evidence for secondary structure of GAG chains in the solid state (Section 1.1.3.4). The axial disaccharide repeat distance (in nm) for GAG chains in a 2 fold single stranded helix from the solid state structures seems to be related to the proportion of induced helix (Table 6.5).

As discussed in Section 5.3.1 PLL has no intrinsic periodicity in hydrophobicity in the sequence for either α-helix or ß-strand and so it is easy to imagine that upon binding to GAG chains, it would be moulded into the helical conformation of the GAG chain. With the exception of hyaluronic acid and heparan sulphate, there is a noticeable trend for an increased proportion of induced helix with the decreasing length of the disaccharide repeat distance (Table 6.5). It is tempting to speculate that in the case of the PLL/GAG interaction that the secondary structure of the GAG chain is the controlling factor in controlling the degree of induced helix. Perhaps the intrinsic secondary structure of the GAG chain (Section 1.1.3.4) is acting as a template, the shorter the axial disaccharide repeat distance the better the fit to PLL in the alpha helical conformation.

The two fold helical conformation of heparin in the solid state has been demonstrated to be preserved in solution (Mulloy et al 1993), in a combined NMR and molecular modelling study. This study demonstrated that heparin in solution existed in a two fold helical state (2 disaccharides per turn), with an axial disaccharide repeat of 0.84 nm (i.e. the same dimensions as that in the solid state). In addition three sulphates from successive residues formed a cluster on one side of the polysaccharide chain, the next cluster was on the opposite side of the chain and offset. The carboxyl

groups from the iduronic acidic residues were midway between these sulphate clusters.

Since the translation per residue of an peptide in an α-helix is ~1.5 Å and there are 3.6 residues/turn, the distance covered by 1,2 and 3 turns of an α-helix are 0.54, 1.08 and 1.62 nm respectively. The value for 3 turns of an α helix (i.e. 11 residues) is approximately that covered by 2 disaccharides units of heparin (1.64 nm). Similarly for C4S, 1 disaccharide covers a distance of 0.98 nm and this fits poorly to the distance covered by 2 turns of an α-helix.

Table 6.5: A comparison of induced helix and disaccharide repeat distance

GAG class	% Induced Helix	Axial disaccharide repeat (nm)
Hep	>80	0.82-0.84
C6S	80	0.93
DS	60	0.94-0.97
C4S	~20	0.98
HS	0	0.93
Hyaluronic	0	0.98
REFERENCE	Gelman et al Section 1.1.3.6	Nieduszynski et al 1989

However the axial disaccharide repeat distance is not the only factor that is probably in operation since, no helix is induced upon binding of PLL to heparan sulphate and hyaluronic acid. Heparin and heparan sulphate differ in the proportion of N sulphate groups (60 and 45 % respectively), so perhaps the controlling factor is dependent on the appropriate spatial distribution of sulphate groups on the GAG chain in 3 dimensions

6.2.3 Peptide/GAG interactions

The periodicity of the basic residues within a number of peptides where the amount of induced secondary structure after binding GAG's had been determined was

examined in order to formulate a method to rationalise the dominant induced secondary structure. It is theorized by the writer that there are three contributing factors determining the dominant secondary structure. These are:

1. The tendency of the peptide to fold into an α-helix or ß-strand. This can be quantified by the calculation of the amphipathic indices of the hydrophobic moment profile of the peptide (Section 5.2.5) in the helical and strand regions.

2. The number of attractive contacts been the sulphate groups of the GAG chain (and possibly the carboxyl groups) with the side chains of the basic amino acid side chains if the peptide is folded into an alpha helix when compared to those when it is in a beta strand.

3. The number of repulsive contacts between the side chains of acidic amino acids and the sulphate groups on the GAG chain if the peptide is folded in an alpha helix compared to those when folded into a beta strand.

The first two factors have been discussed at length by a number of authors, however the discussion of these factors has always been performed separately. Cardin and Weintraub discussed in their original paper (Cardin and Weintraub 1989) that the two consensus motifs showed prominent amphipathic profiles in both α-helical and ß-strand conformations. Two peptide fragments of apolipoprotein E, Apo E 129-169 and Apo E 202-243 have been synthesized and their interaction with heparin has been characterised (Cardin et al 1991). Apo E 129-169 bound in a predominantly α-helical conformation, whereas Apo E 202-243 bound with a predominantly ß-strand conformation. The authors calculated the hydrophobic moment profiles of fragments over the range 80° to 180°for each of these peptides and used this to rationalise the binding behaviour of these peptides. Apo E 136-157 displayed a major amphipathic periodicity at 100° whereas Apo E 211-228 had a prominent periodicity at 165°. In these examples the peptide bound to heparin in a conformation that matched the maximum amphipathicity for the peptide (at 100° or 165°). However most of their

discussion of amphipathic secondary structures in their paper and all of the subsequent papers by other authors have stressed amphipathic helices for GAG binding sites. Hydrophobic moment analysis (Sections 5.2.5 and 5.3.1) of peptide sequences has shown that different secondary structures have characteristic profiles, it also allows the calculation the amphipathic secondary structure (α-helix or ß-strand) occurring by chance (Donnelly et al 1993). However amphipathic indexes cannot be the only factor involved since on this basis ATIII 123-139 would be predicted to fold into an alpha helical conformation upon binding heparin since the indices for α-helix and ß-strand are 2.055 and 1.423 respectively. However the conformation of the peptide bound to heparin has been determined experimentally to be a ß-strand form (Lellouch and Landsbury 1992).

Model building studies of Apo B P-2 (RLTRKRGLKLATALSLSNK) a peptide known to bind C6S strongly (Camejo et al 1988) demonstrated that two basic amino acids are separated by 10-15 Å, when the peptide is folded into an α-helical conformation. These distances were appropriate for 2 point contact for models of C6S disaccharides. However the authors also pointed out that ß-strand models of the same peptide also allowed for similar contacts. The distinct spatial distribution of basic residues in structurally defined heparin binding sequences has been reported and states that 2 basic residues (most frequently arginine) 20 Å apart are on opposite sides of an alpha helix (Margalit et al 1994). In peptides that bind in a ß-strand conformation the distance is 23.5 Å with the basic residues on opposite sides of the strand. The authors also reported that this distance was appropriate for binding the pentasaccharide binding units of the heparin chain.

The third assertion that acidic residues can influence the binding of GAG's by peptides has received the least discussion. The consensus sequences with the exception of position 5 of Cardin and Weintraub's consensus sequence the type II, have a distinct tendency against acidic residues. The binding of heparin to chemokines has demonstrated that the inclusion of acidic residues within the GAG binding site can have marked effects on the specificity of the binding of heparin (Witt and Lander 1994).

6.2.3.1 A stereochemical model for GAG binding

A simple one dimensional model was formulated using the above factors. The model involves projecting the entire peptide backbone onto a pure α-helix and a pure ß-strand conformation. The distances between all possible combinations of the basic amino acids in the peptide sequence is then calculated for each conformation, using the rise per residue for α-helix and ß-strand as 0.15 and 0.33 nm respectively (Schulz and Schirmer 1979). The side chains of the acidic and basic residues are considered to be projected at right angles to the axis of the secondary structure. Some flexibility is built into the model by allowing the side chains to wiggle 5°in either direction, this translates into a 8% tolerance in either direction of the disaccharide repeat distance (or multiples thereof). The number of matches between these distances calculated above and the disaccharide repeat distances (or multiples thereof) of the GAG helix, within the 8% tolerance as a fraction of the total number of paired combinations of basic amino acids is then recorded.

In a similar manner the number of contacts between all possible pairs of acidic and basic amino acids, where the distances match the repeat distance for the GAG chain (or multiples thereof) are recorded. The nett number of productive basic contact for each secondary structure is measured as being the total number of productive contacts with the repulsive contact subtracted i.e. those contacts where both basic amino acids are with one disaccharide repeat distance (or multiples thereof) of an acidic amino acids.

Equation 6.2

$$C(\beta) = AI(\beta) \cdot N^{\beta}_{nett}$$

Equation 6.3

$$C(\alpha) = AI(\alpha) \cdot N^{\alpha}_{nett}$$

Where: AI(α) and AI(ß) are the amphipathic indexes for the alpha helical and beta strand region of the hydrophobic moment plots respectively. N^{α}_{nett} and N^{β}_{nett} are the nett number of contact between the peptide and the GAG chain for the peptide in a

α-helical or ß-strand forms respectively.

The peptide folds into a ß-strand conformation if the product of the proportion of matching contact distances and the beta strand amphipathic index of the peptide, the beta stand conformational score C(ß) (equation 6.2), exceeds the analogous figure for the α-helical conformation score C(α) (equation 6.3). Two worked examples of the procedure are outlined Section A5.3.1 and A5.3.2 of Appendix 5.

As can be seen in Table 6.6 the model is able to rationalise the conformation of the two ATIII peptides (ATIII 13-139 and ATIII 121-134) and the modified ATIII peptide (ATIII 121-134ext). In these cases the C(ß) score is higher than the C(α) score. A similar situation exists for the von Willebrand peptide and the PCI peptide in these cases the dominant secondary structure ß-strand and α-helix (for C4S and heparin binding) respectively the C(ß) and C(α) terms dominates. One exception to this model can be noted from the model, this concerns the binding of dermatan sulphate to the PCI peptide. The model indicates no preference for either secondary structure since both C(α) and the C(ß) scores were zero, whereas both of these secondary structures were observed experimentally (Section 5.3.2.4.1). As discussed in Section 1.1.3.4, dermatan sulphate unlike chondroitin sulphate and heparin, does not have extensive NH-carboxyl hydrogen bonds. This results in a reduced tendency for secondary structure of dermatan sulphate in solution.

6.2.3.2 Biological binding behaviour of peptides

In addition to rationalising the induced secondary structure of the peptides tested, the model is also able to rationalise the biological binding behaviour of some peptide/ GAG interactions. Two groups have examined the binding behaviour of peptides where the physiological relevant GAG is not heparin but chondroitin 6-sulphate and heparan sulphate (Camejo et al 1988 and Drake et al 1993 respectively). The first paper involved the identification the peptide fragments of Apo B-100 mediating the interaction of low density lipoproteins (LDL) with arterial proteoglycans (PG). Nine peptide fragments were synthesized and the interaction with agarose bound

chondroitin sulphate proteoglycans (CSPG) was characterised in terms of binding parameters (dissociation coefficient and maximum binding capacity). Competition experiments between the arterial PG/LDL complex and the synthesized peptides were also performed. Three of the peptides synthesized were capable of binding to arterial proteoglycans (i.e. these sections were identified as mediating the interaction of Apo B with CSPG in the arterial wall). These were Apo P-1, P-2 and P-11 respectively. The remaining peptides did not bind to the proteoglycans (Table 6.7).

Table 6.6: Evaluation of the model

Peptide	GAG	C(α)	C(ß)	% α-helix	% ß-strand	Source
ATIII 123-139	Hep	0.275	0.569	8	80	Lellouch and Landsbury
	C6S	0.275	0.476	23	35	1992
ATIII 121-134	Hep	0.225	0.374	6.2	77	Tyler-Cross et al 1994
ATIII 121-134 ext	Hep	0.122	0.303	14.9	39	
Willebrand Tyr^{565}-Ala^{587}	Hep	0.07	0.263	10	60	Sobel et al 1992
PCI	Hep	0.09	0.00	35	17	This study
	C4S	0.180	0.00	22	0	
	DS	0.00	0.00	14	39	

Sequences of peptides; ATIII 123-139: FAKLNCRLYRKANKSSK, ATIII 121-134: K(ßA)FAKLAARLYRKA, ATIII 121-134 ext: AEAAARK(ßA)FAKLAARLYRKA, Willebrand Tyr^{565}-Ala^{587}: YIGLKDRKRPSELRRIASQVKYA, PCI (264-285): SEKTLRKWLKMFKKRELEEY.

As can be seen from the figures in Table 6.7 three of the peptides have the beta strand potential dominating suggesting that the binding of these peptides to chondroitin 6-sulphate would result in formation of significant proportions of beta strand. The remaining peptide (Apo B P-1) would result in the formation of alpha helix after binding chondroitin-6-sulphate. The sequences of the three peptides (Apo B P-1, P-2 and P-11) when projected onto helical wheels demonstrating the Partitioning the polar/nonpolar residues on opposite sides of the helix. This was taking by the authors as evidence that Apo B P-2 should be the most effective binder since only it has five possible charges located in the polar face in close proximity to

each other. A direct test between this writer's stereochemical model and the Camejo's helical model of the binding of these peptides to chondroitin-6-sulphate would be to determine the dominant secondary structure by CD spectroscopy. For the three peptides where the beta strand potential dominates (ie Apo B P-2, P-11 and P-5) the order of increasing potential [C(ß)] parallels the decreasing values of the disassociation constants.

Table 6.7: Summary of Camejo et al's results

Peptide	C(α)	C(ß)	K_d LDL(nM)
Apo B P-1	0.492	0	413
Apo B P-2	0.125	0.304	800
Apo B P-11	0.204	0.415	510
Apo B P-5	0.00	0.435	95
Control LDL	-	-	95 to 100

Sequences of the peptides; Apo B P-1: LRKHKLIDVISMYRELLKDLSKEA, Apo B P-2 RLTRKRGLKLATALSLSNK, Apo B P-11: RQVSHAKEKLTALTKK, Apo B P-5: RQIDDIDVRFQK. Where C(α): alpha helical conformational score, C(ß): beta strand conformational score, and K_d is the disassociation constant of Apo B peptides/LDL interaction.

A fifteen amino acid residues peptide FN-C/HII (KNNQKSEPLIGRKKTY) derived from the carboxyl terminal heparin binding domain of fibronectin has been demonstrated as the heparin-binding site of fibronectin by the synthesis of the peptide (Drake et al 1993). The structural features responsible for the binding were examined by the construction of variant peptides. The binding activity of the peptides were quantified by two assays. The first measured the ability of the variant peptides to compete with the binding of [^{35}S]HSPG to an affinity column consisting of immobilised FN-C/HII. The second assay measured the ability of these peptides to promote the cell adhesion or compete for cell adhesion in an in-vitro assay. The sequence of the peptide was important for the binding behaviour of the peptide since a scrambled version of the peptide was unable to bind to [^{35}S]HSPG under the conditions of both assays. The active site for heparin binding within the FN-C/HII peptide was localised in the COOH-terminal residues LIGRKK. NMR structural

studies indicated that this region displayed significant multiple-turn or helix-like character. Systematic substitution of the basic residues within the RKK cluster with alanine results in a decreasing ability to inhibit the binding of [^{35}S]HSPG to FN-C/HII affinity column and the cell binding assay. Of all the peptides tested only FN-C/HII and the RKA variants were active in the cell binding assay.

The stereochemical model is also able to rationalize the binding behaviour of these peptides (Table 6.8). In this case the model was relaxed slightly so that wiggles of the side chains of acidic and basic residues of up to 7°were permitted. This resulted in a 12% tolerance of the fits to the axial disaccharide repeats of heparan sulphate (0.93nm). The importance of the RKK cluster is demonstrated by the fact that all of the allowable contacts involve these residues. In the case of the active peptides the helical potential dominates for the bound peptide. The decrease in the activity of the variant peptides (V-RKA AND V-RAA) when compared to FN-C/HII is paralleled by an increase in the helical score C(α). In contrast the two inactive peptides either had no dominant term, or the beta strand score C(ß) dominated (V-AAA and FN-C/HII SCRM respectively).

Table 6.8: FN-C/HII peptide results

Peptide	C(α)	C(ß)	% Inhibition of Binding to [^{35}S]HSPG affinity column
FN-C/HII	0.159	0.116	98
V-RKA	0.182	0.106	72
V-RAA	0.447	0	43.9
V-AAA	0	0	1.6
FN-C/HII-SCRM	0.138	0.342	1.8

Sequence of FN-C/HII SCRM: KEPKTGIRQNKSKNLY

6.2.3.3 Discussion of the model

The model is composed of three main elements. Two of which have previously been discussed by other workers in this field, the contribution of acidic residues being the exception. But the elements have **never** to the writer's knowledge been integrated into **a single coherent model** to describe the binding of GAG's to peptides. The elements are: amphipahtic profiles, the spacing of basic residues and the influence of acidic residues.

The model only considers the distribution of acidic and basic amino acids within the sequence when calculating the number of contacts. As a result of this fact the model is one dimensional. It only considers whether the residue is the right distance apart for GAG contact. But the residue could be on the wrong side the of α-helix (or ß-strand) for the interaction to actually occur. The model examines contacts that are whole number multiples of the axial disaccharide repeat, however in the true situation the existence of contacts at distances that are at fractions of the repeat distance existing are perhaps more likely. However in the initial stages of the development of the model such contacts were not considered. Examination of structural/computer models of chains composed of the major disaccharide repeats of each GAG class may suggest the existence of further contacts. This may result in the full justification of the existing GAG binding protein consensus sequences. A potential fault of this model is that it appears to ignoring the existence of the fine structure of the disaccharide sequence in GAG's such as heparan sulphate and heparin. However despite of the existence of fine structure (Sections 1.1.1.2 and 5.3.2.4.2) emerging evidence suggests that the fine structure may be concentrated within short regions of the sequence.

The effect of acidic residues on the binding of peptides to GAG's can be directly tested by the synthesis of a modified PCI peptide with all the glutamate residues replaced by glutamine. This has no effect on the amphipathic index, but would result on the basis of the stereochemical model predicting that a ß-strand would be the dominant secondary structure upon binding heparin (c.f. α-helix for the unmodified

peptide).

6.3 Binding strength of GAG/peptide interaction

A complementary model to rationalise the strength of heparin/peptide interactions was formulated using three data sets. Two correlations, one for each of Cardin and Weintraub's consensus sequences between the binding strength of the interaction and an attribute were derived from the peptide sequence. The data sets used in the analysis were as follows:

1. The interaction of seven peptides derived from three serine protease inhibitors (ATIII, PCI and HCII) and platelet factor four with heparin Sepharose (Pratt and Church 1992b).
2. Five peptides derived from transforming growth factor-ß1 (McCaffrey et al 1992).
3. Three peptides derived from heparin binding EGF (Besner et al 1992).

The binding strength of the peptide/heparin interaction in all data sets was quantified in terms of the salt strength required to inhibit 50% of the binding to heparin-Sepharose columns. The buffer used for the binding studies was similar for two of the papers with a pH was 7.4 (McCafferty et al 1992, Pratt and Church 1992b), whereas the remaining paper a used of pH 7.0 (Besner et al 1992).

The elements of the consensus sequence model for the salt strength correlation are broadly similar to the stereochemical model discussed in the previous section in that amphipathic indices are used again (but only for the ß-strand in this case). However there is an additional term used to characterise the amphipathic strand, namely the normalised hydrophobicity of the polar face of the ß-strand (i.e. hydrophobicity of the polar face minus the mean hydrophobicity of the peptide). **No** assumptions are made about the number and/or types of contacts (if any) between the basic residues on the peptide and the sulphates on the GAG chain. The sequences are simply scored as to the number of basic residues conforming to each of Cardin and Weintraub's consensus sequences, using four rules outlined below:

1. Potential sites were identified if the spacing of three or more basic residues matched either of the two consensus sequences.
2. Any of the sites identified in step one that had acidic residues present at positions 1,5 or 6 of type I or positions 1 and 4 of type II were discarded.
3. The number of basic residues in these putative sites, at position 2,3,4,7 and 8 of type I or 2,3 and 5 of type II was then recorded.
4. If a peptide had two potential fits to either of the consensus sequences, the number of basic residues was taken as the mean of each of these sites.

Six of the peptides out of the fifteen peptides in the three data sets were omitted from the data analysis for reasons outlined below. One peptide (PCI random) was omitted because of an acidic residue at position 5 of the putative GAG binding site. The sequences of four peptides (EGF 8-19, A2B, A4A and A3A) did not conform to either of the consensus sequence. Finally while the sequence of PF4 74-85 conformed to a type I consensus sequence, it was omitted because it was known to be folded in an alpha helix in the intact protein (St Charles et al 1989). Full details are shown in Section A5.4 of Appendix 5. The salt strength score for beta strand binding is defined in equation 6.3.

Equation 6.3:

$$S(\beta) = AI(\beta) \cdot H_{nor}^{P} \cdot N_B$$

Where H_{nor}^{P} and N_B are the normalised hydrophobicity of the polar face and the number of basic residues in the GAG binding site respectively.

Correlations for each of the consensus sequences (i.e. type I XBBBXXBX and type II XBBXBX) between the salt strength and S(ß) were found these are shown in Figure 6.2. The correlation coefficients for type I and type II consensus sequences (0.889 and 0.996 respectively) were significant at the 2.5% level of significance for a single tail test (that there is no correlation i.e. that r = 0). So despite the small number of peptides containing either consensus sequence in the three data sets (6 and 3 respectively) it is apparent that the consensus sequence binding model may be correct. The implicit assumption in this correlation is that these peptides bind to

heparin in a ß-strand conformation. The assumption appears to be at least partially valid since the stereochemical model described in the previous section predicts that the majority of the peptides [PCI (264-283) being the exception] should adopt a ß-strand conformation upon binding heparin.

The consensus sequence model used in the formulation of the salt strength binding correlation, only considers acidic residues in the selection of the GAG binding site from the peptides sequence. It makes no comment (unlike the stereochemical model) on which acidic and basic residues may have contacts with the sulphate groups on the GAG chain. The model only considers the degree of fit to the established GAG binding consensus sequences, the hydrophobicity of the polar face, and the tendency to conform to a ß-strand.

Figure 6.2: Salt strength binding correlations

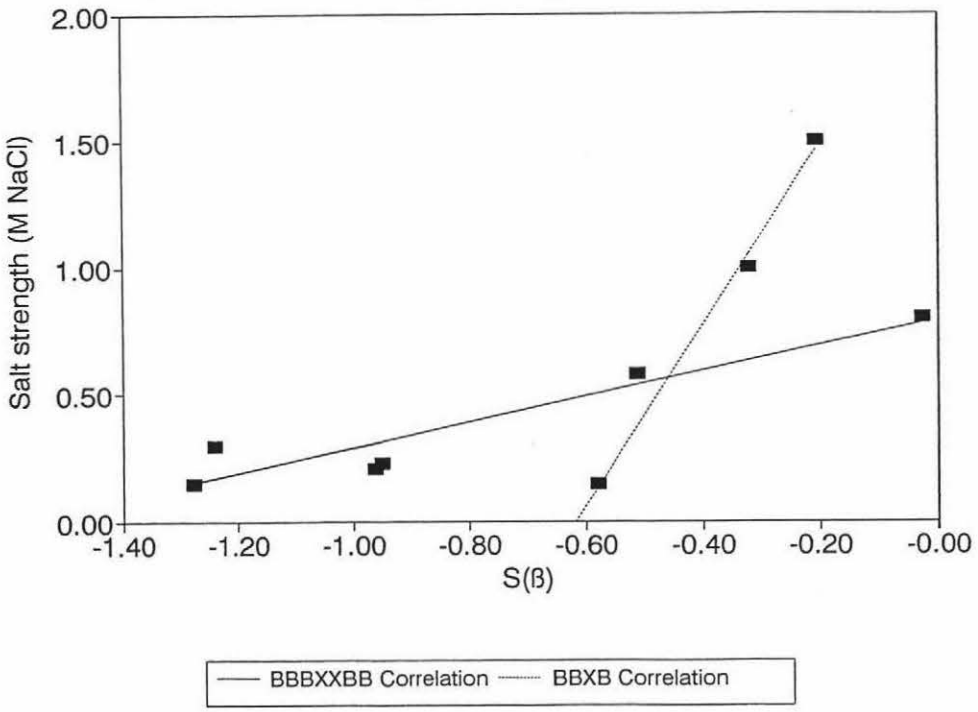

Type I: Constant 0.794, slope 0.502, r^2 0.899

Type II: Constant 2.191, slope 3.551, r^2 0.996

Table 6.9: Summary of peptides for used in the salt strength correlation

Peptide	Sequence	Consensus sequence	Salt strength (M)	S(ß)	Source
PCI 264-283	SEKTLRKWLKMFKKRELEEY	I	0.80	-0.0249	Pratt et al 1992
HC 183-200	FRKLTHRYTLRLFRRNFG	I	0.58	-0.5103	
A2B	DFRKDLGWKWIHEPKGYHA	I	0.23	-0.9524	McCaffrey et al 1992
HC 173-190	KYEITTIHNLFRKLTHRL	I	0.21	-0.9624	Pratt et al 1992
ATIII 124-140	AKLNCRLYRKANKSSKL	I	0.30	-1.241	
ATIII 124-140 Random	LNRCKNAKYSKLSKARL	I	0.15	-1.278	
PCI 264-283 Random	MRTKELKLFKWERLEKLSKY	-	0.38	-	
PF4 74-85	LYKKILKKLLDA	I	0.24	-	
A1A	WKWIHEPKGYHA	-	0.30	-	McCaffrey et al 1992
A2A	DFRKDLGWKW	-	0.23	-	
A3A	PYIWSLDTQY	-	Non binding	-	
HB-EGF 8-19	QALATPNKEEHG	-	Non binding	-	Besner et al 1992
HB-EGF 20-25	KRKKKG	II	1.5	-0.204	
HB-EGF 36-41	LRKYKD	II	1.0	-0.322	
A4A	VGRKPKVE	II	0.15	-0.579	McCaffrey et al 1992

Where S(ß)is the beta strand strength score.

The range of prediction that can be made from the consensus sequence model are somewhat restricted but they include the following.

1. The conformation of the peptides used in the correlation (Table 6.9) upon binding heparin should have significant levels of ß-strand when compared to any helix that may or may not be present.
2. Substitution of the basic residues to nonpolar residues that are not included in the putative consensus sequences should have little or no effect on the strength of binding.

Further experimental work on this model is recommended to validate it and to examine the following points: establish if peptides that bind in an alpha helical mode fit to this correlation, determine if a similar correlation exists for the binding of other GAG's (such as DS, HS, C4S and C6S) to these peptides. It is considered by the writer likely that analogous correlations may exist for peptides folding in an α-helical conformation upon binding heparin.

6.4.1 Specificity of peptide/GAG interactions

Limited experimental work establishing the specificity of peptide/GAG interaction has been reported. The majority of the reports have centred on the characterisation of the heparin/ATIII interaction (Lellouch and Landsbury 1992, Bae et al 1994 and, Tyler-Cross et al 1994). Preliminary studies demonstrating the differential binding of classes of heparin have been reported for von Willebrand factors peptides (Tyler-Cross et al 1993) and transforming growth factor-ß1 (McCafferty et al 1992). Work in the characterisation of the high affinity heparin for the von Willebrand peptide is reported to be underway (Tyler-Cross et al 1993). However all of these studies have yet to demonstrate unequivocally that the binding of these peptides involves specific sequences of sugars on the polysaccharide chain.

6.4.2 ATIII/heparin interaction

The three dimensional structure of ATIII in both the active and inactive forms has been reported (Schredder et al 1994). However neither structure was determined with heparin bound to it and so elucidation of the residues responsible for the interaction have rested with the study of heparin binding mutants of ATIII (Huber and Carrol 1989) and peptide modelling studies (Lellouch and Landsbury 1992, Tyler-Cross et al 1994). The high affinity heparin binding site of ATIII for the pentasaccharide is postulated to reside on the "D" helix (residues F^{123}-A^{134}), however an additional contact at arginine 47 is also thought to be essential. An additional low affinity site (residues 137-149) has also been implicated in heparin binding.

Peptides covering each of these regions (K^{121}-A^{134} and K^{136}-G^{148}) have been synthesized. In addition two peptides covering both the high affinity site and a portion of the low affinity site, the second peptide included both the high and low affinity heparin binding sites (F^{123}-G^{148} and L^{130}-G^{148} respectively). A final peptide with a N terminal extension (AEAAARK) to the K^{121}-A^{134} peptide, to increase the helical content of the peptide was synthesized (K^{121}-A^{134}ext). The interaction of peptides described above with heparin characterised (Tyler-Cross et al 1994). Alanine was substituted for N^{127} and C^{128} in native ATIII to favour helix formation and preclude disulphide bond formation between the peptides. In this series of experiments the binding was characterised by three techniques. These were: CD, isothermal binding calorimetry and competition binding assays. Isothermal binding calorimetry was used to directly characterise the binding of the ATIII peptides to heparin. All the peptides examined demonstrated exothermic and saturatable binding. This technique enables the determination of the thermodynamic binding parameters associated with the binding (i.e. K_d, ΔH and ΔS). Of the five peptides examined (Table 6.10) four of the peptides examined were able to be fitted to a single binding site model. The exception being F^{123}-G^{148} which encompassed both the high and low affinity binding sites.

The competitive binding assay demonstrated that all of the peptides were potent competitors for the binding of heparin in the ATIII/heparin interaction. However the

concentration for 50% inhibition of the binding assay (IC_{50}) for each of the peptides were an order of magnitude higher than the K_d values obtained from the isothermal binding calorimetry binding assay. This discrepancy is due to the different binding interaction measured by the two assays, the competitive binding assay measures specific interactions whereas the calorimetric binding assay measures all binding (ie specific and nonspecific). The high and low affinity heparin appear to bind at different sites on the heparin chain, since the effects of the peptide pairs of peptides (i.e. K^{136}-G^{148} plus K^{121}-A^{134} or K^{136}-G^{148} plus K^{121}-A^{134}ext) were additive in the competitive binding assay when the peptides were incubated at their IC_{50} concentrations. For full inhibition elements of both the high and low affinity binding sites were required.

On the basis of the stereochemical model three (F^{123}-G^{148}, K^{121}-A^{134} and K^{121}-A^{134}ext) of the five peptides were correctly assigned as binding heparin in a ß-strand mode, since the C(ß) scores dominates (Table 6.10). However the C(α) scores dominated for the two remaining peptides (i.e. L^{130}-G^{148} and K^{136}-G^{148}) and these peptides would be expected to bind heparin in an alpha helical manner. These two peptides cover the entire low affinity heparin binding site. The authors stated that these peptides did change conformation on binding of heparin (whether it was α-helical or ß-strand was not stated), but only at very high concentrations of heparin.

The association constants of the peptides for heparin varied over four levels of magnitude with the peptides covering the residues 121 to 135 having the lowest dissociation constant i.e. tightest binding. A correlation between the C(α) scores of the peptide fragments of ATIII high and low affinity sites (i.e. K^{121}-A^{134}ext peptide was omitted) and the logarithm of the disassociation constants (r=0.986, significant at the 2.5% level of significance) was found. Tight binding of the peptide/heparin interaction (defined on the basis of low K_d) is associated with low helical scores [C(α)].

Table 6.10: Summary of peptide modelling of ATIII/heparin interaction

Peptide	K_d	Log K_d	C(α)	C(ß)	IC_{50}
F^{123}-G^{148}	9.3(6.6) x 10^{-7}	-6.032	0.366	0.493	0.30
L^{128}-G^{148}	3.5(0.6) x 10^{-7}	-6.456	0.361	0.173	0.70
K^{136}-G^{148}	1.1(0.1) x 10^{-5}	-4.958	0.469	0	2.00
K^{121}-A^{134}	8.1(2.7) x 10^{-9}	-8.092	0.225	0.374	0.51
K^{121}-A^{134}ext	1.8(0.9) x 10^{-8}	-7.745	0.122	0.303	0.20

Source Tyler-Cross et al 1994. Sequences of the peptides: F^{123}-G^{148}; FAKLNSRLYRKANKSSKLVSANRLFG, L^{128}-G^{148}; LYRKANKSSKLVSANRLFG, K^{136}-G^{148}; KSSKLVSANRLFG, K^{121}-A^{134}; K(ßA)FAKLAARLYRKA K^{121}-A^{134}ext; AEAAARK(ßA)FAKLAARLYRKA.
IC_{50} concentration of the peptide required to inhibit 50% of the ATIII/heparin interaction
Parameters for the C(α) versus K_d correlation: constant 10.972, slope 12.912, r^2 0.986.

A recent paper (Bae et al 1994) has come the closest at demonstrating a specific interaction between specific sugar sequences on the heparin chain and a short peptide. The authors used affinity purified heparin with a immobilised ATIII affinity column to obtain high affinity heparin (ie enriched in the high affinity pentasaccharide sequence). A peptide fragment of ATIII residues 123-139 along with four variants was synthesized. The variants were as follows: replacement of tyrosine 131 with alanine, replacement of lysine 136 with alanine (disrupted consensus), a double mutant with both replacements (modified disrupted peptide) and a scrambled peptide. The peptide sequences are shown in the legend to Table 6.11. The lysine that was replaced in the disrupted peptide was part of a cluster of basic residues which conformed to a type I consensus sequence. The binding of each of these peptides to high affinity heparin was studied with four techniques. These techniques were: heparin affinity chromatography, NMR spectroscopy, fluorescent spectroscopy and a bioassay (performed under competitive and noncompetitive conditions).

The NMR evidence from the interaction of the consensus peptide and the disrupted consensus peptide suggested a major difference in the environment of tyrosine when the peptides were bound to heparin. Steady state nuclear overhauser effect (NOE) spectra suggested further that the tyrosine of the consensus peptide was in a single microenviroment, and was probably in close proximity to the N-acetyl groups of high

affinity heparin (HAH). The disrupted consensus peptide-HAH interaction demonstrated the existence of two resonances for tyrosine in the ratio 93:7 (the minor shift being the same as the specific complex). A close spatial relationship between leucine (126 or 130), probably 130 and the N-acetyl group was also reported.

These results taken together suggest that the consensus peptide binds specifically to the ATIII pentasaccharide binding site of heparin, whereas the disrupted consensus peptide binds nonspecifically. These results are consistent with the results of Tyler-Cross and coworker's (Tyler-Cross et al 1994) which indicated that elements of both the high and low affinity binding sites are necessary for full inhibition of the binding, since lysine 136 is at the start of the proposed low affinity binding site.

The strength of the interaction between the synthesized peptides and unfractionated heparin was quantified by heparin affinity chromatography, with stepwise gradient elution (Table 6.11). Since a very small fraction of the consensus peptide was bound to the affinity column when compared to the other peptides (rearranged and disrupted consensus peptides), this was taken as further proof of specific binding. As has already been discussed the mutation of the lysine had a dramatic effect of the specificity but little effect on the strength of the interaction. This is puzzling since the lysine was part of the consensus sequence. However by using element of the consensus sequence model described in the previous section (Section 6.6) this puzzling results can be rationalised, since the consensus peptide and the disrupted consensus peptide have similar S(ß) values and would be expected to bind at similar salt strengths. Full details on the calculation of these ATIII peptides are shown in Section A5.5 of Appendix 5.

While each of the two model (stereochemical and consensus sequence model) for peptide/GAG interaction developed in this chapter (Sections 6.2.3.1 and 6.3 respectively) are able to rationalise aspects of the binding of the ATIII peptides to heparin, a complete understanding is still lacking.

Table 6.11: Peptide modelling of the specificity of the ATIII/heparin interaction

Peptide	Binding strength (M salt)	% Elution	S(ß)
ATIII 123-139	0.5	50-75	-0.879
Disrupted ATIII 123-139	0.5	90	-0.875
Random	0.25	>96	-0.234

Sequences of the peptides: ATIII 123-139; FAKLNCRLYRKANKSSK, Disrupted ATIII 123-39; FAKLNCRLYRKANASSK, Random FKAKNCRLYRAKSSNLK.

6.4.3 Peptide affinity columns

The use of immobilised peptide columns to fractionate heparin has been reported in two instances (McCafferty et al 1992 and Tyler-Cross et al 1993). The former report concerns the immobilisation of peptide fragments of transforming growth factor ß1 (TGF-ß1) whereas the latter concerns fragments of von Willebrand factor. The interaction of the von Willebrand peptide with heparin was strong, since it required 1 M NaCl to elute the bound heparin. On the basis of a heparin/von Willebrand competition assay results the high affinity heparin was more potent than unfractionated heparin, the $IC_{50's}$ were 11 µg/ml and 75 µg/ml respectively. In the former case two peptides of TGF-ß1 (A1A and A2A) were separately immobilised onto the resin and one of these resin (A2A) was capable of fractionating high and low affinity heparin with a five fold difference in affinity for native TGF-ß1.

6.4.4 Energetics of peptide/heparin interaction

One group has published two reports (Tyler-Cross et al 1993, 1994) characterising the thermodynamics of the binding for seven heparin binding peptides using isothermal titration calorimetry. In all cases the binding was exothermic and saturatable, the $T\Delta S$ term for the peptides tested was small, demonstrating that the binding was enthalphly driven. Furthermore the change in heat capacity associated with the binding was

determined for three of these peptides (ATIII peptides F^{123}-G^{148}, K^{121}-A^{134}ext and von Willebrand peptide Y^{565}-A^{587}). Although the term was negative, it was relatively small suggesting that hydrophobic bonds do not have a major contribution to the binding interaction for the three peptides tested.

6.4.5 Summary

A complete explanation of the origin of the specificity of some peptide/heparin interaction is still lacking. It is apparent that most of interaction is due to ionic bonds i.e. sulphate/basic acid interactions. It has been demonstrated in the case of ATIII/heparin interaction that one section of the peptide is important for tight binding (Tyler-Cross 1994) and one of the basic amino acids is involved in directing the specificity (Bae et al 1994). The remaining elements of the interaction are still being elucidated. It is still not known from the direct examination of experimental results what contact between basic residues and elements on the GAG chain are responsible for the specificity.

The two complementary models developed in this chapter viz the stereochemical model (Section 6.2.3.1) and consensus sequence model (Section 6.3) are able to rationalise elements of the binding behaviour of ATIII peptides in terms of the binding parameter (Tyler-Cross et al 1994) and the salt strength required to disrupt binding (Bae et al 1994).

6.5 Sequence specific binding

It is not known at present whether the majority of the biological binding behaviour of GAG's is mediated by sequence specific protein binding, however there is evidence that the four known examples (Section 1.3.1) may soon be joined by further sequences. A simple method for quantifying the interaction of GAG's with proteins (termed affinity co-electrophoresis) has been reported (Lee and Lander 1991). The method involves the electrophoresis of labelled heparin through zones containing samples of purified proteins at different concentrations. If heparin interacts with the protein its movement will be retarded, examination of the degree of retardation at the different protein concentration

allows the disassociation constant to be measured. The method appears in principle to be an application for studying the specificity of peptide/GAG interactions. If the protein binds selectively to different fractions of the labelled heparin, the heparin will migrate as a broad band or as two bands. This technique has been used to examine the prevalence of specificity in extracelluar matrix proteins (SanAntonio et al 1993) in which the interaction of laminin, fibronectin, thrombospondin and type I collagen with heparin were tested. Heterogeneity in the binding of heparin to type I collagen, laminin and fibronectin was demonstrated. This could indicate the existence of specific carbohydrate sequences on the GAG chain mediating the binding. Strongly bound heparin to one of these proteins also bound strongly to the remaining two. The high affinity binding of heparin to these proteins was demonstrated not to be based on net charge or chain length. However the difference in affinity between the high and low affinity heparin was modest, 5-30 fold compared to 1000 fold for the well characterised ATIII/heparin interaction.

Affinity coelectrophoresis has also been used to demonstrate the differential binding of heparin by two chemokines IL-8 and GRO-α (Witt and Lander 1994) with a 16 and 24 fold difference in the binding of high and low affinity heparin respectively. The heparin binding sites are contained in the 24 C-terminal residues, and conform to Cardin and Weintraub's type I consensus sequences. The three dimensional structures of these two proteins are known. These two proteins exhibit substantial selectively in heparin binding over two related proteins (PF4 and NAP-2 have 1.6 and 2.3 fold differences in affinity respectively). A significant difference between the four proteins is the occurrence of an acidic residues at position 6 of the consensus sequence in IL-8 and Gro-α compared to their absence in PF4 and NAP-2. The authors made the suggestion that sections of heparin with short regions of undersulphation should accommodate these two proteins more easily than uniformly of highly sulphated regions. A direct prediction that heparan sulphate should bind IL-8 and Gro-α to the same extent as heparin was tested and found to be correct.

6.6 CHAPTER SUMMARY

A critical examination of the five proposed consensus sequences (Sections 1.3.2 and 6.1.2 to 6.1.5) on proteins for the binding of GAG's has led the writer to conclude that their are two consensus sequences for continuous GAG binding sites (viz Cardins type I and II). However these are modules from which the complete GAG binding site on proteins is built from. The criteria seem to be the spacing of basic residues.

Examination of the conformational changes of synthetic peptides upon binding heparin has led to the development of a stereochemical model for GAG binding on peptides. The model is composed of three elements: amphipathic profiles of the peptides, and the spacing of acidic and basic residues within the peptide sequence.

This model is able to rationalise the dominant secondary structure induced when the peptides bind C6S (two examples) and heparin. In addition published data for the binding behaviour of ApoB peptides and fibronectin peptides binding to C6S and heparan sulphate respectively was also rationalised by the writer.

A correlation between attributes derived from the peptide sequence and the strength of the peptide/ heparin interaction, as judged by the salt concentration required to inhibit 50% of the binding was also established. This correlation led to a complementary model for GAG/peptide interaction, termed the consensus sequence model for GAG binding.

The two models for peptide binding to GAG's proposed by the writer are compared in Table 6.12. As can be seen the two models are broadly similar. The principle differences between the two models are the treatment of acidic residues, and the weighting of the contribution of basic residues. The stereochemical model predicts that acidic residues can inhibit basic contacts, whereas the consensus sequence model only considers acidic residues that are within the consensus sequence.

Table 6.12: A comparison of the two GAG binding models

Attribute	Stereochemical	Consensus
Amphipathic secondary structure	Amphipathic indexes used to score the interaction for α-helix/ß-strand	The product of AI(ß) and normalised hydrophobicity is used to quantify the interaction
Contacts	Predicts which basic residues that are making contact with the GAG chain in terms of the spacing of the basic residues	Only considers basics within consensus sequence
Weighting of basic residues	All basics that have contacts are weighted equally	Basic residues within consensus sequences are weighted equally
Acidic residues	Can inhibit basic contacts	Only considers in the selection of the GAG binding site

CHAPTER 7: CONCLUSION

7.1 INTRODUCTION

The overall aim of this thesis was to examine the possibility of using immobilised polypeptide chains for the isolation of pure GAG fractions. Earlier published work on the interaction of PLL with GAG's in the solution phase (Sections 1.1.3.6) suggested that immobilised PLL could be a novel method to fractionation GAG's. Earlier attempts (Suzuki and Koide 1984a, 1984b) to exploit this interaction were unsuccessful in mimicking the solution binding behaviour of PLL The binding of short polylysine chains to GAG classes was examined using PLL chains of defined length with known orientation (i.e. immobilised through the C terminus). Three lengths of PLL were examined in an attempt to determine the minimum length for the differential binding behaviour of PLL. To simplify the analysis of the binding behaviour of the PLL resins three GAG standards of known properties were prepared and characterised.

Two other aspects of the thesis were as follows: the examination of the binding of two peptides (PCI 264-283 and thrombospondin) with these standards as possible alternative peptides for immobilisation for possible use as bioaffinity ligands for GAG's. The biological binding behaviour of short peptides to GAG's reported in the biochemical literature was used to propose two complementary models explaining different aspects GAG/peptide interaction.

The content of this thesis is divided into four broad areas. These are:

1. The isolation and characterisation of the GAG standards.
2. The characterisation of the binding of these GAG standards to short resin bound polylysine chains of defined length (4, 8, and 12 lysine residues), followed by the comparison of the behaviour of the same GAG standards to long PLL chains.
3. Solution binding studies of three peptides to the GAG standards.

4. An examination of the literature results on the binding of short peptides to GAG's resulted in the proposal of two complementary models of aspects of GAG/peptide interactions.

7.2 GAG STANDARDS

It is the writer's considered opinion that to be able to fully understand and/or characterise the binding behaviour of the GAG classes to either chromatographic resins or polypeptide chains, pure GAG fractions of known properties **must** be used. It was for this reason that three GAG standards representing the GAG classes CS, DS and heparin were prepared and/or characterised during this thesis. Published technology for the purification of DS using the fractional precipitation of the calcium salts of DS by ethanol (Meyer et al 1956) was found to be satisfactory for the preparation of a pure DS fraction. The remaining standards (CS and heparin) were used as supplied. All three GAG standards were characterised by five different techniques. These were:

1. Cellulose acetate electrophoresis
2. C^{13} NMR spectroscopy
3. The charge density (i.e. sulphate to carboxyl ratio) was measured
4. The average molecular weight of the samples was determined
5. Finally the optical rotation of each sample was measured

On the basis of the above criteria two of the GAG standards (CS and DS) were regarded as being homogenous for the purposes of this study. The C^{13} spectra of both CS and DS were identical to published spectra for GAG's of this type. In addition the optical rotation and charge density for each of these GAG's were within the expected range for GAG's for their classes.

The heparin samples could be separated into two fractions (fast and slow moving heparin) by cellulose acetate electrophoresis. The existence of slow and fast heparin has long been known. The principal differences between the two being that fast

heparin has a lower molecular weight and is less sulphated compared to slow moving heparin. These two types of heparin were separated on a preparative scale using a published fractionation precipitation method using 2M KOAc at pH 5.7 (Scott et al 1968). During the characterisation of slow and fast heparin fraction, two novel properties of these fractions were elucidated. C^{13} NMR spectroscopy demonstrated that the spectra of fast heparin was more complex, i.e. indicating that it had a wider range of disaccharide units when compared to slow heparin. The fast heparin had almost double the number of peaks compared to slow heparin 40 and 25 peaks in the spectra respectively. Elements of the structure of fast heparin were similar to those of heparan sulphate. In addition the levels of a particular sugar (Idu2OS) in fast and slow heparin were determined by a recently published assay (Piani et al 1993). The levels in fast heparin were approximately half of the levels in slow heparin. These differences between fast and slow heparin, i.e. the complexity of the C^{13} NMR spectra for fast heparin and the higher levels of Idu2OS in slow heparin to the writer's knowledge have not been described in the biochemical literature before. While the heparin was able to be fractionated into two homogenous subfractions, i.e. slow and fast heparin, it was decided by the writer to use unfractionated heparin in the binding studies.

7.3 GAG BINDING BEHAVIOUR OF PLL RESINS

The principal observation of the solution binding behaviour of PLL for GAG's which makes it attractive as a novel fractionation method is that it binds DS more strongly than heparin. The different GAG classes are also able to induce α-helices in PLL chains upon binding PLL chains. The extent of α-helix formation depends upon the GAG class (Section 1.1.3.6). Three lengths of short PLL chains with 4, 8 and 12 lysine residues (immobilised through the C-terminus) were synthesized by the writer to probe what length was required for this effect.

The binding of the GAG standards to the K_xG series resin was examined in terms of the stoichiometry of binding (i.e. the number of lysine bound per disaccharide unit) and the binding strength of DS and heparin (w.r.t. CS). As a control a PLL chain of

similar length to that used in the earlier solution binding studies (Gelman et al, Section 1.1.3.6) was immobilised and the binding of the GAG standards was characterised in the same manner. The relative binding strength of DS to all four resins, i.e. K_xG (with x= 4,8, or 12) and the PLL resin were identical within experimental error. The relative binding strength from these resin binding studies was between the values from the earlier PLL-resin (Suzuki and Koide 1984a) and the solution binding studies of Gelman's group (Blackwell et al 1977). There were indications that the relative binding strength of heparin within the K_xG series resins were different since the relative binding strength decreased form 1.6 to 1.34 as the number of lysines residues in the chain increased from 4 to 12. The binding behaviour of the PLL-resin was identical to the solution binding behaviour of the PLL in solution. The expectation of tight binding of DS to PLL chain was not achieved for both the PLL and K_xG series resins. The stoichiometry of the binding of the GAG standards to these resins reinforced the conclusion for the relative binding strength i.e. that the mode of binding may be different. In addition the results from the K_xG-Resin series suggest that the binding may be in terms of a ß-strand rather than the α-helical mode that was suggested for the earlier solution binding studies (Section 1.1.3.6) for longer PLL chains (with 500 residues).

The binding of three lengths of PLL chain (with 8, 126 and 633 residues) with the GAG standards in solution was studied to probe the preliminary conclusion of the resin binding results. Two aspects of the binding were examined, the solution conformation upon binding the GAG standards and the stoichiometry of the interaction. These studies confirmed that the mode of binding of the GAG standards to K_xG occurred via a radically different conformation compared to the earlier solution binding studies (Section 1.1.3.6), with ß-strand being the dominant secondary structure rather than the expected α-helix. In addition conformational studies of the GAG/PLL complexes for the longer PLL chains (with 126 and 633 residues) that were studied suggested that while the extent of the induced helix followed the order CS < DS < heparin, the length of the PLL chain had some effect. The shorter PLL chain (126 residues) having decreased amounts of induced α-helix. The reason why DS was not bound more strongly than heparin was not able to

elucidated in this thesis but explanations could be:

1. The charge density (i.e. sulphate to carboxyl ratio) of the DS used in this study was between that of the earlier resin binding study (Suzuki and Koide 1984a, 1984b) and the solution binding study described in section 1.1.3.6 (were 1.2 versus 1.0 and 1.4 respectively). Since the charge density has been demonstrated in some cases to be important for the binding strength of some protein/GAG interactions the effect could be due to this.

2. The mode of binding is different for the K_xG-resin series with ß-strand being the dominant secondary structure being the dominant secondary structure rather than α-helix. This may be the reason for the loss of the differential binding behaviour.

7.4 GAG BINDING PETIDES

The biological properties of GAG's are primarily mediated by their binding to protein (Jackson et al 1992). Limited information exists in the literature on the effects of the binding of different GAG classes on the conformation of GAG binding peptides. To the writer's knowledge there are only two examples. These are the binding of PLL chains to the various GAG classes (Blackwell et al 1977) and the interaction of heparin or C6S to a peptide fragment of ATIII residues 123-139 (Lellouch and Landsbury 1992). Since studies of this type seem to provide useful clues of the specificity of the GAG/peptide interaction, the interaction of the GAG standards with two important peptides PCI (264-283) and the thrombospondin peptide fragment, was examined. CD spectroscopy was used to determine the dominant secondary structure induced in the peptide upon binding the relevant GAG standards.

The binding of the PCI (264-283) peptide to the different GAG standards induced different secondary structures. For CS and heparin, α-helix was the dominant secondary structure, whereas for DS the ß-strand conformation dominated. However heparin and DS had approximately twice the level of induced secondary structure

than that induced for CS. The order of induced α-helix in the PCI peptide for the various GAG standards (Hep > CS > DS) paralleled the reported biological activities of the GAG's for mediation of the biological activity in the intact protein. The strength of the interaction of DS and heparin with the PCI peptide was measured by determining the concentration of salt required to inhibit 50% of the interaction. The values determined were 0.1 and 0.3 M salt for DS and heparin respectively. The binding of the thrombospondin peptide to the various GAG classes resulted in no detectable change in the conformation of the peptide. The binding behaviour of the PCI peptide for the various GAG standards suggested that it may be a candidate for immobilisation and the examination of its ability to fractionate the GAG classes.

7.5 MODELS OF THE GAG/PEPTIDE INTERACTION

The final part of this thesis is the proposal of two complementary models to rationalize the binding behaviour of GAG binding peptides with GAG's (principally heparin) reported in the biochemical literature. The proposal of these models is in the writer's opinion the most far reaching and important results of the thesis.

A critical examination (Sections 6.1.2 through 6.1.5) of the five different consensus sequences for GAG binding sites on proteins that have been proposed (Section 1.3.2) suggested that there may be only two fundamental GAG binding consensus sequences. These were the two that were initially proposed by Cardin and Weintraub (Cardin and Weintraub 1989). An additional feature of the binding site as suggested by two groups (Margalitt et al 1993, Yang et al 1994) is that the spacing of single pairs of basic residues is important for the binding of GAG's.

7.5.1 Stereochemical model

The first model proposed by the writer's is the stereochemical model. It centres around the spacing of multiple pairs of basic residues when the peptide is folded into an α-helix or ß-strand. Three components are used to predict the effect of GAG binding to the peptide. These are:

1. The tendency of the peptide to fold into an α-helix or ß-strand. This is predicted in terms of the amphipathic profiles of the peptide (Sections 5.2.5 and 5.3.1).
2. The number of attractive complexes between pairs of basic residues and the axial disaccharide repeat distance of each GAG class when it is folded into a 2-fold helical structure in solution.
3. The number of repulsive contacts between pairs of acidic and basic residues on the peptide and the sulphate groups on the GAG chain.

While the first factors have been separately discussed previously in the literature by several authors (Cardin et al 1991 and Camejo et al 1988 respectively), each factor by themselves are unable to completely rationalise the binding behaviour of GAG binding peptides. The final point (number 3 above) to the writer's knowledge has not been discussed at all in the biochemical literature, although the specificity of the binding of heparin to two proteins has been demonstrated to be greatly influenced by the presence of acidic residues (Witt and Lander 1994).

The assumption used by the writer in the development of the stereochemical, that acidic residues influence the conformation of the peptide in the GAG/peptide complex is the most novel feature of this model. It is directly testable by the synthesis of analog peptides with any acidic residues that may be present (i.e. asp or glu) being replaced by aspargines or glutamines respectively. If the assumption has any validity the conformation of these peptides should change in a predictable manner.

The main assumption of the stereochemical model developed by the writer is that the whole peptide is projected into a pure α-helix or ß-strand when examining the probable conformation of the bound peptide. This may be partly true for short peptides (i.e. less than 20 residues), however for longer peptides such as Apo B 3345-3381 and Apo E 202-243 (Cardin et al 1989, 1991 respectively) this may not be case.

The model was able to successively rationalise the binding behaviour in terms of the dominant secondary structure that was induced when peptides bound heparin (5 cases) or CS (2 cases). The biological binding properties of ApoB peptides to C6S (Camejo et al 1988) and a 15 residue peptide derived from fibronectin, FN-C/HII to heparan sulphate were both successfully rationalised using the above model.

7.5.2 Consensus sequence model

The strength of the interaction between heparin and nine heparin binding peptides containing type I or Type II Cardin and Weintraub consensus sequences has been measured by three groups (Besner et al 1992, McCaffrey et al 1992 and Pratt and Church 1992). A correlation for each of the consensus sequences between an attribute derived from the peptide sequence and the binding strength determined by the above authors was discovered by the writer. The single assumption of this model is that the peptides used in the correlation bound to heparin in a conformation that was in a predominantly ß-strand form. It is this assumption that can be experimentally tested.

7.5.3 Implications of the models

There are a number of implications of the two models discussed above. To test if these models have any basis in fact a number predictions can be made. These predictions can be directly tested using available tools to the writer. The predictions are as follows:

1. Substitution of acidic residues within GAG binding peptides to their amide forms should result in changes in the induced conformation when these peptides bind heparin. These changes should occur in the manner predicted for the stereochemical model.
2. The strength of the interaction between heparin and peptides containing the consensus sequences should be able to be predicted using the consensus sequence model.

The most exciting implication of the models is that it may be possible to design a GAG binding peptide that could selectively bind particular GAG classes e.g. a peptide that binds C6S over heparin. Peptides of this type **do not** exist naturally since the binding of GAG's to proteins follows the following order (Section 1.1.2):

Heparin > HS > DS > CS > Hyaluronic acid

A corollary of these models is that if the specificity and strength of the binding of GAG's to peptides is simply dependent upon the appropriate spacing of basic residues in a particular secondary structure, it should be possible in principle to design a peptide mimetic for use as an affinity ligand for binding and fractionating GAG's. It is reasonable to expect that the mimetic could be much less expensive and more robust than a synthetic peptide for large scale isolation.

7.6 OUTLINE OF FUTURE WORK

A future research worker will find a number of fertile and novel areas to examine resulting from the writer's effort during this study. Further analysis of the consensus sequences of GAG binding sites and the validation of the two models proposed by the writer cry out for further experimentation.

There appears to be a the tendency for particular basic amino acids to occur in particular positions within the consensus sequences of GAG binding peptides. This can be examined in two ways. These are:

1. The protein sequence data bases should be examined to see if additional amino acid sequences should be examined to see if additional AA sequences conforming to the putative GAG binding consensus sequences can be found. These new sequences should be analyzed statistically to see if the trend for particular basic amino acids are still valid.
2. Arginine residues within GAG binding peptides that have already been characterised (such as ATIII 123-139) should be changed to lysine and/or

histidine. The binding behaviour of the modified peptides should then be characterised in terms of the conformation, strength of the interaction and specificity of the interaction to see if there are any changes.

The solution conformations of the nine peptides (Section 6.3) used in the consensus sequence model should be determined by CD spectroscopy, to see if the prediction that these peptides bind in predominantly ß-strand conformation is correct. CS and DS affinity columns should also be prepared and the strength of the interaction of the 9 peptides with each of these columns should be determined, to see if similar salt strength correlations exist for CS and DS.

The various basic residues in the PCI peptide should be serially changed to alanine and the conformation of these modified peptides when bound to GAG's should be compared to the predicted conformation on the basis of the stereochemical model. The acidic residues in the PCI peptide should also be separately serially modified to there amide forms. The solution conformation upon binding GAG's should again be compared to prediction that can be made from the stereochemical model.

Appendix 1: Supplementary material to Chapter 1.

A1.1: GAG properties

Table A1.1: Properties of the GAG's Used by Gelman

GAG class	Molecular weight (kdaltons)	Charge density
Hyaluronic acid	230	0.00
KS	16	1.17
HS	23	0.99
C4S	60	1.00
C6S	25	1.00
DS	9	1.40
Heparin	11	2.30

Table A1.2: Elution behaviour of GAG's on Suzuki's PLL resin

GAG Class	Charge Density	NaCl concentration for elution (M)	Gelmans binding strength
Hyaluronic acid	0.00	0.32	0.50
Chondroitin	0.00	0.36	-
KS	1.90	0.80	-
C4S	1.00	0.86	0.80
DS	1.00	0.91	>2.0
C6S	1.00	0.95	0.27
HS	0.99	1.20	-
Heparin	2.80	1.35	1.5

Table A1.3: Ionizing groups per disaccharide units of GAG's

GAG	Number of carboxyl groups	Number of sulphate groups	Total number of charged groups
Hyaluronic acid	1	0	1
KS	0	0.9-1.8	0.9-1.8
Chondroitin	1	0	1
C4S	1	0.1-1.3	1.1-2.3
C6S	1	0.1-1.3	1.1-2.3
DS	1	1.0-3.0	2.0-4.0
HS	1	0.4-2.0	1.4-3.0
Heparin	1	1.6-3.0	2.6-4.0

Adapted from Breen et al 1976 and Lindahl and Hook 1978

A1.2 Heparan sulphate proteoglycans (HSPG) and amyloidoses

The presence of HSPG in amyloid deposits has been established by differential staining with Alcian blue and immunochemistry. Differential staining of GAG's with Alcian blue is achieved by varying the concentration of magnesium chloride (Scott and Dorly 1965). Antibodies directed against either the core protein or the HS chains of HSPG has established the presence of HSPG in prion protein plaques of Gerstmann-Straussler Syndrome, Creutzfeldt-Jacob and Scrapie (Snow et al 1990).

Common features of **all** amyloid deposits include heparan sulphate proteoglycans and the serum amyloid protein (SAP). The common features of the proteins that comprise amyloid deposits are: small size (3-30 kdaltons), they are polyanionic (high content of dicarboxylic acid), and exhibit a high proportion of ß-sheet amino acids (Sipe 1992).

HSPG and SAP comprise the amyloid enhancing factor, which in conjunction with

inflammation lead to the formation of amyloid deposits (Kiselevsky 1990).

There are some suggestions that the outside of amyloid deposits may be coated with dermatan sulphate proteoglycans. Decorin, a dermatan sulphate proteoglycan has been established by the use of 3 monoclonal antibodies to be present on the outside of spherical amyloid core (Snow et al 1992).

Why are HSPG colocalising? There are two possible reasons for this. These are:

1. They may be more common at the site of deposition.
2. The chains are more flexible therefore they may bind easier to components of the amyloid deposits.

"GAG's may influence the deposition of amyloid protein should GAG accumulate in the tissue prior to amyloid formation. This phenomenon has been observed in the early stages of collagen fibril formation where the presence of GAG determined the rate and size of fibrils" (Guiroy et al 1991).

In several cases the identity of the HSPG has been established to be Perlecan, a basement membrane component (Ailles et al 1993). There is some suggestion however that this may not always the case. Differences in the types of HS and HSPG fragments have been detected (Vangool et al 1993) using antibodies directed against the core protein and HS chains.

SAP binds HSPG and dermatan sulphate PG (it binds HSPG better) and heparin competes for the binding of PG (Hamazaki 1988 and 1989). The binding affinity for peptide fragments of SAP to heparin has been measured as a high affinity interaction (Hamazaki 1987).

A pathogenic mechanism for Alzheimer's disease and Scrapie involving "one dimensional crystallization" has been recently reported (Jarrett and Lansbury 1993). The process involves nucleation dependant polymerization, a phenomena which is common

e.g. protein crystallization and sickle-cell haemoglobin fibril formation. Experiments with model peptides of Alzheimers disease and Scrapie lend some support to this concept (Jarrett et al 1993 and Come et al 1993). Proteoglycans may act as heterogeneous seeds for polymerization or perhaps in the case of Scrapie, they catalyze a conformational change in the prion protein.

A1.2.1 Alzheimer's Disease

The amyloid precursor protein (APP) has been shown to bind to heparan sulphate proteoglycans. APP exists in five isoforms. The brain isoform binds the most strongly out of the three isoforms tested. The solid phase immunoabsorbant binding assay used was also able to indicate that the heparan sulphate chains played only a minor role in the binding process (Narindrasorasak et al 1991). Heparin partially competed for the binding of HSPG suggesting that the HS chains play some role in the binding. The synthesis of the ßA4 (the major protein component of amyloid deposits in AD) and fabrication of A4 affinity columns demonstrated that HSPG bound with high affinity. Removal of the heparan sulphate chains from the proteoglycan diminished, but did not abolish the binding (Buee et al 1993). ßA4 residues 1-28 and 1-40 bound heparin in a pH dependant manner suggesting that HS chains play a role in the binding of ßA4 to HSPG (Brunden et al 1993). The high affinity binding between Alzheimer's disease APP and laminin using solid phase immunoabsorbent assays has also been characterised (Narindrasorasak et al 1992). Laminin like HSPG is a component of the basement membrane

There is preliminary evidence for changes in the disaccharide composition of the HS making up the HSPG expressed into the culture medium when fibroblasts from AD patient are compared to normal fibroblasts (Zebrower et al 1992). The incorporation of radioactive sulphate into CSPG and HSPG was increased. But only in the case of HSPG did the disaccharide patterns after digestion with enzymes change. There was an increase in the 6-sulphated disaccharide and a corresponding decrease in the non sulphated disaccharide. The results suggest that the relative activities of heparan sulphate sulphotransferases are different in tissues and cells isolated from patients with

Alzheimers disease. In addition changes in the degree and extent of sulphation of HSPG caused by the alteration in sulphotransferase activities may have a profound effect on many neuronal proteases and be an important factor in the aetiology of Alzheimers disease.

HSPG is known to accumulate in both intracellular and extracelluar NFT (neuro fibrillar tangles) of patients with Alzheimer's disease. The disaccharide structure is different in the E-NFT and I-NFT as shown by the ability of basic fibroblast growth factor to bind to ENFT but not I-NFT (Perry et al 1991 and Sieolak et al 1991). Perry's group have suggested that the binding of HSPG to NFT may explain the insolubility of this deposit. The high negative charge of the HSPG allows the deposit to concentrate and protects it from attack from proteolytic enzymes.

A1.2.2 AA Amyloidosis

AA amyloidosis occurs as a secondary response to underlying inflammatory disorders. A unique protein (MW 8.5 kdaltons) known as amyloid A protein has been isolated as the main component of the amyloid deposits of this disorder. This protein corresponds to two thirds of the amino terminus of a naturally occurring serum protein known as serum amyloid A (SAA). A close temporal and ultrastructural relationship between HSPG and AA amyloid protein has been demonstrated. Regardless of the organ involved (spleen or liver) or the method of induction (Snow et al 1991). It has recently been established that induction of Perlecan (the HSPG associated with the disorder) gene expression **precedes** amyloid formation in this disorder (Ailles et al 1993).

A1.2.3 Prion disorders

Prion are composed largely if not entirely of prion protein (PrP^{Sc} in the case of scrapie). The formation of PrP^{Sc} from the cellular prion protein PrP^{C} is a post-translation process. To date no chemical modifications of PrP^{C} have been detected. The in vivo function of PrP^{C} is not known. Mice without PrP^{C} seem normal but are completely resistant to prion infection. The proportion of secondary structures in PrP^{C} and PrP^{Sc} has recently

been determined. The conversion from the normal cellular precursor to the prion protein involves a large increase in the ß sheet content (Pan et al 1993). Further more, any treatment that destroys the ß sheet content of PrP^{Sc} seems to also destroy the infectivity of the prion particle (Safar et al 1993). Limited proteolysis of PrP^{C} leads to a release of a protease resistant core that aggregates into amyloid fibrils. The formation of PrP^{Sc} occurs relatively slowly after PrP^{C} reaches the cell surface. Soon after its formation, it is exposed to lysosomal or endosomal proteases and truncated at the N terminus. Once PrP_{res} is formed it is resistant to complete degradation. HSPG have been shown to colocalise with amyloid deposits associated with prion disorders. The binding of endogenous GAG seem to be important for prion replication (Caughy and Raymond 1993). Heparan sulphate has been shown to augment the accumulation of PrP^{Sc} in scrapie infected cultured cells (Gabizon et al 1993). However the addition of low molecular weight heparin to scrapie transformed cells changes this course and leads to phenotypic reversion. It is interesting to speculate that HSPG might be the cellular factor responsible for the conformational change from PrP^{C} to PrP^{Sc}.

Appendix 2: Supplementary material to Chapters 2 and 3

A2.1 Worked examples of viscosity molecular weight determination

A worked example of the processing of the viscosity data to determine the intrinsic viscosity is shown in Table A2.1. The concentration of the dermatan sulphate solution was measured using the uronic acid assay (Section 2.2.4.6). The mean transit times in the viscometer for four different concentration of DS relative to the blank were measured. The relative viscosity of each sample (ratio of samples versus blank) was calculated and converted to specific viscosity by subtraction of 1). The reduced viscosity is the ratio of the specific viscosity and the DS concentration. The intrinsic viscosity was calculated from the intercept of a plot of the reduced viscosity versus the DS concentration.

Table A2.1: Data processing for viscosity determination

DS concentration (g/100 ml)	Time (sec)	Relative viscosity	Specific viscosity	Reduced viscosity
0	464.04			
0.0562	489.53	1.0549	0.0549	0.9769
0.09634	509.98	1.0990	0.0990	1.0280
0.1265	526.69	1.1350	0.1350	1.0672
0.1499	538.84	1.1612	0.1612	1.0754

A2.2 Worked examples of calculation of substitution menu

The substitution levels of a peptide resin throughout the synthesis of a peptide resin can be calculated, and compared to experimentally determined values. This gives some indication of the integrity of the synthesis. A worked example for the automated synthesis of the K_4G resin is outlined below, where the original amine substitution of the starting material was 0.53 mmol/g. If all the coupling reactions go to completion

(i.e. 100% coupling), the total moles of amine on the resin will remain constant. However the coupling of each amino acid to the resin increases the total weight of the resin.

Weight added = 0.53 X 10^{-3} X (MW glycine-18)

= 0.53 X 10^{-3} X 57.1

= 0.0303 g

Total weight 1.032 g

substitution = 0.53/1.0303

= 0.514

second AA (Nε-Boc)Lys

Weight added = 0.53 X 10^{-3} X 228.2

= 0.1209

Total weight 1.1529 g

Substitution = 0.53/1.1598

= 0.459

The steps in the calculation are usually displayed in a tabular form (Table A2.2)

Table A2.2: Substitution menu for K_4G

Aminoacid	Expected total weight (g)	Expected amine substitution (mmol/g)
GLY	1.0303	0.514
LYS	1.1598	0.459
LYS	1.2807	0.414
LYS	1.4405	0.368
LYS	1.5614	0.339

Appendix 3: Supplementary material to Chapter 4

A3.1 Data analysis of GAG binding to ion exchange resin

A comparison of the binding behaviour of eight resins (principally ion exchange) that have been used in the past to separate GAG's has been reported (Bohn and Kalbhen 1971a, 1971b). The authors studied the interaction of pure GAG samples with each of these resins. Elution of bound GAG's was by step gradients with sodium chloride. The data described in their papers was processed to enable the relative binding strength of two of the two resins (Dowex 1X2 and ECTEOLA-cellulose) to be evaluated. The cumulative elution curves for these two resins are displayed in Figures A3.1 and A3.2.

Figure A3.1: Cumulative Elution of GAG's from Dowex 1X2 resin

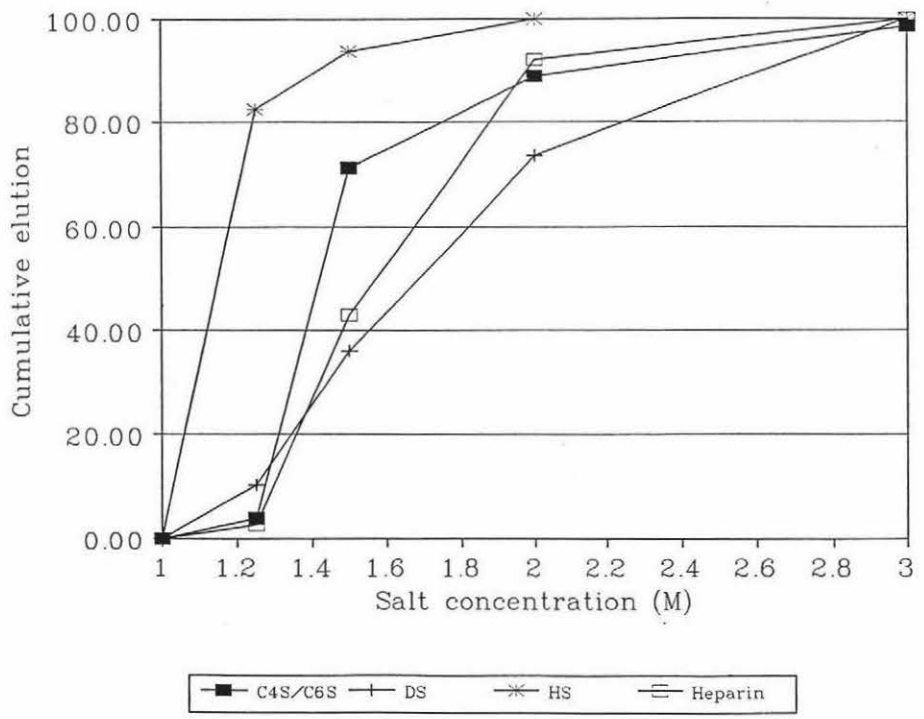

Source of data: Bohn and Kalbhen 1971

Table A3.1: Binding of GAG's to two ion exchange resins

GAG	DOWEX:Salt concentration for 50% elution	RBS	ECTEOLA: Salt concentration for 50% elution	RBS
Chondroitin sulphate	1.42	1.00	1.04	1.00
Dermatan sulphate	1.57	1.18	1.19	1.14
Heparin	1.68	1.10	1.66	1.59
Heparan Sulphate		<0.84	-	-

Figure A3.2: Cumulative Elution of GAG's from ECTEOLA-cellulose

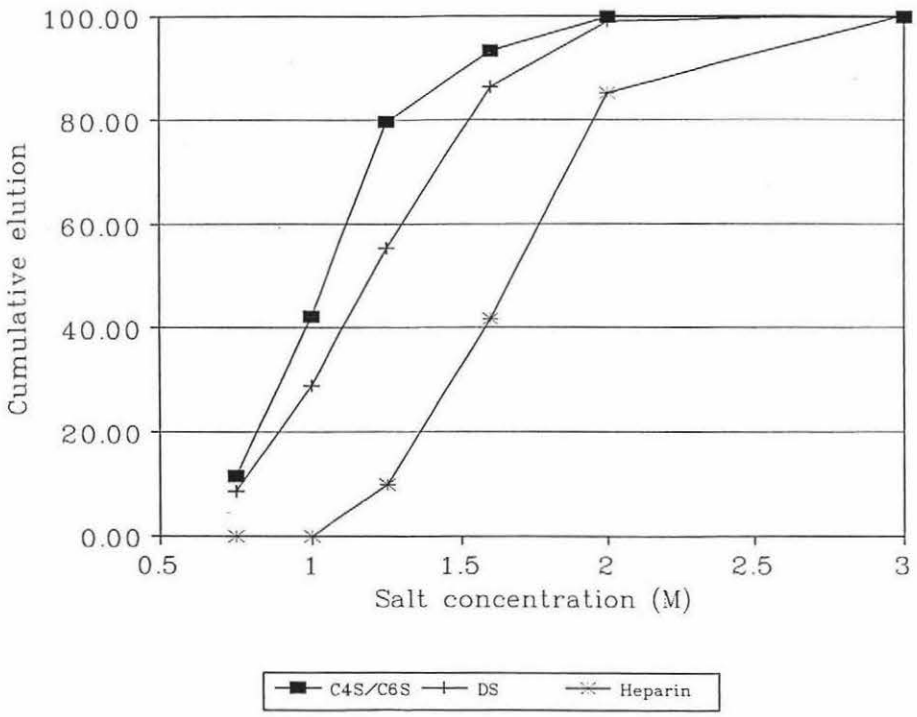

Source of data: Bohn and Kalbhen 1971

A3.2 GAG binding to peptide resins

Table A3.2: K_4G resin ECONO system runs

GAG	$M_{0.25}$	$M_{0.50}$	$M_{0.75}$	RBS
CS	0.93	1.18	1.43	
CS	1.08	1.33	1.63	
		Mean= 1.26		1.00
Heparin	1.58	1.76	1.90	
Heparin	1.51	1.71	1.88	
		Mean=1.74		1.41 (0.1)

Table A3.3: K_4G resin FPLC runs

GAG	Gradient type	$M_{0.25}$	$M_{0.5}$	$M_{0.75}$	RBS	mg Loaded	mg Recovered
DS	Shallow	1.3	1.60	1.80	1.38	1.12	0.86
	Shallow	1.5	1.68	1.80	1.45	1.73	1.66
CS	Shallow	0.88	1.16	1.44	1.00	12.7	9.4
DS	Steep	1.31	1.49	1.71	1.43	5.78	0.15 FT 4.6 ET
CS	Steep	0.76	1.04	1.34	1.00	12.7	0.3 FT 9.5 ET
Hep	Steep	1.38	1.67	1.91	1.61	13.3	7
	Steep	1.36	1.65	1.87	1.59	13.3	1.00 FT 9.6 ET
			Mean=1.66		1.57[1]		

Key: CS; Chondroitin sulphate, DS; Dermatan sulphate, Hep; Heparin, RBS: Relative binding strength. $M_{0.25}$, $M_{0.50}$, $M_{0.75}$ are the salt concentration required to elute 25, 50 and 75% of the bound GAG.

Table A3.4: K_8G resin FPLC runs

GAG	$M_{0.25}$	$M_{0.50}$	$M_{0.75}$	RBS	mg Loaded	mg Recovered
Heparin	1.49	1.76	1.95	1.52	13.3	7.8 ET
	1.33	1.66	1.96	1.43	13.3	0.3 FT 10.3 ET
	1.36	1.64	1.84	1.41	13.3	0.5 FT 10 ET
		Mean= 1.69		1.46		
DS	1.3	1.63	1.80	1.41	5.8	5.2
	1.4	1.58	1.78	1.36	5.8	5.5
		Mean= 1.61		1.38		
CS	0.81	1.15	1.49	1.00	12.7	9.5
	0.85	1.16	1.46	1.00	12.7	9.7
		Mean= 1.16		1.00		

Key: CS; Chondroitin sulphate, DS; Dermatan sulphate. RBS: Relative binding strength, FT: unbound GAG, ET salt eluted fraction.

Table A3.5: $K_{12}G$ resin FPLC runs

GAG	$M_{0.25}$	$M_{0.50}$	$M_{0.75}$	R.B.S	mg Loaded	mg recovered
CS	1.48	1.65	1.82		6.56	7.41
	1.43	1.63	1.93		6.56	7.34
	1.50	1.76	1.93		6.56	6.45
		1.68 (4.2% cov)		1.00		
DS	2.00	2.10	2.32	1.25	5.74	5.8
	2.22	2.27	2.38	1.35	5.74	6.74
	2.22	2.34	2.61	1.39	5.74	6.39
		2.24 (5.5% cov)		1.33		
Heparin	2.07	2.25	2.39	1.34	6.81	5.50
	2.05	2.18	2.36	1.30	6.81	5.35
	2.20	2.34	2.45	1.39	6.81	4.95
		2.26 (3.6%cov)		1.34		

Table A3.6: PLL resin FPLC runs

GAG	$M_{0.25}$	$M_{0.50}$	$M_{0.75}$	R.B.S.	mg loaded	mg recovered
CS	0.33	0.55	0.82		2.24	1.61
	0.33	0.51	0.72		1.68	1.52
	0.45	0.62	0.95		1.12	1.06
		0.56 (9.9% cov)		1.00		
DS	0.52	0.80	1.09	1.43	2.12	1.51
	0.60	0.80	1.09	1.43	1.59	1.46
	0.56	0.76	0.98	1.36	1.59	1.65
		0.79 (2.9% cov)		1.41		
Heparin	0.81	1.09	1.35	1.95	1.41	1.67
	0.88	1.17	1.38	2.09	1.08	1.18
	0.84	1.05	1.30	1.78	0.71	1.17
		1.10 (5.5% cov)		1.96		
Mucopolysaccharide mixture	0.55	0.87	1.22	1.55	1.98	2.00
	0.53	0.75	1.03	1.34	1.32	1.64
	0.58	0.85	1.13	1.52	7.94	5.14
	0.51	0.84	1.13	1.50	7.94	6.3
		0.83 (6.4% cov)		1.48		

A3.2 Sample calculation of stoichiometry of GAG binding to polylysine resin

Resin K_8G, substitution 1.72 mg/g (dry resin), 8% dry weight

Molecular weight of GAG disaccharides (based on elemental analysis results) 439, 472 and 557 for chondroitin sulphate, dermatan sulphate and heparin respectively.

Chondroitin sulphate capacity 36 mg/g

mmol amino groups per g of wet resin = 1.72 X 0.08

= 0.1376

CS capacity (mmol/g) = 42/439

= 0.095

Stoichiometry (i.e. lys/disaccharide unit) = 0.1376/0.095

= 1.45

Appendix 4: Supplementary material to Chapter 5

A4.1:Calculation of hydrophobic moments

A sample calculation of the hydrophobic moment for the PCI ((264-283) peptide at one angle (i.e. 80° or 1.396 radians) is shown in Table A4.1. The hydrophobicities (column 2) for the amino acids used in the calculation are those of Eisenberg's group (Eisenberg et al 1984). The hydrophobicities of each amino acid are normalised (H_n) i.e the difference from the average hydrophobicity of all residues before, being used in the Fourier transform equation (equation 5.3). The vector component of the normalised hydrophobicities i.e. $H_n$sinNδ and $H_n$cosNδ are recorded in column's 7 and 9 of Table A4.1 respectively). The square of the cumulative sum of each component is then calculated (base of column 7 and 9 respectively) and added. This is the square of the hydrophobic moment at this angle. As can be seen the figure is 19.96. It follows that the moment at 80° is 4.437 (or 0.221 per single residue). The calculation is repeated for the remaining angles between 0° to 180^0.

A4.2 CD spectral data for peptide/GAG complexes

The secondary structures α-helix, ß-strand and the unordered (or random) forms of polypeptide chains have different CD spectral profiles. The profile for the α-helix displays a typical double minimum at 222 and 208-210 nm with a maximum in the 191-193 nm range. ß-strands have two bands a negative one near 216-218 nm and a positive one near 195-200 nm. Finally the unordered form has a strong negative and band near 220 nm which may be either positive or negative.

Additional material used in the characterisation of the CD spectra of the poly-peptide/GAG complexes studied is shown in tabular form in Tables A4.1 to A4.5. The ellipticities at the maximum and minima of the spectra are shown in these tables. For comparative purposes the ellipticities at 208, 218 and 222 nm are also recorded. These results for each peptide clearly demonstrate that the CD spectral

Table A4.1: Sample calculation of hydrophobic moment at 80^0 degree's for PCI peptide

Residue	H	H_n	Nδ	sinNδ	cosNδ	$H_n$sinNδ	Cum $H_n$sinNδ	$H_n$cosNδ	Cum $H_n$cosNδ	
S	-0.26	0.20	1.396	0.985	0.176	0.20	0.192	0.035	0.035	
E	-0.62	-0.17	2.79	0.759	-0.94	-0.1290	0.0668	0.160	0.195	
K	-1.1	-0.65	4.188	-0.866	-0.5	0.5629	0.630	0.325	0.520	
T	-0.18	0.28	5.584	-0.643	0.766	-0.1800	0.450	0.215	0.735	
L	0.53	0.99	6.980	0.643	0.766	0.6366	1.087	0.758	1.493	
R	-1.76	-1.31	8.376	0.86	-0.5	-1.1266	-0.040	0.655	2.148	
K	-1.1	-0.65	9.772	-0.342	-0.94	0.2223	0.182	0.611	2.759	
W	0.37	0.83	11.168	-0.985	0.174	-0.8176	-0.636	0.144	2.903	
L	0.53	0.99	12.564	0.0002	1	0.0002	-0.636	0.990	3.893	
K	-1.1	-0.65	13.960	0.984	0.174	-0.6396	-1.276	-0.113	3.780	
M	0.26	0.72	15.356	0.342	-0.940	0.2462	-1.030	-0.677	3.103	
F	0.61	1.07	16.752	-0.866	-0.5	-0.9266	-1.957	-0.535	2.568	
K	-1.1	-0.65	18.148	-0.643	0.766	0.4180	-1.539	-0.498	2.070	
K	-1.1	-0.65	19.544	0.643	0.766	-0.4180	-1.957	-0.498	1.572	
R	-1.76	-1.31	20.940	0.866	-0.5	-1.1345	-3.092	0.655	2.227	
E	-0.62	-0.17	22.336	-0.342	-0.94	0.0581	-3.034	0.160	2.387	
L	0.53	0.99	23.732	-0.985	0.174	-0.9752	-4.009	0.172	2.559	
E	-0.62	-0.17	25.128	0.004	1	-0.0007	-4.010	-0.170	2.389	
E	-0.62	-0.17	26.524	0.985	0.17	-0.1675	-4.178	-0.029	2.360	
Y	0.02	0.48	27.920	0.339	-0.984	0.1627	-4.015	-0.472	1.888	
Mean	-0.455					(Cum $H_n$sinNδ)^2	16.120	(Cum $H_n$cosNδ)^2	3.565	19.69

envelope changes upon binding the GAG standards and in addition different GAG's can induce different conformations in the peptide backbone.

Table A4.2: PLL (long)/GAG interaction

	Maximum		Minimum		Θ 208 ($X10^{-4}$)	Θ 218 ($X10^{-4}$)	Θ 222 ($X10^{-4}$)
	Wavelength	Value ($X10^{-4}$)	Wavelength	Value ($X10^{-4}$)			
PLL alone	0	0	197.8	-7.149	-2.224	-0.2859	-0.176
CS	-	-	-	-	-	0.2628	-3.595
DS	193.2	11.84	205.8 255.8	-4.033 4.498	-3.987	-3.491	-4.237
Heparin	191.8	8.306	206.2 223	-3.886 -3.788	-3.63	-3.027	-3.595

Table A4.3: PLL (short)/GAG interaction

	Maximum		Minimum		Θ 208 ($x10^{-4}$)	Θ 218 ($x10^{-4}$)	Θ 222 ($x10^{-4}$)
	Wavelength	Value (X 10^{-5})	Wavelength	Value (X 10^{-5})			
PLL alone	217	0.1443	197.8	-2.072	-4.725	1.364	1.084
CS	_	_	198.6	-2.063	-7.715	-1.142	-0.2352
DS	189.4	1.109	202.6 224.6	1.478 -0.725	-10.06	-5.337	-6.614
Heparin	195.2	2.178	226.6	0.9885		-5.936	-8.388

Table A4.4: K_8G/GAG interaction

	Maximum		Minimum				
	Wavelength	Value ($X10^{-3}$)	Wavelength	Value ($X10^{-5}$)	208 ($X10^{-4}$)	218 ($X10^{-3}$)	222 ($X10^{-3}$)
Peptide	218	8.52	197	1.438	3.03	8.52	7.13
CS	216	1.053	196.8	0.9792	1.807	8.788	7.112
DS	218.6	6.77	198	0.612	1.364	5.068	4.13
Heparin	216.4	8.537	198	1.438	3.728	1.302	1.268

Table A4.5: PCI peptide/GAG interactions

	Maximum Θ		Minimum Θ				
	Wavelength	Value	Wavelength	Value	Θ208 ($X10^{-4}$)	Θ218 ($X10^{-4}$)	Θ222 ($X10^{-4}$)
Peptide alone	-	-	200.6	-7.141	-3.896	-7.926	-6.405
CS	187	6.664	227.8 207	-3.827 6.32	-4.25	-2.238	2.819
DS	189	4.382	205	8.71	-8.00	-4.68	-4.851
Heparin	192.4	2.421	207 225	-1.875 -1.52	-1.887	-1.406	1.492

Table A4.6: Thrombospondin peptide/GAG interaction

	Maximum		Minimum				
	Wavelength	Value ($X10^{-4}$)	Wavelength	Value ($X10^{-4}$)	Θ 208 ($X20^{-4}$)	Θ 218 ($X20^{-4}$)	Θ 222 ($X20^{-4}$)
Peptide alone	229	1.35	202	-1.33	-1.194	-5.924	-2.183
CS	228.6	0.089	201.4	-1.248	-1.028	-5.424	-2.316
DS	229.6	0.0999	200.1	-1.355	-1.083	-5.437	-2.266
Heparin	228.0	0.1778	199.8	1.338	-1.048	-4.724	-1.268

A4.3 Sample calculation for stoichiometry of solution binding

The end points for the blank and complex titration (for 1 hour complex formation i.e. before complex equilibrium) in Figure 5.9 are 39 and 73.9 µl respectively. The conditions used in the blank and complex solution are outlined below.

	Volume added µl		
	Blank	Complex	
Buffer	500	500	
Heparin	400	400	1.45 mg/ml
Water	100	70	
PLL solution	-	30	12.1 mg/ml

The concentration of heparin in the incubation mixture is 0.58 mg/ml.
Let the concentration of heparin in the complex mixture, at this stage be x.

$$73.9x = 39 \times 0.58$$

Solving the above equation for x, results in the figure for heparin in the complex tube as 0.306 mg/ml. Since the initial concentration was 0.58 mg/ml, 0.274 mg of heparin must be complexed by 0.363 mg of PLL. The amount of PLL bound per unit weight of heparin can be calculated.

Stoichiometry = 0.363/0.274

= 1.325 mg PLL/mg heparin

However the PLL was supplied by the manufacturer as a hydrobromide salt. The residue molecular weight of the lys.HBr unit is 208 (manufacturer data). To convert the crude PLL concentration to the actual concentration a correction factor is required (residue MW of lys/residue MW of lys.HBr).

Correction factor= 128.18/208

=0.6163

Hence mg PLL/mg Hep = 0.6163 X 1.325

= 0.8197

The enable a direct comparison of the binding behaviour of the PLL chains (with 126 and 633 residues) and the K_xG series resin, the number of lysines bound per disaccharide unit is calculated.

moles of lysine = 0.8197/128.18

= 6.39 µmol

moles of heparin disaccharides = 1/557

= 1.79 µmol

Stoichiometry of binding = 6.39/1.79

= 3.57 lysines are bound per disaccharide unit

The process is repeated for the other time points until the complex has reached equilibrium.

Appendix 5: supplementary information to Chapter 6

A5.1 Distribution of acidic, aromatic and basic residues within consensus sequences

The overall frequency of basic amino acids lysine, arginine and histidine in proteins is 7%, 5%, and 2% respectively or 50, 36, 14 expressed as percentage of the total basic residues (Flinta et al 1986)

A5.1.1 Cardin and Weintraub type I

The sequences displayed in Table 2 of Cardin and Weintraub's original paper (Cardin and Weintraub 1989) on the two consensus sequences are analyzed in Table A5.1.

Table A5.1: Distribution of residues within type I consensus sequences,

Residue	Overall distribution	Position			
	Observed (expected)	2	4	3	7
K	53 (49.5)	43.8 (50)	64.7 (50)	57.1 (50)	60.7 (50)
R	40 (35.6)	50 (36)	29.4 (36)	39.3 (36)	32.1 (36)
H	6 (13.9)	6.3 (14)	5.9 (14)	3.6 (14)	7.1 (14)
χ^2 value	5.281	10.448	10.33	9.04	6.113
Total residues	99	16	17	28	28
Residue type	Position	1	5	6	8
Acidic		3 (12)	3 (12)	7 (12)	3 (12)
Aromatic		6(8)	11 (8)	3 (8)	6 (8)
χ^2 value		7.25	7.875	5.205	7.25

The null hypothesis for the basic residues was that the proportion of lysine, arginine and histidine in the consensus sequence is just a reflection of the proportion of these basic residues in proteins (cutoff for the hypothesis 9.21 at the 1% level of

significance). Similarly for acidic and basic residues the null hypothesis is that the frequency is just a reflection of their overall frequency in proteins (cutoff for the hypothesis 6.635 at the 1% level of significance).

With position 2,3, and 4 there are four possible arrangement of basic residues, these are BBB, XBB, BBX, and XBX. The expected proportions of these four types can be calculated.

Sample calculation:

Probability (BBB)= Prob (basic at 2)X 1 X Prob (basic 4)

= 0.57 X 1 X 0.61

= 0.348

In Cardin and Weintraub's (Cardin and Weintraub 1989) data the fourth possible outcome (ie XBX) was not observed, so the remaining outcomes (BBB, XBB, and BBX) were normalised to 1.

Table A5.2: Distribution of the outcomes at position 2,3 and 4

Type	Observed (expected)	Probability
XBB	42.9 (31.5)	0.2626
BBX	39.3 (26.7)	0.222
BBB	17.9 (41.8)	0.348
χ^2 value	23.73	

A5.1.2 Cardin and Weintraub's type II consensus sequence

The analysis of sequences in Table 1 of Cardin and Weintraub's original paper (Cardin and Weintraub 1989)on the two consensus sequences is shown in Table A5.3.

Table A5.3: Distribution of the residues within the type II consensus sequence

Residue	Overall distribution	Position		
	Observed (expected)	2	3	5
K	45.2 (50)	55.6 (50)	63.2 (50)	21.1 (50)
R	41.9 (36)	27.8 (36)	26.3 (36)	68.4 (30)
H	12.9 (14)	16.7 (14)	10.5 (14)	10.5 (14)
Total number	62	18	19	19
χ^2 value	1.514	3.016	6.97	46.74
		Position		
		1	4	6
Acidic		0 (12)	0 (12)	25 (12)
Aromatic		25 (8)	12.5 (8)	5.3 (8)
χ^2 value		48.1	14.53	14.99

A5.1.3 Sobel's et al consensus sequence

The sequences that were used by Sobel's group to propose the consensus sequence are analyzed in Table A5.4. Because of the small number of basic amino acids at position 2,3, 11 and 12 the test of the distribution of basic amino acids was not attempted.

A5.2 Preferred ligand for sulphate binding

The results of the analysis of the two papers (Chakrabarti 1993, Copley and Barton 1994) that have discussed the ligands for sulphate binding are shown in Table A5.5. The amino acids were divided into four groups. These were:

1. Strong preference amino acids; arg, lys, his, and ser.
2. Slight preference; tyr and trp.

3. No preference; thr, asp, asp, glu, gln, and gly.
4. A preference against; cys, met, phe, val, ile, leu, phe and ala.

Table A5.4: distribution of the residues within Sobel's Consensus sequence

Residue	Overall Distribution Observed (expected)	Position		
		6	7	8
R	42.6 (36)	62.5 (36)	11 (36)	62.5 (36)
K	44.7 (50)	44.4 (50)	44.4 (50)	25 (50)
H	12.8 (14)	0 (14)	44.4 (14)	12.5 (14)
Total number	47	8	9	8
χ^2 value	1.875	36.64	84	32.17

The observed amino acid frequency as sulphate ligands was compared to the average frequency in eukaryotic proteins using the chi squared test. The null hypothesis is that the order of occurrence of the amino acids as ligands for 98 sulphates in 58 crystallographically determined protein structures is just a reflection of their average occurrence in eukaryotic proteins.

The statistical analysis confirmed the idea that the frequency of arginine, lysine, histidine and serine were preferred since the chi squared value shown in column 7 of Table A5.5 exceeded the cutoff value (shown within the brackets). The slight preference for tyrosine and tryptophan as sulphate ligands was not significantly different from the values expected in an average eukaryotic protein. This does not imply that these amino acids cannot act as ligands for sulphate, it simply means that they are not preferred. In a similar manner the third group of amino acids (T, D, N, Q, and G) were also at levels that would be expected in an average eukaryotic protein. Finally the levels of the of amino acids in the fourth group (C, M, P, V, I, L, P and A) was confirmed to be significantly different for the levels in an average eukaryotic protein.

Table A5.5: Preferred ligands for sulphate binding

Amino acid	Chakrabarti's data	Copley and Barton's data	Pooled data	% Observed	% Expected	Chi squared test
R	24	25	49	23.9	5	
K	14	19	33	14.7	7	
H	10	7	17	7.6	2	
S	16	25	41	18.2	7	113.51 (11.345)
Y	7	10	17	4.40	3	
W	3	1	4	1.80	1	1.293 (6.635)
T	3	7	10	4.4	6	
D	6	0	6	2.7	6	
N	6	4	10	4.4	4	
E	2	7	9	4.0	6	
Q	8	1	9	4.0	4	
G	12	9	21	9.3	8	7.153 (15.086)
C	0	0	0	0	3	
M	0	0	0	0	2	
P	0	0	0	0	5	
V	0	0	0	0	7	
L	0	0	0	0	7	
I	0	2	2	0.9	5	
F	1	1	2	0.9	4	
A	2	1	3	1.30	9	36.353 (18.475)
			Total	225		
Sulphates	35	63	98			
Proteins	22	36	58			

Table A5.6: Preference Among Basic Ligands

Amino acid	Ligand Number (% of total)	Expected
Arg	49 (49.5)	36
Lys	33 (33.3)	50
His	17 (17.2)	14
Total	99	
	Chi squared value	11.371

Adapted from: data in Chakrabarti (1993) and Copley and Barton

The cutoff value for the value for rejection of the null hypothesis 9.21 at the 1% level of significance.

A5.3 Worked examples for stereochemical model

A5.3.1 Peptides with no acidic residues

ATIII 123-139 sequence:FAKLNCRLYRKANKSSK (Lellouch and Landsbury 1990).

The sequence contains 6 basic residues with the spacing (numbering from residue 125), 4, 7, 8, 11 and 15. There are 15 different paired combinations of 6 basic residues, using the rise distances for residues packed into α-helices and ß-strand (0.15 and 0.33 nm respectively) the distances between all combination of the basic amino acids for each secondary structure.

The distances between the basic residues of the peptide in each correlation are compared to the disaccharide repeat distance (and its multiples) for heparin (figures are shown in column 2 of Table A5.7). There are 2 matches when the peptide is in the alpha helical conformation, compared to 7 when it is in a beta strand conformation (potential contact for each conformation are indicated in bold). The fraction of productive contact is then calculated from the ratio of the number of

basic amino acids for this peptide. The conformational scores for α-helix and ß-strand are then calculated by using equation's 6.2 and 6.3 (Section 6.2.3.1).

Table A5.7: Multiples of Disaccharide repeat distances for GAG's

Number of Disaccharides	Heparin	C6S	DS	HS
1	0.83	0.93	0.95	0.93
2	1.66	1.86	1.90	1.86
3	2.49	2.79	2.85	2.79
4	3.32	3.72	3.80	3.72
5	4.15	4.65	4.79	4.65
6	4.98	5.58	5.70	5.58
7	5.81	6.51	6.65	6.51
8	6.64	7.44	7.60	7.44

Table A5.8: Distances between basic residues in an alpha helical conformation

Residue						
125	0	0.6	1.05	1.2	1.65	2.25
129	0.6	0				
132	1.05	0.45	0			
133	1.2	0.60	0.15	0		
136	**1.65**	1.05	0.60	0.45	0	
139	2.25	**1.65**	1.20	1.05	0.6	0

Table A5.9: Distances between basic residues in a beta strand conformation

Residue						
125	0	1.32	2.31	2.64	3.63	4.95
129	1.03	0				
132	**2.31**	0.99	0			
133	**2.64**	1.32	0.33	0		
136	3.63	**2.31**	1.32	0.99	0	
139	**4.95**	**3.63**	**2.64**	**2.31**	1.32	0

A5.3.2 Peptides containing acidic residues

A5.3.2 Peptides containing acidic residues

Heparin cofactor II peptide (residues 173 to 190) sequence
KYEITTIHNLFRKLTHRL
The distances between the basic residues and the acidic residues for each conformation are calculated, the results are shown in Table A5.10

Table A5.10: Distances between acidic and basic residues

Residue	α- helical conformation	ß-strand conformation
173	0.30	0.66
180	0.75	**1.65**
184	1.35	2.97
185	1.50	**3.30**
188	1.95	**4.29**
189	2.10	**4.62**

As can seen from Table A5.10 none of the acidic residues are within one disaccharide repeat (or multiples thereof) of any of the basic residues when the peptide is folded into an α-helical conformation. However if the peptide is folded into a ß-strand conformation 4 of the basic residues (residues 180, 185, 188 and 189) are within contact distances.

Table A5.11: Distances between basic residues in a alpha helical conformation

Residue						
173	0	1.05	1.65	1.80	2.25	2.40
180	1.05	0				
184	**1.65**	0.60	0			
185	1.80	0.75	0.15	0		
188	2.25	1.20	0.60	0.45	0	
189	**2.40**	1.30	0.75	0.60	0.15	0

The putative contacts of the basic residues comprising HC 173-190 when the peptide is folded into a ß-strand conformation in shown in Table A5.12. Two of the potential contacts are inhibited (indicated in italics) because both of the basic residues are within the influence of the acidic residue. The remaining putative basic amino acid contact are indicated in bold. In summary on the basis of the stereochemical model, there would be expected to be 2 and 5 contact of the peptide and heparin, for the α-helical and ß-strand conformation respectively.

Table A5.12: Distances between basic residues in a beta strand conformation

Residue						
173	0	2.31	3.63	3.96	4.95	5.28
180	**2.31**	0				
184	3.63	1.32	0			
185	**3.96**	*1.65*	0.33	0		
188	**4.95**	*2.64*	1.32	0.99	0	
189	**5.28**	2.97	**1.65**	1.32	0.33	0

5.3.3: Peptide data for stereochemical model

The procedure was repeated for the remaining peptides an outline of the steps in the calculation is shown in Table A5.13.

Table A5.13: Summary of the peptides used in the stereochemical model

Peptide	GAG	$N_B(N_{TOT})$	N(α)	N(ß)	AI(α)	AI(ß)	C(α)	C(ß)
K121	Hep	5(10)	1	3	2.253	1.245	0.255	0.374
K121 ext	Hep	6(15)	1	5	1.831	1.011	0.122	0.303
F^{123}-G^{148}	Hep	7(21)	4	10	1.924	1.036	0.366	0.493
F^{130}-G^{148}	Hep	5(10)	2	3	1.809	0.575	0.362	0.173
K^{136}-G^{148}	Hep	3(3)	1	0	1.489	0.698	0.496	0
Von Will	Hep	7(21)	1	6	1.466	0.923	0.07	0.263
PCI	Hep	7(21)	2	4	1.898	0.415	0.09	0.00
	DS		0	6			0.180	0.00
	C4S						0.00	0.00
ATIII 123	Hep	6(15)	2	6	2.055	1.423	0.275	0.569
	C4S		0	2			0.275	0.476
FN-C/HII	HS	5(10)	2	3	0.794	0.388	0.159	0.116
V-RKA	HS	4(6)	1	1	1.096	0.640	0.183	0.106
V-RAA	HS	3(3)	1	0	1.340	0.489	0.447	0
V-AAA	HS	2(1)	0	0	1.174	1.036	0	0
FN-C/HII Scrm	HS	5(10)	1	4	1.381	0.856	0	0.342
Apo P1	C6S	7(15)	4	0	1.845	0.474	0.492	0
Apo P2	C6S	7(15)	2	7	0.939	0.652	0.125	0.304
Apo P5	C6S	2(3)	0	2	1.554	1.409	0	0.435
Apo P11	C6S	6(15)	2	6	1.528	1.037	0.204	0.415

N_B: Number of basic amino acids, N_{TOT}: Number of combinations of basic amino acids, N(α) and N(ß); Number of contacts in α-helical and ß-strand conformation respectively, C(α) and C(ß); conformational score for α-helical and ß-strand conformation respectively.

5.4 Peptide data for consensus sequence binding model

A summary of the steps in the calculations for the peptides used in the consensus sequence model is shown in Table A5.14

Table A5.14: Summary of peptides used in the consensus sequence model

Peptide	AI(ß)	Normalised hydrophobicity	N_B	Source
ATIII 124-140	1.103	-0.375	3	Pratt et al 1992
ATIII 124-140 Random	1.469	-0.290	3	
PCI 264-283	0.415	-0.020	3	
PCI 264-283 Random	0.795	-0.03	-	
HC 173-190	1.119	-0.215	4	
HC 183-200	0.802	-0.159	4	
PF4 74-85	0.433	-0.083	4	
A1A	0.839	-0.150	-	McCaffrey et al 1992
A2A	1.707	-0.490	-	
A3A	1.357	-0.177	-	
A4A	0.839	-0.230	3	
A2B	1.322	-0.240	3	
HB-EGF 8-19	0.649	-0.072	-	Besner et al 1992
HB-EGF 20-25	0.680	-0.10	3	
HB-EGF 36-41	0.825	-0.13	3	

A5.5: Specificity of ATIII peptide heparin interaction

The specific interaction of the ATIII peptide (residues 123-139) and variants with heparin has been studied by NMR (Bae et al 1994), the results are interpreted in Table A5.15 using the consensus sequence model. Two of the peptides (ATIII 123-139 and disrupted 123-139) had similar S(ß) scores this parallels that fact that the two peptides bound heparin to the same strength.

two peptides bound heparin to the same strength.

Table A5.15: Data treatment for Bae et al's peptides

Peptide	AI(ß)	Normalised polar hydrophobicity	Number basic in consensus	S(ß)
ATIII 123-139	1.423	-0.206	3	-0.879
Disrupted ATIII 123-139	1.364	-0.321	2	-0.875
Random	0.966	-0.081	3	-0.234

REFERENCES

Adams J.C and Watts F.M. (1993) Development 117:1183-1198

Adrade-Gordon P. and Strickland S. (1990) P.N.A.S. 87:1865-1869

Ailles L, Kislevsky R,and Young I.D. (1993) Lab. Invest. 69:443-448

Arad O. and Houghten R.A. (1990) Peptide Research 3:42-50

Bae J, Desai U.R, Caldwell E.E.O, Weiler J.M and Linhardt R.J. (1994) Biochem. J. 301:121-129

Barany G, Kneib-Cordonier N, Mullen D.G. (1987) Int. J. Peptide Protein Res. 30:705-739

Bengtsson G, Olivecrona T, Hook M, Riesenfield J, and Lindahl U. (1980) Biochem. J. 189:625-633

Bergmann K and O'Konski C.T. (1963) J. Phys. Chem. 67:2169-2177

Bergy E.J. and Stinson M.W. (1988) Infection and immunity 56:1715-1721

Besner G.E, Whelton D, Crissman-Combs M.A, Steffen C.L, Kim G.Y and Brigstock D.R (1992) Growth Factors 7:289-296

Blackwell J, Schodt K.P, and Gelman R.A. (1977) Federation Proceedings 30:98-101

Blumenkrantz N and Asboe-Hansen G (1973) Anal. Biochem 54:484-489

Bohn R. and Kalbhen D.A. (1971a) J. Chrom. 62:399-408 Abstract in English, paper in German

Bohn R. and Kalbhen D.A. (1971b) J. Chrom. 62:409-415 Abstract in English, paper in German

Bourin M, and Lindahl U. (1993) Biochem. J. 289:313-330

Breen M, Weinstein H.G, Blacik L.J,Borcherding M.S and Sittig R.A. (1976) *Methods in Carbohydrate Chemistry* VII:100-115 Edited by Whister and Bemiller

Brunden K.R. (1993) J. Neurochem 61:2147-2154

Buee L, Ding W, Delacourte A. and Fillit H. (1993) Brain Research 601:154-163

Burke C, Mayo K.H, Skubitz A.P.N, and Furcht L.T. (1991) J. Biol. Chem 266:19407-19412

Camejo G, Olofsson S.O, Lopez F, Carlsson P. and Bondjers G. (1988) Arteriosclerosis 8:368-377

Cappelletti R, Delross M. and Chiarugi V. (1979a) Analytical Biochemistry 93:37-40; (1979b) ibid 99:311-315

Cardin A.D. and Weintraub H.J.R. (1989) Arteriosclerosis 9:21-32

Cardin A.D, Jackson R.L, Sparrow D.A, Sparrow J.T, (1989) Annal. N.Y. Acad. Sci. 556: 186-193

Cardin A.D, Demeter D.A, Weintraub H.J.R, Jackson R.L. (1991) Methods in enzymology 203:556-583

Castellot J.J, Choay J, Lormeau J.C, Petitou M, Sache E and Karnovsky M.J. (1986) J. Cell. Biol. 102:1979-1984

Casu B, Torri G, and Vercellotti J.R. (1979) Pharmacol. Res. Comm. 11:297-301

Casu B, Moretti M, Oreste P, Torri G. and Vercellotti J.R. (1980) Arzneim.-Forsch 30:1889-1892

Casu B. (1985) Advances in Carbohydrate Chemistry 43:51-134

Casu B, Petitou M, Provasoli M, and Sinay P. (1988) T.I.B.S. 13:221-225

Casu B, (1989) Chapter 2, p25-49 in *Heparin: Chemical and Biological Properties. Clinical Applications*. Lang and Lindahl (eds)

Caughey B. and Raymond G.J (1993) J. Virol. 67:643-650

Chakrabarti B and Park J.W. (1980) CRC Crit. Rev. Biochem. August: 225-313

Chakrabarti P. (1993) J. Mol. Biol 234:463-482

Cheng F, Yoshida K, Heingard D, and Fransson L.A. (1992) Glycobiology 2:533-561

Come J.H, Fraser P.E and Lansbury P.T. (1993) P.N.A.S 90:5959-5963

Copley R.R. and Barton G.J. (1994) J.Mol.Biol 242:321-329

Cornette J.L, Cease K.B, Margalit H, Spouge J.L, Berzofsky J.A and DeLisi C (1987) J. Mol. Biol 195:659-685

Choi S.H and Stinson M.W. (1989) Infection and immunity 57:3834-3940

Culp L.A, Laterra J, Lark M.W, Beyth R.J, and Tobey S.L. (1986) *Functions of Proteoglycans* p158-183 Ciba Foundation Symposium 124 Edited by Evered and

Whelan.

Dawes J. (1988) Anal. Biochem. 174:177-186

de Beer M.C, de Beer F.C, Mc Cubbin W.D, Kay C.M and Kindy M.S (1993) J. Biol. Chem 268: 20606-20612

Donnelly D, Overington J.P, Ruffle S.V, Nugent J.H.A and Blundell T.L (1993) Protein Science 2:55-70

Drake S.L, Varnum J, Mayo K.H, Letourneau P.C, Furcht L.T, and McCarthy J.B (1993) J. Biol. Chem. 268:15859-15867

Englebretsen D.R. and Harding D.R.K.(1992a) p 597-598 in Peptides: chemistry and biology, Proceedings of the Twelfth American Peptide Symposium Edited by JA Smith

Englebretsen D.R. and Harding D.R.K. (1992b) Int. J. Peptide Protein Res 40:487-496

Englebretsen D.R. and Harding D.R.K. (1993) Peptide Res. 6:320-329

Englebretsen D.R. and Harding D.R.K. (1994a) Int. J. Peptide Protein Res. 43:546-554

Englebretsen D.R. and Harding D.R.K. (1994b) Peptide Res. 7:136-139

Englebretsen D.R. and Harding D.R.K. (1994c) Peptide Res. In Press

Eisenberg D, Weiss R.M and Terwilliger T.C (1984) P.N.A.S. 81:140-144

Farooqui A.A, Yang H, Horrocks L.A (1994) J. Chrom 673:149-158

Farndale R.W. (1986) Biochimica Biophysica Acta 883:172-177

Fields G.B and Noble R.L (1990) Int. J. Peptide Protein Res. 35:161-214

Flinta C, von Heijne G. and Johansson J. (1983) J. Miol. Biol 168:193-196

Flinta C, Persson B, Jornvall H. and von Heijne G. (1986) Eur. J. Biochem 154:193-196

Fransson L.A, Huckeby T.N, and Nieduszyski I.A. (1978) Biochem. J. 175:299-309

Fransson L.A. (1985) *The Polysaccharides* Vol 3:337-415 Edited by Aspinall G.O.

Fransson L.A, Havsmark B, and Silverberg I. (1990) Biochem. J. 269:381-388

Fraser P.E, Nguyen J.T, Chin D.T, and Kirschner D.A. (1992) J. Neurochem 59:1531-1540

Gabizon R, Meiner Z, Halimi M. and Ben-Sasson S (1993) J. Cell. Phys 157:319-325

Gallagher J.T, Turnbull J.E and Lyon M. (1992) Int. J. Biochem 24:553-560

Gatti G, Casu B, Hamer G.K. and Perlin A.S. (1979) Macromolecules 12:1001-1007

Geiger M, Priglinger U, Griffin J.H. and Binder B.R. (1991) J. Biol. Chem. 266:11851-11857

Gelman R.A. and Blackwell J, (1973a) Archives of Biochemistry and Biophysics 159:427-433

Gelman R.A, Rippon W.B, and Blackwell J. (1973b) Biopolymers 12:541-558

Gelman R.A, and Blackwell J. (1973c) Biopolymers 12:1959-1974

Gelman R.A, and Blackwell J. (1973d) Biopolymers 13:139-156

Gettin P, Patson P.A. and Schapira M. (1193) Bioessays 15:461-467

Gigli M, Consonni A, Ghiselli G, Rizzo V, Torri G, and Naggi A. (1992) Biochemistry 31:5996-6003

Gigli M, Ghisilli G, Torri G, Naggi A, and Rizzo V. (1993) Biochimica Biophysica Acta 1167:211-217

Goetinck P.F, Stirpe N.S, Tsonis P.A, and Carlone D. (1987) J. Cell. Biol. 105:2403-2408

Gorin P.A. (1981) Adv. Carbohydrate Chem. 13:104-210

Gu K, Liu J, Pervin A and Linhardt R.J. (1993) Carbohydrate Res. 244: 369-377

Guiroy D.C, Yanagihara R, and Gajusek D.C (1991) Acta. Neuropathol. 82:87-92

Guo N, Krutzsch H.C, Negre E, Zabrenetsky V.S. and Roberts D.D. (1992) J. Biol. Chem. 267:19349-19355

Guimond S, Maccarana M, Olwin B.B, Lindahl U, Raprager A.C. (1993) J. Biol. Chem 268:23906-23914

Habuchi H, Yamagata T, Iwata H, and Suzuki S. (1973) The J. Biol. Chem. 248:6019-6928

Hamazaki H. (1987) J. Biol. Chem. 262:1456-1460

Hamazaki H. (1988) Biochem. Biophysics. Res. Commun 150:219-224

Hamazaki H. (1989) Biochimica Biophysica Acta 998:231-235

Hamer G.K, and Perlin A.S. (1976) Carbohydrate Res. 49:37-48

Herrmann M, Suchard S.J, Boxer L.A, Waldvogel F.A and Lew P.D (1991) Infection and immunity 59:279-288

Holme K.R. and Perlin A.S. (1989) Carbohydrate Res. 186:301-312

Hook M, Bjork I, Hopwood J, and Lindahl U. (1976) FEBS letters 66:90-93

Hounsell E.F.(1989) Chap 2 12-20 in Keratan sulphate: chemistry, biology, chemical pathology Edited by H Greiling and JE Scott. Published by Biochemical Society (London)

Jackson R.L, Busch S.J, and Cardin A.D. (1991) Physio. Rev 71:481-539

Jarrett J.T, and Lansbury P.T. (1993) Cell 73:1055-1058

Jarrett J.T, Berger E.P and Lansbury P.T. (1993) Biochemistry 32: 4693-4697

Jaseja M, Rej R.N, Sauriol F. and Perlin A.S. (1989) Can. J. Chem 67:1449-1456

Jaques, (1977) *Determination of Heparin and Related Sulphated Mucopolysaccharides* in Methods of Biochemical Analysis 24:203-312

Jeanloz R.W. (1965) *Methods in Carbohydrate Chemistry* V:114-118 Edited by Whister and Bemiller

Jenning A and Smith C.P. (1980) Methods in carbohydrate chemistry VIII:Article 12

Kan M, Wang F, Xu J, Crabb J.W, Hou J and McKeehan W.L. (1993) Science 259:1918-1921

Kennedy J.F. (1979) *Proteoglycans: Biological and Chemical Aspects in Human Life* Published by Elsevier

Kisilevsky R. (1990) Lab. Invest. 63:589-591

Kisilevsky R. (1992) J. Int. Med. 232:515-516

Kjellen L. and Linhadl U (1991) Ann. Rev. Biochem 60:443-475

Klinger M.M., Margolis R.U. and Margolis R.K. (1985) J.Biol.Chem. 260:4082-4090

Kovensky J. and Cirelli A.F. (1993) Carbohydrate Res. 245:361-365

Lages B., and Stivala S.S. (1973) Biopolymers 12:127-143

Lee M.K. and Lander A.D. (1991) P.N.A.S 88:2768-2772

Lellouch A.C, and Lansbury P.T. (1992) Biochemistry 31:2279-2285

LKB (1987) Biolynx™ 4175 Instruction manual

Li S.F.Y. 1992 Capillary electrophoresis: principles, practise and applications Journal of chromatography press Vol 52 Elsevier (Amsterdam)

Liang O.D, Ascencio F, Fransson L.A, and Wadstorm T. (1992) Infection and immunity 60:889-906

Liang X, Babbiuk L.A and Zamb T.J (1993) Virology 194:233-243

Lindahl U., and Hook M. (1978) Ann.Rev.Biochem 47:385-417

Lycke E., Johansson M. Svennerholm B. and Lindahl U. (1991) J. Gen. Virol 72:1131-1137

Mach H, Volkin D.B, Burke C.J, Middaugh C.R, Linhardt R.J, Fromm J.R, Loganathan D. and Mattsson M (1993) Biochemistry 32:5480-5489

Maimone M.M. and Tollefsen D.M (1990) J. Biol. Chem 265:18263-18271

Margalit H, Fischer N, and Ben-Sasson S.A. (1993) J. Biol. Chem 268:19228-19231

Mascellani G, Liverani L, Bianchini P, Parma B, Torri G, Bisio A, Guerrini M. and Casu B. (1993) Biochem. J. 296:639-648

Mbemba E, Czyrski J.A and Gattegno L. (1992) Biochimica Biophysica Acta 1180:123-129

McCubbin W.D, Kay C.M, Narindrasorasak S, Kiselevsky R. (1988) Biochem. J. 256:775-783

McCaffrey T.A, Falcone D.J and Du B. (1992) J. Cell. Physio. 152:430-440

Melrose J and Ghosh P. (1993) Journal of Chromatography 637:91-95

Meyer K, Davidson E, Linker A, and Hoffman P (1956) B.B.A. 21:506-518

Meyer B, Thurnberg L, Linhahl U, Larm O, and Leder I.G. (1981) Carbohydrate Res 88: C1-C4

Mukherjee D.C., Park J.W., and Chakrabarti B. (1978) Archives of Biochemistry and Biophysics 191:393-399

Mulloy B, Forster M.J, Jones C. and Davies D.B. (1993) Biochem. J. 293:849-858

Naka D, Ishii T, Shimomura T, Hishida T, and Hara H. (1993) Experimental Cell. Res 209: 317-324

Narindrasorasak S, Lowery D, Gonzalez-DeWhitt P, Poorman R.A, Greenberg B. and Kisilevsky R (1991) J. Biol. Chem. 266:12878-12883

Narindrasoasak S, Lowery D.E, Altman R.A, Gonzalez-DeWhitt P.A, Greenberg B.D and Kisilevsky R. (1992) Lab. Invest. 67:643-652

Nevaldine and Kassell, (1971) Biochimca et Biophysica Acta 250:207-209

Neville G.A, Mori F, Holme K.R, Perlin A.S. (1989) J. Pharm. Sciences 78:101-104

Nieduszynski I. (1989) Chapter 3 in *Heparin: Chemical and Biological properties* Edited by D.A. Lane and U. Lindahl

Nilsson K. and Mosbach K. (1980) Eur. J. Biochem 112:397-402

Ogamo A, Uchiyama H, and Nagasawa K (1980) B.B.A 626:477-485

Ogamo A, Yamada T, and Nagasawa K (1987) Carbohydrate Res. 165:275-280

Ogamo A, Metori A, Yamada T, and Nagasawa K (1990) Carbohydrate Res. 198:157-162

Pantoliano M.W, Horlick R.A, Springer B.A, Van Dyk D.E, Tobery T, Wetmore D.R, Lear J.D, Nahapetian A.T, Bradley J.D and Sisk W.P (1994) Biochemistry 33:10229-10248

Pan K.M, Baldwin M, Nguyen J, Gasset M, Serban A, Groth D, Mehlhorn I, Huang Z, Fletterick R.J, Cohen F.E and Pruiser S.B. (1993) P.N.A.S. 90:10962-10966

Park J.W. and Chakrabarti B. (1978) Biochimica Biophysica Acta 544:667-675

Parthasarathy N, Goldberg I.J, Sivaram P, Molloy B, Flory D.M, and Wagner W.D (1994) J. Biol. Chem 269:22391-22396

Perry G, Siedlak S.L, Richey P, Kawai M, Cras P, Kalaria R.N, Galloway P.G, Scardina J.M, Cordell B, Greenberg B.D, Ledbetter S.R and Gambetti P. (1991) J.Neurosci 11:3679-3683

Piani S, Casu B, Marchi E.G, Torri G. and Ungarelli F. (1993) J. Carbohydrate Chem. 12:507-521

Poblacion C.A. and Michelacci Y.M. (1986) Carbohydrate Res. 147:87-100

Pratt C.W., and Church F.C. (1992a) J.Biol.Chem. 267:8789-8794

Pratt C.W., and Church F.C. (1992b) J.Biol.Chem. 267:8795-8801

Predki P.F., Whitfield D.M. and Sarkar B. (1992) Biochem.J 281:835-841

Radhakrishnamurthy B., Dalferes E.R., Ruiz H., and Berenson G.S. (1977) Anal.Biochem 82:445-454

Rej R.N., Holme K.R., and Perlin A.S. (1990) Can.J.Chem. 68:1740-1745

Richard E.C, Strohl M.M, and Nielsen R.G. (1991) Anal. Biochem 197:197

Roden L, Baker J.R, Cifonelli A, and Mathews M.B.(1972) Methods in Enzymology 28:73-140

Safar J, Roller P.P, Gajdusek D.C. and Gibb C.J. (1993) Protein Science 2;2206-2215

San Antonio J.D, Slover J, Lawler J, Karnovsky M.J. and Lander A.D. (1993) Biochemistry 32:4746-4755

Sanderson P.N, Huckerby T.N. and Nieduszynski I.A. (1984) Biochem. J. 223:495-505

Sanderson P.N, Huckerby T.N. and Nieduszynski I.A. (1989) Biochem. J. 257:347-354

Sanderson R.D, Turnbull J.E, Gallagher J.T and Lander A.D. (1994) J. Biol. Chem 269:13100-13106

Schreuder H.A, de Boer B, Dijkema R, Mulders J, Theunissen H.J.M, Grootenhuis P.D.J and Hol W.G.J. (1994) Nature; structural biology 1:48-54

Schiffer M. and Edmundson A.B. (1967) Biophysical J. 7:121-135

Schodt K.P, Gelman R.A and Blackwell J. (1976) Biopolymers 15:1965-1977

Schultz G.E and Schrimer R.H.(1979) Principles of protein structure Springler-Verlag (New York)

Scott J.E, Stacey and Tigwell M.J. (1968) Biochemistry Journal 105(S), 50p

Scott J.E, and Tigwell M.J. (1978) Biochem. J. 173:103-114

Scott J.E, and Heatley F. (1982) Biochem. J. 207:139-144

Scott J.E (1988a) Biochem. J. 252:313-323

Scott J.E (1988b) Ciba Found. Symp. 143: 6-20 in The biology of Hyaluronan , Ed. by D. Evered and J. Whelan

Scott J.E. (1991) Biochem. J. 275:267-268

Scott J.E. (1992) FASEB. J. 6:2639-2645

Scott J.E. (1994) Biochem. J. 298:221-222

Siedlak S.L, Crass P, Kawai M, Richey P and Perry G (1991) J. Histochem. and Cytochem. 39:899-904

Sipe J.D. (1992) Ann. Rev. Biochem. 61:947-975

Snow A.D, Bramson R, Henderson M, Wight T.N, and Kisilevsky R. (1991) J. Histochem. Cytochem 39:1321-1330

Snow AD Henderson M Nochlin D, Kresse H and Wight TN (1992) J. Histochem. Cytochem 40:105-113

Snow A.D, Sekiguchi R.T, Nochlin D, Kalaria R.N. and Kimata K. (1994) Amer. J. Path. 144:337-347

Sobel M., Soler D.F., Kermode J.C., and Harris R.B. (1992) J.Biol.Chem. 267:8857-8862

St. Charles R, Walz D.A and Edwards B.F.P (1989) J. Biol. Chem 264:2092-2099

Stone A.L and Epstein P. (1977) Biochimica Biophysica Acta 497:298-306

Stuckey J.A, St Charles R, and Edwards B.F.P (1992) Proteins; Structure, Function, and Genetics 14:277-287

Suzuki and Koide (1984a) Analytical Biochemistry 137:101-105

Suzuki and Koide, (1984b) *Purification of Heparan Sulphate*. Japanese patent number 58171, 403. Chemical Abstracts 100: 141121k

Talafous J, Marcinowski K.J, Klopman G, and Zagorski M.G. (1994) Biochemistry 33:7788-7796

Thompson L.D, Pantolianno, and Springer B.A (1994) Biochemistry 33:3831-3840

Timpl R. (1993) Experientia 49:417-427

Turnbull J.E. and Gallagher J.T. (1991) Biochem. J. 273:553-559

Tyler-Cross R, Sobel M, Marques D, Soler D.F and Harris R.B (1993) Archives of Biochemistry and Biophysics 306:528-533

Tyler-Cross R, Sobel M, Marques D, and Harris R.B (1994) Protein Science 3:620-627

Uchiayama H, Ogamo A, and Nagasawa K. (1982) Carbohydrate Res 99:87-92

Uchiayama H, Okouchi K, and Nagasawa K. (1985) Carbohydrate Res 140:239-249

Uchiayama H, Kikuchi K, Ogamo A, and Nagasawa K. (1987) Biochimica Biophysica Acta 926:239-248

Vangool D, David G, Lammens M. Baro F, and Dom R. (1993) Dementia 4:308-314

Volpi N, Mascellani G, Bianchini P, and Liverani L (1992) Farmaco 47:841-853

Volpi N. (1993a) J. Chrom. Biomedical appl. 662:13-20

Volpi N. (1993b) Carbohydrate Res. 247:263-278

Wight T.N, Kinsella M.G and Quarnstrorm E.E (1992) Curr. Opinion Cell. Biol. 4:793-801

Williamson M.P and Waltho J.P (1992) Chem. Soc. Rev 21:227-236

Witt D.P. and Lander A.D. (1994) Current Biology 4:394-400

Yang J.T, Wu C.S.C and Martinez H.M. (1986) Methods in Enzymology 130:208-252

Yang B, Yang B.L, Savani R.C, and Turley E.A. (1994) EMBO. J. 13:286-296

Zebrower M, Beebar C. and Kieras F.J. (1992) Biochem. Biophys. Res. Comm 184:1293-1303

Zebrower M. and Kieras F.J. (1993) Glycobiology 3:3-5